Characterization of carbon and nitrogen uptake by marine biota in the Indian Ocean

A THESIS

submitted for the Award of Ph. D. degree of

MOHANLAL SUKHADIA UNIVERSITY

in the

Faculty of Science

by

Arvind Singh

Under the Supervision of

Dr. R. Ramesh, FNA, FASc, FNASc, FTWAS
Senior Professor
Geosciences Division
Physical Research Laboratory, Ahmedabad, India.

DEPARTMENT OF PHYSICS

MOHANLAL SUKHADIA UNIVERSITY

UDAIPUR

2011

CERTIFICATE

I feel great pleasure in certifying the thesis entitled "**Characterization of carbon and nitrogen uptake by marine biota in the Indian Ocean**" by Arvind Singh under my guidance. He has completed the following requirements as per Ph.D. regulations of the University

(a) Course work as per the university rules.

(b) Residential requirements of the university.

(c) Presented his work in the departmental committee.

(d) Published/accepted minimum of one research paper in a referred research journal,

I am satisfied with the analysis of data, interpretation of results and conclusions drawn.

I recommend the submission of thesis.

Date: 2011

Prof. R. Ramesh
(Supervisor)
Physical Research Laboratory
Ahmedabad, India.

Countersigned by
Head of the Department

DECLARATION

*I Mr. Arvind Singh, S/o Mr. Bhisham Singh Bhadoriya, resident of Room No. - 203, Thaltej Hostel, PRL residences, Navrangpura, Ahmedabad - 380009, hereby declare that the research work incorporated in the present thesis entitled "***Characterization of carbon and nitrogen uptake by marine biota in the Indian Ocean***" is my own work and is original. This work (in part or in full) has not been submitted to any University for the award of a Degree or a Diploma. I have properly acknowledged the material collected from secondary sources wherever required. I solely own the responsibility for the originality of the entire content.*

Date:

Arvind Singh
(Author)

Dedicated To

my family

Acknowledgements

Whatever little I know today, I owe it to my teachers, friends, colleagues and family members rather than reading the printed pages and it is a great pleasure to thank all who supported me with dedicated spirit and have been part of my life at PRL.

First and foremost I offer my sincerest gratitude to my thesis supervisor, Prof. Rengaswamy Ramesh, who has motivated me throughout my thesis period with his patience and knowledge whilst allowing me the room to work in my own way. He made oceanography an easy subject for me with his style of teaching otherwise I would have taken a little longer while changing my subject from Physical Sciences to Ocean Sciences. I must thank him for regularly inviting me to weekend get togethers at his home. Aside from having a fun time, this offered me a unique opportunity to interact with other professors informally and discuss rather freely about research. Prof. Ramesh has been an immense help throughout my time and I have learnt to extract wisdom from his anecdotes, witticism and uniquely own eccentricities! My culinary skills have been boosted too thanks to him ("A chemist must always be a good cook!"). I am deeply indebted to all that he has taught me.

I am grateful to Drs. Marcel M.M. Kuypers and Gaute Lavik, at Max Plank Institute for Marine Microbiology (MPIMM), Bremen, Germany, for teaching me the complexity of nitrogen cycle within a few weeks and motivating for doing research in this field. They offered me the chance to do a significant part of my thesis work at MPIMM. I thank Hang, Yudi, Sergio, Moritz, Hannah, Tim, Abdul, Birgit, Daniela, Gabi, Thomas, Sabine and other members of MPIMM for making my stay memorable at Bremen. It was grateful that Dr. Wajih Naqvi's visit coincided with mine at MPIMM. I thank him for explaining to me many processes that occur in the Arabian Sea. I must thank POGO-SCOR for providing me the fellowship for the project. It was a fantastic experience through which I gained developed my skill set and was exposed to different work ethics in science.

I thank Dr. Anna Godhe for offering me the chance to perform culture experiments, and participate in Mesocosm experiment in future. She has taught me the biological aspect of oceanography. I also thank her daughter Nina and husband Dr. Johan Burman for having making my stay at Mangalore a very comfortable and fun-filled one!

I gratefully acknowledge Prof. M.M. Sarin for his advice, and critical comments during various stages of this thesis work. I am very much indebted to Drs. Sunil Singh, Bhas Bapat, R.P. Singh, R. Rangarajan, Dileep Angom and Prof. J.N. Goswami for teaching the various subjects during course work. I thank Profs. Utpal Sarkar and Anjan Joshipura for their cordial nature and cooperation as Dean

of the institute.

I am specially thankful to Dr. J.S. Ray for his most supporting words and informal scientific discussion during various parties. He stands testament to the fact that a jovial attitude can go a long way!

I thank Dr. M.G. Yadava and R.A. Jani for discussions and helping me in the lab. N. B. Vaghela is thanked for helping me whenever I had any sort of problem in designing any experiment. I thank Drs. Ravi Bhushan, R.D. Deshpande, Vinai Rai, K.K. Marhas, Anil Shukla, D.K. Rao and all the members of Planetary and Geosciences Division for their constructive comments and suggestions during various area seminars and reviews. Their guidance always helped me to improve the quality of the research work.

I am grateful to Dr. M.S. Sheshshayee for providing all the facilities for my sample analyses at University of Agricultural Sciences, Bengaluru.

I am thankful to Profs. Ashok Ambastha and Venkatakrishnan for describing to me the beauty of the Sun. I thank Brajesh, Sanjay, Raja, Shibu ji, Nandita ji, laxmilal ji, Manish, Alkesh, Sanjeev, Ram and their family for making my days memorable at USO.

I am very grateful to all the members of the Computer Center, Library, Purchase, Accounts, Stores and PRL dispensary. My special thanks go to Mrs. Nandini Rao and Mr. Nirav Vaidya for their help during procuring chemicals and instruments for my thesis work. I would also acknowledge people from different sections of PRL: V. Ranganathan, G.P. Patel, N.D. Bhawsar, R.S. Gupta, Parul Parikh, Bankim, Keyur, Senthil, Pradeep, Manan, Sivadasan, Hitendra and others for their help in various stages.

I owe a special appreciation to Profs. B.L. Ahuja and Rajesh Pandey for encouragement during various stages, which has helped me to improve this work. The Physics Department and the Ph.D. section of Mohan Lal Sukhadia University, Udaipur has provided the support I have needed to produce and complete my thesis.

I acknowledge Drs. S. Prasanna Kumar (NIO, Goa), M. Sudhakar, N. Anil Kumar, M. M. Subramaniam, Ravi Mishra (NCAOR, Goa), R.M. Dwivedi, Mini Raman (SAC, Ahmedabad) for giving me the opportunity to participate in various research cruises. Thanks are due to my friends Arvind Sahay and Suhas for making the cruises memorable. I thank the captains, crew and participants in the cruises and Ministry of Earth Sciences for ship time. I also thank ISRO-GBP for funding provided for the cruises.

I spent quality time with my younger friends Anwar, Siddharth, Rahul and Saurabh. I learnt from them in many ways from playing Volleyball to solving puzzles. Kaustubh and Vikas were great company with academics and otherwise. I wish them all a very bright future.

I also benefited from my seniors at PRL who inspired me throughout my thesis work. I thank Subimal, Manish Tiwari, Neeraj Rastogi, Santosh Rai, Morthekai, Antra and Rajesh Kushwaha. Special thanks to Tarun Jha for running the fun-show 24 hrs with positive energy. His jokes saw me through a tough day at work!

Collective and individual acknowledgments are also owed to my labmates Amzad, Ashutosh and Rohit. They were always very supportive and always guided me in the right direction. Scientific discussions with them were always very fruitful and enjoyable. My special thanks to Naveen, Shreyas and Satya who have always been an infinite source of encouragement and criticism to my academic career.

During my initial time at PRL, Gyana, Bhavik, Vishal, Anil Ohlan, Anil Tyagi, Praveen, Kallol, Charu, Bindu, Sumita, Waliur, Kirpa, Alok and Sumanta have created lively atmosphere. I thank them all for making my life easy at PRL.

In my daily work, I have been blessed with a friendly and cheerful group. Heartfelt thanks goes out to Ashwini, Vimal, Pankaj, Vineet, Soumya, Bhaswar, Anand, Sandeep, Sreekanth, Ashok, Rohit, Rabiul, Suman, Chauhan, Jayati, Raju, Zulfi, Ketan, Patra, Neeraj, Arvind Saxena, Nita, Digu, and Aditya. All the research scholars of JRF 07-10 batches have been supportive and I wholeheartedly wish them the best.

Words fail in expressing love, strength and inspiration of my family for me. My little niece Anjali who asks me every time I talk with her "*Mamu, aap kab tak padai karte rahoge* (How long will you be studying)?" This question makes me think deeply if I am doing something worthwhile. The question is still left unanswered but at least I came out alive with a doctoral thesis!

Abstract

Primary productivity is mostly limited by the unavailability of reactive nitrogen in the sunlit surface layer of tropical oceans. The supply of such new nitrogen to the surface ocean is through upwelling, N_2 fixation by diazotrophs, riverine flux and atmospheric deposition. The relative and absolute importance of these processes in the Indian Ocean is studied here.

N_2 fixation is estimated directly for the first time using the $^{15}N_2$ tracer technique in the Arabian Sea during the spring inter-monsoon 2009. Estimates are double the values reported earlier and can account for a substantial fraction of the nitrogen gained by the Arabian Sea. Carbon uptake rates are also estimated using the ^{13}C tracer technique. Further, contribution of atmospheric deposition and riverine fluxes to new productivity in the two biogeochemically different basins of the northern Indian Ocean, the Arabian Sea and the Bay of Bengal, is presented. A upper bound of the contribution of atmospheric deposition to new productivity in the northern Indian Ocean is $\sim$2.5%. On an average 1.73 Tg N y^{-1} is deposited into the northern Indian Ocean through dry and wet depostion of aerosols. On the other hand, most of the dissolved inorganic nitrogen ($\sim$81% in the case of the Arabian Sea and 96% in the case of the Bay of Bengal) through riverine flux is not transported to the ocean and is consumed on the course of the rivers or in the estuaries. Coastal Bay of Bengal and Arabian Sea receive $\sim$0.38 Tg N y^{-1} and $\sim$0.06 Tg N y^{-1}, respectively, through rivers. A large variation in the contribution of DIN through river fluxes to new productivity is found in both these basins. Our estimate of nitrogen fluxes through N_2 fixation, aerosols and rivers is a step towards significantly reducing the uncertainty in the global nitrogen budget.

Application of stable isotopes is extended further by simulating nitrogen loss process in the Arabian Sea. An equation describing isotopic fractionation in open systems, wherefrom material is not only removed with isotopic fractionation, but fresh material of a different isotopic composition is added from an external source, is derived. This model is further applied to understand other oceanographic processes as well. With the help of a new data set, spatiotemporal variation in the oxygen isotopic composition and salinity (δ^{18}O-S) relation of the northern Indian Ocean is studied. While the results are consistent with positive P-E (excess of precipitation over evaporation) over the Bay of Bengal and negative P-E over the eastern Arabian Sea, a significant spatiotemporal variability in the slope (also intercept) of the relation is observed in the Bay; the temporal variability is difficult to discern in the Arabian Sea. Both the slope and intercept appear to be sensitive to rainfall; the slope (intercept) is higher (lower) during years of stronger monsoon. The observed variability in the δ^{18}O-S relation implies that caution needs to be exercised in paleosalinity estimations, especially from the Bay of Bengal, based on δ^{18}O of marine organisms.

Key words: Marine Carbon Cycle, Marine Nitrogen Cycle, Nitrogen fixation, The northern Indian Ocean, Rayleigh fractionation, Aerosol deposition, Riverine flux

Abbreviations

α	fractionation factor between product and source
ϵ	enrichment factor i.e. (α-1)$\times 10^3$
δ^{18}O	Oxygen isotope composition of water with VSMOW as standard
δ^{15}N	Nitrogen isotope composition of PON with air as standard
‰	per mil (or parts per thousand)
Anammox	Anaerobic Ammonium Oxidation
DIC	Dissolved Inorganic Carbon
DIN	Dissolved Inorganic Nitrogen
DNRA	Dissimilatory Nitrate Reduction to Ammonium
EA	Elemental Analyzer
EP	Export productivity
FIM	Fall Inter monsoon
FORV	Fishery and Oceanographic Research Vessel
GC	Gas Chromatograph
GNIP	Global Network on Isotopes in Precipitation
HNLC	High-nutrient, low-chlorophyll
IAEA	International Atomic Energy Agency
IAPSO	International Association for the Physical Sciences of the Ocean standard seawater
IPCC	Intergovernmental Panel on Climate Change
IRMS	Isotope Ratio Mass Spectrometer
IRS-P4-OCM	Ocean Colour Monitor on Indian Remote Sensing Satellite IRS-P4
ISRO-GBP	Indian Space Research Organisation - Geosphere Biosphere Programme
ITCZ	Inter Tropical Convergence Zone
JGOFS	Joint Global Ocean Flux Study
JRF	Junior Research Fellow
MLD	Mixed Layer Depth

N_r	Reactive Nitrogen
N/P	Nitrate to Phosphate ratio
N/Si	Nitrate to Silicate ratio
NARM	Narmada
NCAOR	National Centre for Antarctic and Ocean Research
ND	no data available
NIO	National Institute Of Oceanography
NOAA-AVHRR	National Oceanic and Atmospheric Administration-Advanced Very High Resolution Radiometer
NP	New Productivity
OMZ	Oxygen Minimum Zone
ORV	Oceanographic Research Vessel
PAR	Photosynthetically Active Radiation
POC	Particulate Organic Carbon
POGO	Partnership for Observation of the Global Oceans
PON	Particulate Organic Nitrogen
PP	Primary Productivity
ppmv	parts per million volume
PRL	Physical Research Laboratory
R	Ratio of heavier to lighter isotopes
S	Salinity
SAC	Space Applications Centre
SCOR	Scientific Committee on Oceanic Research
SIM	Spring Inter monsoon
SM	Summer monsoon
SOM	Soil Organic Matter
SST	Sea Surface Temperature
TAD	Total (wet + dry) atmospheric nitrogen deposition

TRMM	Tropical Rainfall Measuring Mission
UNESCO	United Nations Educational, Scientific and Cultural Organization
VSMOW	Vienna Standard Mean Oceanic Water
WM	Winter monsoon
WMO	World Meteorological Organization

Contents

List of Figures

List of Tables

Chapter 1

Introduction

Carbon dioxide (CO_2), one of the most important green house gases in the Earth's atmosphere, increased from ∼280 ppmv (parts per million volume) to ∼380 ppmv during the last 250 years [*Solomon et al.*, 2007]. This rate of increase, due to anthropogenic activities, is around an order of magnitude higher than that has occurred for millions of years [*Doney and Schimel*, 2007]. Ocean is one of the key components in regulating the Earth's atmosphere as it absorbs around one quarter of the CO_2 emitted to the atmosphere by human activities. All the processes that influence the oceanic uptake of CO_2 are controlled by climate. Therefore, any changes in climate may alter the uptake of CO_2 by the ocean. However, understanding of the response of ocean CO_2 to changes in climate is inadequate due to the limited data on CO_2 removed by the oceans [*Houghton*, 2007].

Ocean exchanges carbon with atmosphere mainly by two processes. First, cold and dense waters at high latitudes, enriched in dissolved CO_2, sink to the deeper oceans. This localized sinking, associated with the Meridional Overturning Circulation is termed the solubility pump. This sinking flux is approximately balanced by diffuse upward flux of DIC (dissolved inorganic carbon) into tropical surface waters. The second process is biological through which there is a net removal of (CO_2) from the atmosphere to the deeper ocean, known as the biological pump. This is more efficient in the tropical oceans, e.g., the area of the present study -

the northern Indian Ocean.

Marine biological productivity is defined as the rate of carbon fixation during photosynthesis at the ocean surface, measured in units of mg C $m^{-2}d^{-1}$. There is a supply of this fixed carbon from the sunlit layers of the ocean (i.e., the top ~100 m) to the darker, deeper layers through biological pump, termed as export productivity. This is approximately equal to 'new productivity', the fraction of the productivity sustained by the input of new nutrients into the euphotic zone, over annual time scales [*Eppley and Peterson*, 1979]. The efficiency of the biological pump is driven by the availability of nutrients, especially macronutrients such as reactive nitrogen (N_r) in the tropics. N_r is known to limit the biological productivity in the surface ocean in many regions [*Broecker*, 1974]. Thus, nitrogen is an essential nutrient for growth of marine biota and hence understanding the processes by which nitrogen is added to the oceans are important. This is the one of the objectives of the present study.

1.1 Marine Nitrogen Cycle

Nitrogen, as a building block in the amino acids, is a fundamental player in marine biogeochemical cycles. The fluxes of nitrogen within and among its reservoirs comprises the global nitrogen cycle (Figure 1.1). Molecular nitrogen (N_2) is most abundant (78% by volume) in the Earth's atmosphere, but can be directly utilized only by a specific group of marine microorganisms. Most other organisms prefer oxidized or reduced forms of nitrogen, i.e., N_r (e.g., NO_3^-, NH_4^+ etc.). Nitrogen enters the surface ocean through the following processes related to the marine nitrogen cycle.

1.1.1 N_2 fixation

N_2 fixation is a microbially mediated process performed by several types of bacteria and algae. In this process, molecular nitrogen gets converted to ammonium (Figure 1.1) -

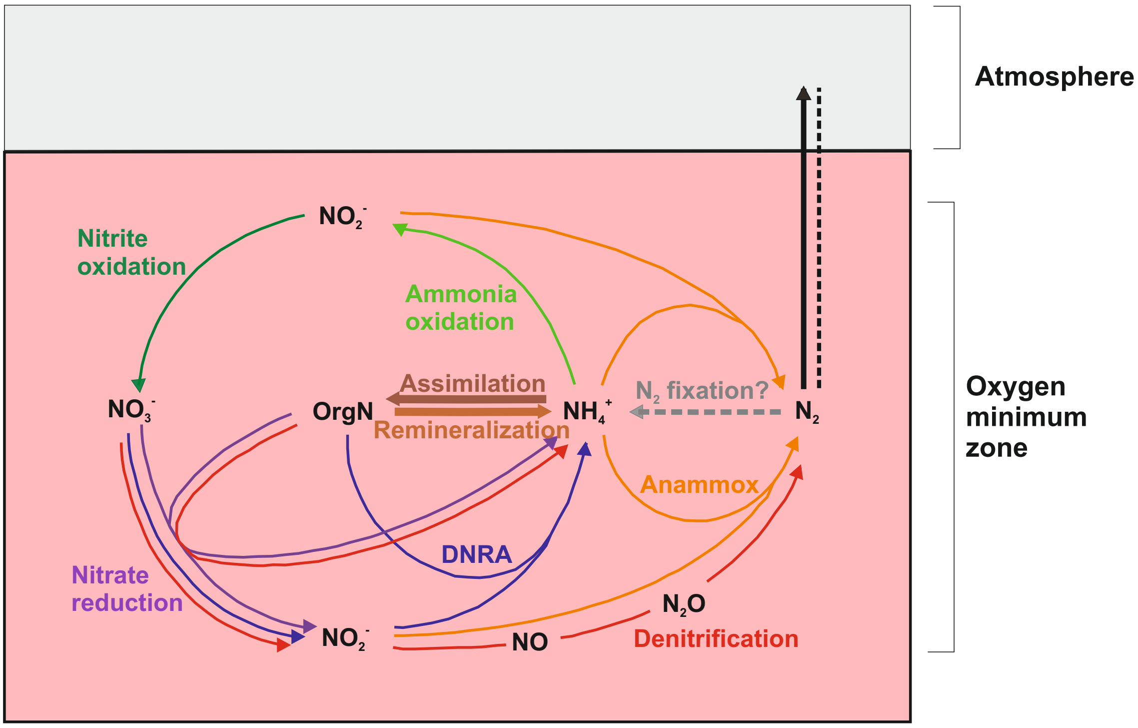

Figure 1.1: The nitrogen cycle in oceanic oxygen minimum zones. N_2 can be produced by both anammox (orange) and denitrification (red). Both nitrate reduction (purple) and dissimilatory nitrate reduction to ammonium (blue) are also remineralization processes. Nitrification is divided into two steps: ammonia oxidation (light green) and nitrite oxidation (dark green). N_2 fixation is also shown (gray dashed). Source: *Lam et al.* [2009]

$$N_2 + 8H^+ + 8e^{-1} \rightarrow 2NH_3 + H_2$$

As discussed earlier, the surface water of the ocean is deficit in N_r. Nitrate is the main compound present in the surface water on which marine productivity depends. However, in the absence of N_r, a specific group of microorganisms-diazotrophs, can utilize N_2, despite the fact that large energy (226 kcal/mol) is required to break the triple bond (N≡N). These microorganisms convert N_2 into ammonium with their special enzyme, nitrogenase, and in this way 'new' nitrogen is introduced into the ocean. Such microorganisms like *Trichodesmium* occur in the Arabian Sea under favorable conditions, i.e., in the absence of N_r and higher Sea Surface Temperature (SST). Fe is the key micronutrient which may decide the fate of N_2 fixing microorganisms.

N_2 fixation has the potential to influence the sequestration of CO_2 by introducing 'new' nitrogen which supports primary productivity. Diazotrophs are involved in a global feedback of the climate system and this feedback exhibits complex dynamics on varying time-scales. The hypothesized feedback mechanisms will have the following components - the rate of N_2 fixation can impact the concentration of atmospheric CO_2; CO_2 concentrations in the atmosphere can influence the climate; the climate system, in turn, can influence the rate of N_2 fixation by controlling the supply of Fe associated with dust, and by influencing the stratification of the upper ocean. Humans play an important role in this feedback cycle by their influence on dust production, through agriculture at the margins of deserts, and by emissions of CO_2 into the atmosphere. These influences can lead to a cyclic feedback system, particularly on longer time-scales. Consequently, a large challenge in the contemporary biogeochemical oceanography is to understand the regional to global scale controls on N_2 fixation in the sea [*Karl*, 2002].

1.1.2 Nitrification

Nitrification is an aerobic process in which microorganisms obtain energy by converting ammonium to nitrate (Figure 1.1). This happens in two stages - in the first stage, the oxidation of ammonium to nitrite is performed by a group of organisms called *Nitrosomonas*; in the second stage, another group of organisms-*Nitrobacter*, are responsible for the oxidation of the nitrite to nitrate.

$$NH_4^+ + 3/2O_2 \rightarrow NO_2^- + H_2O + 2H^+ \qquad \Delta G = -290\ kJ/mol$$

$$NO_2^- + 1/2O_2 \rightarrow NO_3^- \qquad \Delta G = -82\ kJ/mol$$

1.1.3 Assimilatory nitrate reduction

Uptake of nitrate by an organism and its incorporation through nitrate reduction is known as assimilatory nitrate reduction (Figure 1.1). It is an important input of nitrogen for many microorganisms.

1.1.4 Ammonification

Ammonification (Remineralization) is conversion of organic nitrogen in to ammonium through microbial process (Figure 1.1). This is part of decomposition of organic matter by heterotrophic microbes.

1.1.5 Denitrification

Denitrification is a multi-step heterotrophic reduction of nitrate to molecular nitrogen ($NO_3^- \rightarrow NO_2^- \rightarrow NO \rightarrow N_2O \rightarrow N_2$), but only when the process leads all the way to N_2 production (Figure 1.1) then only it meets the proper definition of denitrification [*Zumft*, 1997]. In addition to nitrogen sink, heterotrophic denitrification is regarded as the major remineralization process in the Oxygen Minimum Zones (OMZs) because heterotrophic bacteria release NH_4 from organic matter while respiring NO_3.

1.1.6 Anammox

It is very well established now that apart from denitrification, <u>an</u>aerobic <u>amm</u>onium <u>ox</u>idation (anammox) - chemolithoautotrophic process that fixes inorganic carbon - is also cause for N_r loss from the ocean [*Kuypers et al.*, 2003; *Lam et al.*, 2009; *Lam and Kuypers*, 2011] (Figure 1.1). Anammox mainly occurs if oxygen concentration is less than 1.1 μM. The overall reaction for anammox has been suggested as follows-

$$NH_4{}^+ + 1.32NO_2{}^- + 0.066HCO_3{}^- + 0.13H^+ \rightarrow$$
$$0.26NO_3{}^- + 1.02N_2 + 0.066CH_2O_{0.5}N_{0.15} + 2.03H_2O$$

The occurrence of anammox in seawater was first reported in the Black Sea [*Kuypers et al.*, 2003] and Golfo Dulce [*Dalsgaard et al.*, 2003]. Neither oxygen nor sulfide were detectable at the depths where anammox was observed.

1.1.7 DNRA

Dissimilatory Nitrate Reduction to Ammonium (DNRA) is a microbial process in which nitrate/nitrite is reduced to ammonium (Figure 1.1). This process has previously been considered unimportant, however, recent research has shown DNRA to be of importance in marine nitrogen cycle [*Brandes et al.*, 2007; *Lam et al.*, 2009].

1.1.8 Nitrate Reduction

The dissimilatory reduction of nitrate to nitrite is the first step in denitrification and DNRA, but it is also an independent process (Figure 1.1). More microorganisms have potential of reducing nitrate to nitrite without denitrifying or ammonifying [*Gonzalez et al.*, 2006; *Zumft*, 1997].

The present study mainly deals with N_2 fixation and dintrification in the northern Indian Ocean.

1.2 Ocean-atmosphere-land interaction

Ocean gains nitrogen through atmosphere (dry and wet deposition of aerosols) and land (riverine fluxes) besides N_2 fixation [e.g., *Chen and Chen*, 2006]. Upwelling/eddy diffusion is another inherent nitrogen source to photic zone of the ocean but this occurs in limited and specific areas of the ocean, e.g., in the western Arabian Sea during summer. Nitrogen inputs from fertilizer use on land and waste discharge are also probably limited to the coastal regions.

1.2.1 Atmospheric Nitrogen Deposition

N_2 is the most stable molecule in the Earth's atmosphere. It is chemically unreactive at the atmospheric temperature and pressure and combines with other elements only under extreme conditions or when catalyzed by enzymes. All other forms of nitrogen (oxidized and reduced) are derived from N_2. N_2 is converted to N_r by either N_2 to NH_3 or by converting N_2 to NO via both natural and anthropogenic processes.

In addition to N_2 fixation, lightning is another natural process which converts N_2 to N_r, though this process has less global importance now. With industrial revolution, fossil fuel burning has become the dominant anthropogenic process for N_r creation. The high temperature and pressure provide energy for N_r creation during fossil fuel combustion.

N_r, which is present in the atmosphere, is deposited into the ocean by two ways: wet deposition - aerosols settles with rain over the ocean; and gravitational force leads to dry deposition of N_r. Depositional velocities and scavenging ratio required to estimate wet and dry deposition of N_r suffer from considerable uncertainties as they depend on complex interactions of various parameters, e.g. wind speed, particle size [*Duce et al.*, 1991]

Atmospheric nitrogen inputs are often poorly represented in the study of the open ocean anthropogenic impacts [e.g., *Duce et al.*, 1991; *Jickells*, 2006], however, potential importance of atmospheric deposition to the new productivity in the open ocean is discussed. Atmospheric deposition of N_r may account for up to ∼3% of marine new productivity [*Duce et al.*, 2008]. *Bange et al.* [2000] have estimated nitrogen deposition through aerosol in the Arabian Sea is to be 1.5 Tg N y^{-1}.

1.2.2 Nitrogen fluxes through rivers

Nitrogen, in addition to supply of through atmosphere, is also supplied through river via erosion and weathering processes. The most productive areas in the oceans are coastal region because of supply of nutrients through rivers and coastal upwelling. Though the N_r flux through atmosphere and rivers are modest but with increasing human activities they have potential to alter subsurface water chemistry by altering the Redfield Ratio (C:N:P :: 106:16:1).

An enigma appeared while estimating the nitrogen loss and gain rates; these are not in balance. Ocean loses ∼400 Tg N y^{-1} and fixes ∼200 Tg N y^{-1}. Suggested reasons for the nitrogen deficit are - either there are other less well-studied or currently unknown exist processes that fix substantial amounts of N_r [*Codispoti*, 2007]. The loss processes are studied in detail and the possibility of a decrease in the nitrogen loss term in the total nitrogen budget is less likely, while the gain processes are still poorly understood [*Codispoti*, 2007]. This motivated to revise N gain processes (e.g., N_2 fixation) with the better tools available now.

Stable isotopes provide a tool in studying biogeochemical cycles in the Ocean. Their applications are discussed in detail below:

1.3 Stable Isotopes and their applications

The atomic nuclei of an element having different number of neutrons are called isotopes. There are two types of isotopes present in the nature - radio isotopes and stable isotopes. Radioisotopes are important to measure time, e.g. age or circulation times of ground water, while stable isotopes are useful as tracers in the hydrology, biogeochemistry, geochemistry, etc.

H, C, N, O and S are the elements whose stable isotopes are of practical importance. The stable isotopes of C and N, focus of the present study in the biogeochemical cycle, serve as tracers in estimating the carbon and nitrogen fluxes.

Isotopic molecules with differences in mass have different reaction rates. This leads to isotopic fractionation. Isotopic fractionation is a physical phenomenon which causes changes in the relative abundances of isotopes due to their differences in mass. The isotopic fractionation that accompanies the evaporation of water from the ocean and other surface waters and the reverse process of rain formation account for the most notable changes. As a result, meteoric waters are depleted in the heavier isotopic species of H and O relative to ocean waters, whereas waters in evaporative systems, such as lakes and plants, are relatively enriched.

Stable isotopes are measured as the ratio of two isotopes of a given element, i.e. R = Abundance of the rarer isotope/Abundance of the more abundant isotope. For nitrogen, which has two stable isotopes - ^{14}N and ^{15}N, with abundances of 0.99634 and 0.00366, respectively, isotope ratio is given as

$$R = \frac{^{15}\mathrm{N}}{^{14}\mathrm{N}} \approx 0.0037$$

Measuring an absolute isotope ratio requires sophisticated mass spectrometric equipment. Further, measuring this ratio would lead often to problems in comparing data sets from different laboratories. However, our interest is only in comparing the variations in stable isotope ratios rather than actual abundance, and so a simpler approach is used. Rather than measuring a true ratio, an apparent ratio is measured by gas source mass spectrometry. The apparent ratio differs from the true ratio due to operational variations and will not be constant between machines or laboratories or even different days for the same machine. However, by measuring a known reference on the same machine at the same time, we can compare our sample with a reference.

As fractionation processes do not impart large variations in isotopic concentrations, $\delta-$ values are expressed as the parts per thousand or permil (‰) difference relative to the reference.

$$\delta^{15}\mathrm{N} = \left(\frac{(^{15}\mathrm{N}/^{14}\mathrm{N})_{\mathrm{sample}}}{(^{15}\mathrm{N}/^{14}\mathrm{N})_{\mathrm{air}}} - 1 \right) \times 1000‰ \tag{1.1}$$

A δ value that is positive, say +10‰, signifies that the sample has 10‰ more $^{15}\mathrm{N}/^{14}\mathrm{N}$ than the reference (air), or is enriched by 10‰ or 1% more $^{15}\mathrm{N}/^{14}\mathrm{N}$ than the reference. Similarly, the value for a sample depleted relative to the reference by this amount would be expressed as $\delta^{15}\mathrm{N}_{air}^{sample} = -10‰$.

Artificially enriched (99%) stable isotopes of carbon ($^{13}\mathrm{C}$) and nitrogen ($^{15}\mathrm{N}$) are used in this study. Contribution of $^{15}\mathrm{N}$ tracer in the biogeochemical cycling is well-established, evidences of nitrogen as limiting nutrient are aggregated from $^{15}\mathrm{N}$ studies [*Owens and Watts*, 1998]. $^{15}\mathrm{N}$ tracer is introduced into oceanography to separate the fraction of primary productivity into new and regenerated productivity in the photic zone (oceanic depth upto where 1% of surface sunlight reaches) of the ocean [*Dugdale and Goering*, 1967]. *Dugdale and Goering* [1967] introduced a conceptual model assuming the photic zone to be as a close box. The microorganisms present in the zone may obtain nitrogen into two ways - (i) nitrogen is recycled in organic matter decomposition inside the zone, (ii) lateral or vertical transport of nitrogen from outside the zone. Productivity supported by nitrogen produced inside the photic zone is regenerated productivity while that supported by externally added nitrogen is new productivity. It is assumed in this model that the form of new nitrogen is nitrate and that of regenerated nitrogen is ammonium. ^{15}N in the form of gas is used in the present study for measuring N_2 fixation [*Montoya et al.*, 1996]. In addition, ^{13}C is also used for primary productivity (carbon assimilation) estimations [*Slawyk et al.*, 1977]. Methodology of using stable isotopes is provided in the next chapter.

In addition to estimating the carbon and nitrogen uptake rates, applications of stable isotopes are extended further in the present study in understanding the processes. The heaviour isotopes get enriched in the reservoir during physicochemical processes because they move slowly during transformations. Such transformations modify isotope ratio (R), causing isotopic fractionation. In nature, isotope fractionation occurs during physical and chemical reactions such as evaporation and precipitation of calcite. Isotope ratios in various compounds are measured and then used to trace the process. Isotopic evolution of such systems is explained by the Rayleigh equation as discussed below.

1.3.1 Rayleigh equation

Rayleigh equation [e.g., *Mook*, 2006] is applied to a system where a substance is continuously removed. Lets consider a reservoir, e.g., a lake from where water evaporates. During the evaporation, the remaining water becomes enriched in the heaviour molecules compared to the water vapor.

Let us consider a reservoir that loses material due to any physicochemical process with isotopic fractionation at a constant temperature. At any instant the stable isotope ratio is given by

$$R = \frac{N^*}{N} \tag{1.2}$$

where N^* and N are respectively the number of molecules containing the heavier and lighter isotopes of a given mass of the same element (e.g. oxygen; $H_2{}^{18}O$ and $H_2{}^{16}O$). Differentiating equation (1.2)

$$\mathrm{d}R = \frac{\mathrm{d}N^*}{N} - \frac{R\mathrm{d}N}{N} \tag{1.3}$$

After making a few assumptions like (i) abundance of the heavy isotope is much smaller than that of the light isotope ($N^* << N$) at all times, hence $N^* + N \sim N$, (ii) process is isothermal (iii) The substance removed is in isotopic equilibrium with the reservoir and (iv) there is no isotopic gradient in the reservoir at any time, Rayleigh equation is obtained from equation the (1.3)

$$R = R_0 f^{\alpha-1} \tag{1.4}$$

where R_0 is the initial isotopic ratio, f is remaining fraction in the reservoir and α is fractionation factor. In the present study, this equation is extended further and applied to a few oceanographic processes where material is not only being removed but added as well, simultaneously [e.g., *Mook*, 2006, *Ramesh and Singh*, 2010].

In the first two examples, the derived equation is applied to understand the denitrification in the Arabian Sea, and soil organic matter decomposition processes [*Ramesh and Singh*, 2010]. Equation is further applied to understand oxygen isotopic composition ($\delta^{18}O$) and salinity relation in the surface water of the northern Indian Ocean.

1.4 The northern Indian Ocean

The northern Indian Ocean is divided into two parts - the Arabian Sea in the western and the Bay of Bengal in the eastern side of the Indian subcontinent, both being enclosed in the north at similar latitudes. Though they are like twin seas but are different in many aspects. They form excellent sites to study the variability in the biogeochemistry of the oceans.

Unlike other oceans, the northern Indian Ocean, being bounded by the Asian land mass to its north, suffers a strong seasonal reversal in the wind direction, well known as the monsoon circulation. During June-September (the southwest or summer monsoon), strong winds blow from ocean towards land resulting in intense upwelling in the northwestern Arabian Sea. Evaporation over the Arabian Sea (275 cm y^{-1}) is estimated to be higher than that over the Bay of Bengal (250 cm y^{-1}; [*Prasad*, 1997]). River discharge and overhead precipitation together exceed evaporation in the Bay of Bengal. This flux imbalance causes the export (advection) of less saline water to the Arabian Sea [*Rao and Sivakumar*, 2003], e.g., the East India Coastal Current (EICC) transports low salinity water from the Bay to the southeastern Arabian Sea during winter. The West India Coastal Current (WICC) carries this water northward [*Wyrtki*, 1973; *Han and McCreary*, 2001; *Schott and McCreary*, 2001] and decreases the surface salinity of the eastern Arabian Sea. In contrast, during summer, the eastward flowing Indian Monsoon Current carries high-salinity water from the Arabian Sea to the Bay of Bengal [*Prasanna Kumar and Prasad*, 1999; *Vinayachandran et al.*, 1999].

Rainfall over the Indian subcontinent is derived from the northward movement of the Inter-Tropical Convergence Zone (ITCZ) during June-September and its withdrawal during October-November [*Gadgil*, 2003]. The rainfall varies seasonally, regionally and annually over the region. Most Indian plains receive a major fraction (∼80%) of the annual rainfall during summer. The highest rainfall occurs along the west coast and northeastern regions of the Indian peninsula. During

December-February (the northeast or winter monsoon), cool and dry air from the Himalayas enhances evaporation in the northeastern Arabian Sea causing convective mixing [*Madhupratap et al.*, 1996], while there is little rainfall over most of India; southeastern India gets its major share of rain during this period. Upwelling and winter mixing during summer and winter, respectively, bring nutrient from the deep to the surface in the Arabian Sea which results in enhancing the productivity [*Madhupratap et al.*, 1996; *Prasanna Kumar and Prasad*, 1996; *Prakash and Ramesh*, 2007]. On the other hand, high riverine fluxes stratify the Bay of Bengal surface water, limiting surface productivity [*Kumar et al.*, 2004a; *Singh et al.*, 2010]. The Arabian Sea is one of most productive regions in the world oceans and also hosts perennially-intensified denitrification zone [e.g., *Madhupratap et al.*, 1996; *Naqvi et al.*, 2005].

An interesting study, productivity during summer in the western Arabian Sea show increasing trend from 1997 to 2004 as observed from the ocean color data. This trend has been attributed to the warming of the Eurasian land mass [*Goes et al.*, 2005]. However, such a trend is not observed in the northeast Arabian Sea [*Prakash and Ramesh*, 2007; *Prasanna Kumar et al.*, 2010]. *Naqvi et al.* [2010a] reanalyzed the data and have also ruled out such increasing trend. These studies suggest that there is still much more to be understood in the Arabian Sea with the improved techniques.

1.4.1 Previous studies on N_2 fixation

Significant amount of work on new and primary productivity has been done in the northern Indian Ocean over the last two decades [e.g. *Owens et al.*, 1993; *McCarthy et al.*, 1999; *Watts et al.*, 1999; *Watts and Owens*, 1999; *Sambrotto*, 2001; *Kumar et al.*, 2004a; *Prakash et al.*, 2008; *Kumar et al.*, 2010; *Gandhi et al.*, 2010a, b], however, no direct estimates on N_2 fixation are made despite the reports on the seasonal occurrence of *Trichodesmium* blooms in the Arabian Sea [*Devassy et al.*, 1978; *Capone et al.*, 1998; *Parab et al.*, 2006]. Presence of diazotrophic

γ-proteobacteria has also been reported in the Arabian Sea [*Bird et al.*, 2005], they release fixed nitrogen to the ocean water, making it available to the other non-diazotrophic species [*Letelier and Karl*, 1996]. Indirect measurements (C_2H_2 reduction technique) suggested that 3.3 Tg y^{-1} is fixed in the Arabian Sea which is an order of magnitude less than the denitrification rates [*Bange et al.*, 2005 and references therein]. The present study reports the first direct measurements (using $^{15}N_2$ tracer) of N_2 fixation in the Arabian Sea during spring intermonsoon.

Hypothesis of heterotrophic N_2 fixation in the Wadden Sea is tested with a slight modification in the technique for measuring the same in the water. This technique will be helpful in estimating N_2 fixation in the northern Indian Ocean.

1.4.2 Previous studies on Nitrogen inputs through Aerosols and rivers

The concentration of nitrate in the aerosol over the major part of the Arabian Sea is governed by the seasonal variability of the air mass origin [*Tindale and Pease*, 1999; *Naqvi et al.*, 2005]. Due the the seasonal shift of ITCZ, aerosols in the Arabian Sea during summer and winter, respectively, faithfully preserve the signature of air originating from the Southern and Northern Hemispheres. This is evidenced by correlating nitrate in the aerosol with ^{210}Pb [*Sarin et al.*, 1999].

Realizing the importance of aerosols in the biogeochemistry, it is suggested that the higher chlorophyll in the Arabian Sea than in the Bay of Bengal is not merely controlled by nutrients by vertical mixing but also critically depend on atmospheric inputs [*Patra et al.*, 2007]. Aerosols supply 1.2 Tg N y^{-1} via wet and dry deposition in the Arabian Sea [*Bange et al.*, 2000], while no such estimates are available for the Bay of Bengal. With the limited data available, aerosol nitrogen contribution to new productivity is found to be minor in the Arabian Sea. In the present study, such estimates have been revised with the more data becoming available, by dividing the Arabian Sea into three different zones i.e. western, central and eastern, since the origin of aerosols in these zones may be different. In addition, estimates are also presented for the Bay of Bengal.

No estimates have been made so far for riverine nitrogen contribution to the new productivity for the northern Indian Ocean. *Naqvi et al.* [2010b], assuming a constant concentration of N_r, have estimated nitrogen fluxes through rivers in the Arabian Sea is to be 0.6 Tg N y^{-1}. In the present study, contribution of riverine nitrogen inputs to the new productivity in the northern Indian Ocean is discussed.

1.4.3 Previous studies on δ^{18}O-salinity relation

A limited set of δ^{18}O values of precipitation over the Indian subcontinent is available from the web site for Global Network on Isotopes in Precipitation [*IAEA/WMO*, 2006]. *Araguas-Araguas et al.* [1998] have shown that there is an 'amount effect' in the monsoon precipitation, i.e., higher amount of rainfall is more depleted in ^{18}O (∼-1.5 ‰ per 100 mm of monthly rainfall). δ^{18}O values of direct precipitation over the Bay of Bengal and the Arabian Sea are ∼-2 ‰ and ∼-1 ‰, respectively [*Bowen and Revenaugh*, 2003]. Reported δ^{18}O values of the runoff to the Bay of Bengal from the Ganga river system are similar (∼-6 ‰) [*Ramesh and Sarin*, 1992; *Somayajulu et al.*, 2002]. Additionally, the Bay receives runoff from the Brahmaputra, Irrawady, Mahanadi, Godavari and Krishna rivers [*Lambs et al.*, 2005]. All this adds up to 1.6×10^{12} m^3 y^{-1}, much higher relative to the runoff of 0.3×10^{12} m^3 y^{-1} to the Arabian Sea from rivers viz, Narmada, Tapti, Nethravati and Indus [*Subramanian*, 1993]. The mean δ^{18}O value of the runoff is likely to be as low as ∼-9 ‰ in some years when the summer rains are well above normal [*Delaygue et al.*, 2001]. The major runoff to the Bay derives from the rivers of Himalayan origin [*Ramesh and Sarin*, 1992; *Karim and Veizer*, 2002; *Lambs et al.*, 2005], and increased snowmelt could also lower the mean δ^{18}O of runoff during pre-monsoon (April-May). The mean δ^{18}O value of the runoff to the Arabian Sea from the Indus is ~ -11 ‰ [*Mook*, 1982], while that from the Narmada and Tapti and smaller westbound rivers originating in the Western Ghats is likely to be higher (i.e., more enriched in ^{18}O); however, in years of excess rain/floods or increased Himalayan snow-melt in spring, the mean δ^{18}O of runoff into the Arabian Sea could be significantly lower. Time series data on δ^{18}O of runoff are too sparse to refine these assertions.

Because of the water flux imbalances between the Arabian Sea and Bay of Bengal, both basins experience significant changes in δ^{18}O and salinity through the exchange of surface waters. Because of the geography of the Indian sub-continent, the surface water of the Bay is more diluted by runoff than that of the Arabian Sea, decreasing the surface salinity of the Bay by ∼2 relative to the southern Indian Ocean [*Delaygue et al.*, 2001]. Maximum seasonal variations in salinity of 2 and 8 psu are observed in the Arabian Sea and the Bay of Bengal, respectively [*Delaygue et al.*, 2001; *Rao and Sivakumar*, 2003].

1.5 Scope of the present work

Main aim of the present study is to investigate N_2 fixation rates and primary productivity using $^{15}N_2$ and ^{13}C isotope tracer techniques in the northern Indian Ocean. Objective is further extended to solve the mystery of nitrogen cycle with both the observation and simulation. To fulfill this goal the following work is done

1. N_2 fixation rates are estimated during a *Trichodesmium* bloom period in the northeastern Arabian Sea. The study is aimed to understand nitrogen cycle in the Arabian Sea in a better way.

2. Carbon uptake rates in the surface water during the same period were also investigated. This helps in understanding the role of *Trichodesmium* in the global carbon cycle.

3. Natural isotopic composition of surface suspended particulate matter is estimated in the same cruise which helps to identify sources of nitrogen to the euphotic zone.

4. A technique to measure N_2 fixation rates was the sediments were developed. This is tested in the Wadden Sea. This technique helps in estimating N_2 fixation rates in the sediments in the northern Indian Ocean.

5. Hypothesis of heterotrophic N_2 fixation in the sediments was tested in the Wadden Sea. This helps in modifying the global nitrogen fluxes.
6. Nitrogen loss rates (denitrification) were simulated by revising the Rayleigh fractionation equation. Revised equation is helpful in describing isotopic fractionation in open systems, wherefrom material is not only removed with isotopic fractionation, but fresh material of a different , constant, isotopic composition is added from an external source, at a given rate.
7. Hypothesis of spatiotemporal variability of δ^{18}O-salinity relation in the northern Indian Ocean is tested by both observation and simulation. This study may help in decreasing the uncertainty in the palaeosalinity estimates.
8. Aerosol and riverine nitrogen fluxes, and their contribution into the new productivity, is estimated in the northern Indian Ocean. This would again help in revising the marine nitrogen cycle and understanding the role of anthropogenic activities on the marine productivity.

1.6 Outline of the thesis

The thesis is divided into six chapters, as detailed:

Chapter 1

This chapter gives a brief introduction to the role of the northern Indian Ocean in the global nitrogen and carbon cycles. This further discusses biogeochemical processes controlling these cycles. The chapter briefly touches on the main findings of the earlier studies on this subject in this region. Important findings and scientific questions addressed are presented at the end of this chapter, followed by a chapter-wise summary.

Chapter 2

This chapter gives a brief description of the $^{15}N_2$ and ^{13}C tracer techniques. The chapter also contains the detailed information of the study area, seasons and durations of sampling, and the experimental procedures. Measurement techniques of

δ^{18}O and salinity are also discussed. Calculations of deposition and riverine fluxes from the nitrogen concentration data are presented. Analytical uncertainties are also discussed.

Chapter 3

This chapter presents results of N_2 fixation and primary productivity from the northern Indian Ocean and the Wadden sea. Revised nitrogen fluxes are also presented in the later part of the chapter.

Chapter 4

Rayleigh isotope fraction is revised in this chapter. Nitrogen loss in the ocean is simulated. δ^{18}O-salinity relation is also discussed in this chapter.

Chapter 5

This chapter presents aerosol and riverine nitrogen fluxes and discusses their contribution into the new productivity in the northern Indian Ocean.

Chapter 6

This chapter summarizes the results obtained from the present study and suggests scope for future work.

1.7 Major questions addressed in the present study

The present study has attempted to answer the following scientific problems

1. Is nitrogen cycle in balance in the Arabian Sea?

2. Does N_2 fixation occur in sediments, if yes then how much? Is it significant?

3. Can we quantify theoretically the amount of external nitrogen inputs to the denitrification zones of the Arabian Sea?

4. Could the above theory also explain the observed variation in δ^{18}O-salinity relation in the northern Indian Ocean?

5. Does nitrogen through aerosol deposition significantly contribute to new production in the northern Indian Ocean?
6. How much nitrogen reaches the Arabian Sea and Bay of Bengal through the rivers of the subcontinent? Is this contribution significant to cause additional new productivity?

Chapter 2

Materials and Methods

Methodology used is discussed in three major sections. In the first section, the methodology to measure N_2 fixation rates and primary productivity is discussed. Second section discusses oxygen isotopic composition ($\delta^{18}O$) and salinity measurements of sea surface water samples while the third describes the estimation of aerosol deposition and riverine nutrient fluxes to the ocean.

2.1 Estimation of N_2 fixation rates and primary productivity in the ocean

The C_2H_2 reduction method [e.g., *Capone*, 1993] was widely used in the earlier estimates of N_2 fixation. This method is indirect and based on the number of molecules of C_2H_2 reduced relative to N_2 (C_2H_2:N_2 ~ 3); this ratio varies and introduces significant uncertainties in the estimates of N_2 fixation rate [*Mulholland et al.*, 2006]. Here we have used $^{15}N_2$ gas (99% enriched in ^{15}N) tracer in a direct technique so as to obtain more precise estimates [e.g., *Montoya et al.*, 1996].
A cruise for measuring the N_2 fixation rates and primary productivity estimations was undertaken in the eastern Arabian Sea during the spring intermonsoon. The protocol established by *Montoya et al.* [1996] was followed for the estimation of N_2 fixation rates using $^{15}N_2$ gas tracer technique. Total primary production was

estimated using the ^{13}C tracer following the procedure of *Slawyk et al.* [1977].

A field trip to the Janssand Flat in the Wadden Sea was organized to test the hypothesis of heterotrophic N_2 fixation in the sediments. A new protocol was set up following the method of *Montoya et al.* [1996].

Basic principle

The measurement of N_2 fixation rates relies on the determination of the uptake rate of the 'trace' ^{15}N-labelled nitrogen gas by phytoplankton during deck incubation. Primary productivity is measured as the rate of incorporation of the 'trace' ^{13}C-labelled $NaH^{13}CO_3$ by phytoplankton during such incubations.

Sampling Locations

Arabian Sea

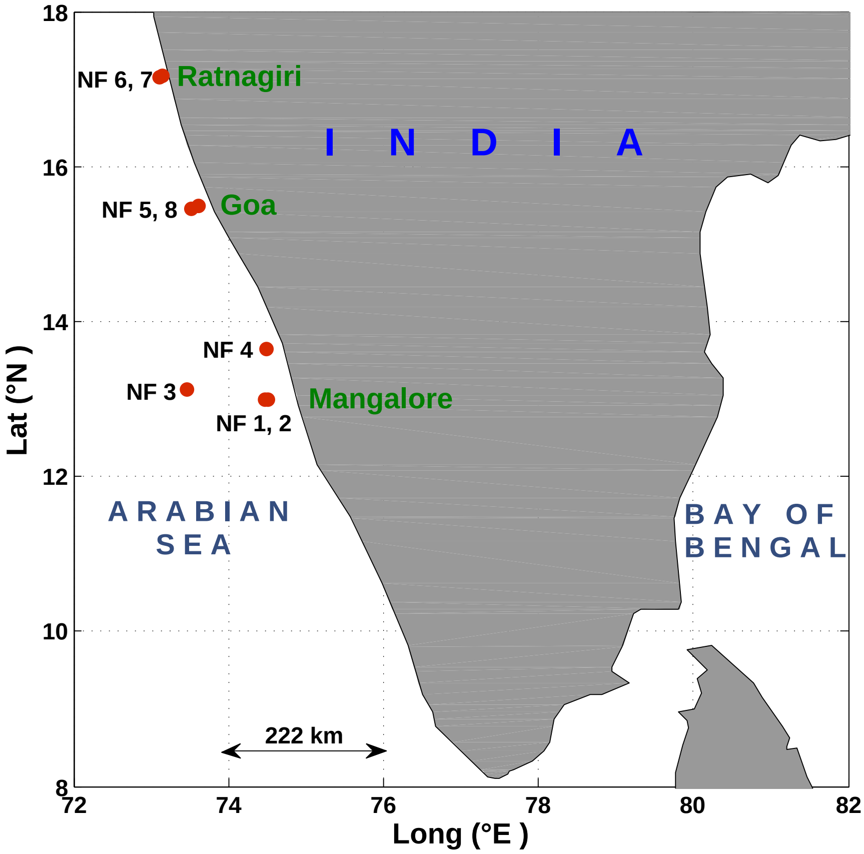

Figure 2.1: Sampling locations in the Arabian Sea during spring (April 2009)

The eastern Arabian Sea is known for the seasonal occurances of *Trichodesmium* blooms [*Devassy et al.*, 1978; *Parab et al.*, 2006; *Gandhi et al.*, 2010a]. The formation of blooms starts in the beginning of March, peaks in May and disappears due to the strong southwest monsoon winds in June. Sampling for the measurements of N_2 fixation and carbon uptake rates was carried out at seven different stations on board ORV *Sagar Kanya* (Cruise # SK 258) during the spring inter-monsoon (16th April to 1st May 2009, station locations shown in Figure 2.1) off Goa, Mangalore and Ratnagiri. Sampling was done wherever *Trichodesmium* bloom was sighted. Stations are named as NF1 to 8. NF3 was located more towards the open ocean than the other stations, no bloom was observed, and therefore N_2 fixation measurement was not carried out. We observed dense blooms at most of the stations during the present sampling period (Figure 2.2).

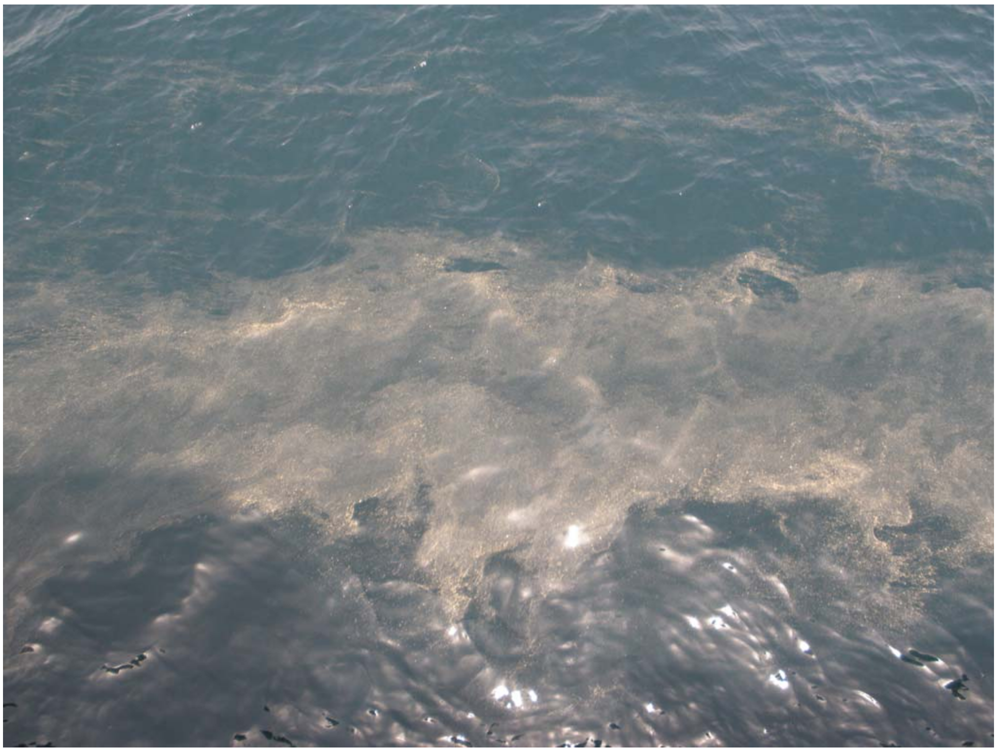

Figure 2.2: An example of *Trichodesmium* blooms observed during the sampling period

Wadden Sea

The study was conducted in a field campaign during 27 – 29^{th} October 2009 on the upper (central) part of the Janssand Flat (Figure 2.3). This area (~11 km^2) is known for semi-diurnal tides, and is covered by ~1.5 to 2 m of water during high tide, becoming exposed to air for about 6 to 7 hrs. during the low tide.

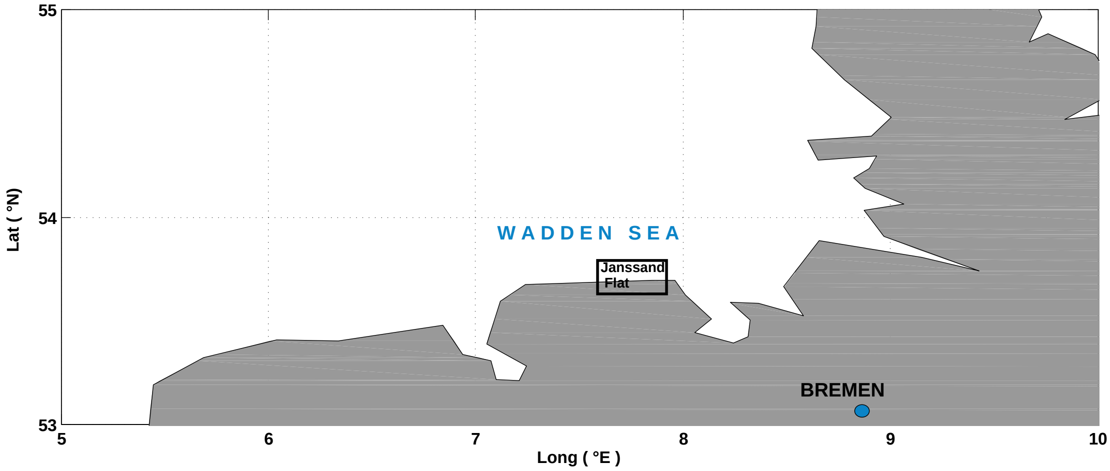

Figure 2.3: Sampling locations in the Janssand Flat

Sampling Strategy

In the Arabian Sea, water samples were collected using a CTD rosette fitted with Niskin/Go-Flo bottles to avoid trace metal contamination. Samples for primary productivity measurements (using ^{13}C tracer) were collected from six different depths to cover the euphotic zone, to the depth of 1% light level of the measured surface photosynthetically active radiation (PAR) in the wavelength band 400-700 nm. These depths correspond to 100, 80, 64, 20, 5 and 1% of the surface irradiance, which is measured using a hyperspectral underwater radiometer (Satlantic Inc.) at each location. The radiometer was operated at each sampling location prior to the sample collection. For N_2 fixation measurements, water samples were collected at four different depths, corresponding to the surface, 5 m, 10 m and 15 m, as *Trichodesmium* is known to be restricted to the surface layers due to its positive buoyancy [*Capone et al.*, 1997; *Capone et al.*, 1998; *Shiozaki et al.*, 2010].

Figure 2.4: CTD sensors and rosette sampler (SeaBird 911 plus)

In the Wadden Sea, all the sediment samples were collected from the central part and surface water was collected from the lower Janssand Flat. The Janssand Flat is characterized by well sorted, fine quartz sands with a mean grain size of 176 μm. On the upper sand flat, permeability of the sediment surface layer permits advective pore water flows [*Huettel et al.*, 2003]. Samples were collected from the three different depths (0-5, 5-10 and 10-15 cm) in the sediments and surface water.

2.1.1 Tracer preparation

^{15}N-labelled Tracers

2 mL of $^{15}N_2$ gas (Cambridge Isotope Laboratories, Massachusetts, USA) was injected using a chromatographic gastight syringe (Hamilton, UK) into vacuum-tight bottles containing the seawater/sediment samples.

^{13}C-labelled Tracer

The ^{13}C-labelled (99 atom% enriched) $NaH^{13}CO_3$ in dry chemical form was procured from Cambridge Isotope Laboratories, Inc. (USA). The working solution of ~0.2 mol C L^{-1} was prepared. For this, 5 g of $NaH^{13}CO_3$ (molecular weight ~85 g) was added in a volumetric flask containing 300 mL of deionized Milli-Q water and mixed thoroughly to make a homogeneous solution. This was later transfered to a polycarbonate bottle (procured from Nalgene, USA) for further use.

2.1.2 Tracer addition

Arabian Sea

Once the samples were collected, the ^{13}C and ^{15}N labeled tracers containing 99 atom % ^{13}C and ^{15}N were added to the samples. 2 mL $^{15}N_2$ gas was added to individual samples in duplicates. For primary productivity estimations, 2 mL $NaH^{13}CO_3$ of 0.2 M concentration is added to each sample. Pre-cleaned ~1.25 L and 2 L polycarbonate bottles (Nalgene, USA) were used for N_2 fixation and primary productivity measurements, respectively, during the deck incubation. All the bottles were filled to overflow before being sealed with a leak-proof septum cap.

Wadden Sea

All N_2 fixation experiments were performed in combination with different ^{13}DIC (99% labelled) and ^{12}DIC (unlabelled glucose) compounds in four different treatments (a) $^{15}N_2$+^{13}C (b) $^{15}N_2$+^{13}C+Glucose (c) $^{15}N_2$+^{13}Glucose and (d) $^{15}N_2$+$^{13}CH_4$. ^{13}DIC was added to a final concentration of 0.42 mM in (a) and

(b) treatments. 42 μM final concentrations of unlabelled and labelled glucose are added to treatments (b) and (c), respectively. A gas-tight syringe (Hamilton, UK made) was used to inject 2 mL of $^{15}N_2$ into all the treatments. Samples from treatments (a)-(c) were taken into 120 mL serum bottles while treatment (d) in 60 mL. Background (natural) samples were also collected from all the sediment depths and surface water.

2.1.3 Incubation

In the Arabian Sea, after addition of the tracers, deck incubation was performed for 4 hrs as suggested by the JGOFS protocol [*UNESCO*, 1994]. To simulate the irradiance at the depths from which samples derived, well-calibrated neutral density filters were put on the sample bottles. The neutral density filters were calibrated using lux-meter in both dry and wet conditions. Subsequently sample bottles covered with neutral density filters were kept in a big plastic tub on the deck and seawater from a depth of 6 m was circulated to regulate the temperature during the incubation from 10:00 to 14:00 Hrs local time at each station.

In the Wadden Sea, the sample bottles were gently mixed and then incubated (6-11 hrs) in triplicates for light and dark separately.

2.1.4 Filtration and preservation

In the Arabian Sea, at the end of incubation, bottles were transferred to the shipboard laboratory and all samples were filtered sequentially through precombusted (4 hrs at 400 ℃) 25 mm diameter and 0.7μm pore size Whatmann GF/F filters. All samples were filtered in dim light under low vacuum (<70mm Hg) using a manifold filtration unit and vacuum pump (procured from Millipore, USA).

In the Wadden Sea, at the end of each experiment, the suspended particles in each bottle were collected by gentle vacuum filtration after ultrasonification for 5 min at low pressure on 25-mm precombusted (480 ℃ for 4 hrs) GF/F filter. The filters were stored in a freezer (-20 ℃). Samples were dried at 60 ℃ in the lab and decalcified for mass spectrometric analysis.

Separate glass cups were used for each tracer to avoid any cross contamination. After filtration, GF/F filters were rinsed using filtered sea-water. The filters were preserved in 47 mm petrislides (procured from Millipore, USA) with the help of clean forceps (separate forceps were used for different tracers). After this, filters were dried in an oven at 50 ℃ overnight and stored for further analysis on mass spectrometer. For the blank correction, the same concentrations of isotopically enriched tracers as in samples, were added to the individual blank samples. Immediately after the addition, the blank samples were filtered.

2.1.5 Mass spectrometric analysis

Figure 2.5: *Thermo Quest's Finnigan Delta plus IRMS at the University of Agricultural Sciences, Bengaluru, India*

To calculate the uptake rate of Nitrogen and Carbon, it is required to measure two parameters (a) total N (or C) content and (b) atom $\%^{15}$N (or $\%^{13}$C) in the post incubation samples. To measure these parameters on GF/F filter samples, Thermo

Quest's Finnigan Delta plus continuous flow Isotope Ratio Mass Spectrometer (IRMS) at the National Facility, University of Agricultural Sciences, Bengaluru, India (Figure 2.5) was used. All mass spectrometric measurements were made by the author. The peripherals attached with the mass spectrometer were Elemental Analyzer (Flash EA 1112 Series, CE Instruments, Italy) and ConFlo III. The instrument and its working principle are discussed below.

Elemental Analyzer (EA)

Elemental analyzer uses the Dumas combustion method for high temperature flash combustion. It consists of two reactors (an oxidation column and a reduction column), water absorber column and Gas Chromatograph (GC). Both the oxidation and reduction columns are made of quartz (melting point ∼1800 ℃) tubes, which are 45 cm in length, with 18 mm outer diameter, and 14 mm inner diameter. Combustion column was prepared by filling quartz tube with chromium oxide (layer thickness ∼10 cm) and silvered cobaltous oxide (layer thickness ∼5 cm), separated (layer thickness ∼1 cm) and bracketed by quartz wool (layer thickness ∼5 cm). Reduction column was prepared by filling quartz tube with reduced copper (layer thickness ∼12 cm) with quartz wool at the top and bottom (∼5 cm). The chemicals required for combustion and reduction columns were procured from IVA Analysentechnik e.K., Meerbusch, Germany. Water absorber column, 10 cm in length, with 5 mm inner diameter, was filled with magnesium perchlorate anhydrous granulate. A molecular sieve made up of zeolite was used in the GC, 100 cm in length, with 4 mm outer diameter, and 1.6 mm inner diameter.

Con-Flo III

Con-Flo III is a device coupling EA and IRMS. It works with an open-split arrangement whereby a gas flow of ∼80-100 mL min^{-1} coming from EA is reduced to ∼0.3 mL min^{-1}, the rate at which gas is introduced into the IRMS. Con-Flo III contains two open split cells: one 'sample section' and the other 'reference section', which split the gases coming from EA and the reference gas cylinder, respectively.

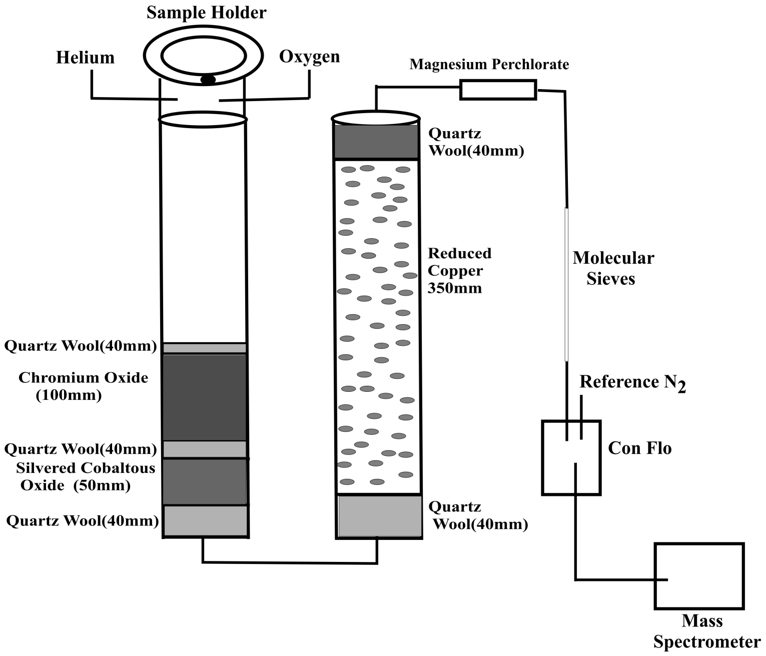

Figure 2.6: Schematic diagram of Elemental Analyzer interfaced with IRMS

Mass Spectrometer

Thermo Quest's Finnigan Delta plus continuous IRMS is a gas source mass spectrometer. In the source, ions are generated by electron (80 eV) impact in high vacuum, and are accelerated by a ∼3 keV potential difference. The accelerated ion beam exits the ion source through a slit (width 0.3 mm), and enters the magnetic sector of field strength 0.75 Tesla. The direction of the uniform magnetic field is perpendicular to the direction of the moving ions. The geometry of the magnetic sector is such that the ion beam enters and exits the magnetic sector at an angle of 26.5°. This is done in order to maintain the radius of flight to be 9 cm. The collector consists of three Faraday cups connected to amplifiers. The elemental analyzer and mass spectrometer are fully automated and are controlled by the Finnigan MAT software ISODAT.

Another mass spectrometer with a similar configuration (installed at Max Plank Institute for Marine Microbiology, Germany of the same company) was used for N_2 fixation measurements in sediments.

Measurement procedure

A quarter of each of the GF/F filter samples was packed into a pellet using a clean silver foil. The rest was preserved for replicate analysis. Samples were then loaded on a turret (sample holder had the capacity of 62 samples) kept on the top of the oxidation chamber. Typically, 62 samples (56 GF/F filter samples and 6 standards) were analyzed in a single run. Standards were kept at 1^{st}, 17^{th}, 32^{th}, 47^{th}, 48^{th} and 62^{th} positions. An automated mechanism allowed the samples to fall one by one into the oxidation chamber. The temperature of the oxidation chamber was maintained at 1100 ℃ with the help of an electric furnace. As soon as a sample fell, a one-second pulse of oxygen was given at a flow rate of 175 mL s^{-1}. When temperature inside the column increased to 1800 ℃ for a moment, an oxygen pulse lead to combustion of the sample with a flash. A constant flow of pure He gas (grade 5,99.999%, procured from *Hydragas*, Bengaluru) was maintained. Cumbustion of the sample produced oxides of C, N and H mainly in the presence of oxygen and oxidising egents (chromium oxide and silvered cobaltous oxide). Therefore, the main gases coming out of the column were CO_2, NO_x and H_2O. These gases were carried by Helium to the reduction column, which contained reduced copper at 680 ℃. Here different oxides of nitrogen were reduced to N_2 gas. CO_2 remained in its oxidized form because of the high affinity of carbon for oxygen. Gases coming out of the column, mainly N_2, CO_2 and H_2O, were passed through the magnesium perchlorate column, which absorbed moisture. The remaining gases were then carried to GC column (maintained at 60 ℃). The gas mixture passed at different rates through the GC column, depending on their various chemical and physical properties and their interaction with the molecular sieve. The function of the molecular sieve was to separate different gases. The retention time for N_2 was less than that for CO_2, as a result of which N_2 moved faster than CO_2 and came out earlier from the chromatographic column. Once the N_2 or CO_2 exited the column, it was injected into the mass spectrometer through the Con-Flo III.

A method of instructing the timing of different events (i.e., on and off times of reference gas, on and off times of elemental analyser and He dilution) was followed. The total data acquisition time for each sample was 450 sec.

For nitrogen measurements, the amplitudes of 28, 29 and 30 mass peaks and their ratios (29/28 and 30/28) were recorded, while for carbon measurements, the amplitudes of 44, 45 and 46 mass peaks and their ratios (45/44 and 46/44) were monitored. Area under the different mass peaks were proportional to the amounts of nitrogen (or carbon) present in the sample. The ratios were measured as atom $\%^{15}$N (or $\%^{13}$C). Standards (Table 2.1) were loaded in varying amounts, ranged from 0.02 to 0.1 mg N (or 0.1 to 0.5 mg C) to calibrate the mass spectrometer for estimating PON (or POC).

Typically, the combustion and reduction columns were changed after ~300 samples, followed by degassing of the system overnight. After checking for leak in the connections, background levels were measured. After this, the internal precision of the mass spectrometer was checked by 'zero enrichment or Standard ON/OFF' method in which a reference N_2 or CO_2 gas was injected repeatedly and its δ^{15}N or δ^{13}C was measured. The reference gas injections gave an internal precision better than 0.1‰. This was followed by δ^{15}N or δ^{13}C measurements of external standards.

Table 2.1: Atom % and its precision for standard materials used (* 1σ standard deviation).

Standard	Quoted atom % ^{15}N (or ^{13}C)	Measured % ^{15}N (or ^{13}C)
Nitrogen		
$(NH_4)_2SO_4$ (IAEA-N-2)	0.373883	0.375116 ± 0.00066*(n=21)
KNO_3 (IAEA-N-3)	0.368188	0.367129 ± 0.00163* (n=17)
KNO_3 (USGS-32)	0.432152	0.432442 ± 0.00244* (n=15)
Carbon		
Starch	1.081719	1.067496 ± 0.00096* (n=73)

For nitrogen, calibrated in-house casein and international standards $(NH_4)_2SO_4$ (IAEA-N-2) and KNO_3 (IAEA-NO-3) were used for checking the external precision. While for carbon, calibrated in-house starch and international standard ANU sucrose were used. The external precisions of the measurements were consistently better than 0.5‰. Error associated with the estimation of amount of nitrogen or carbon present in the sample was less than 10%. While the error was less than 1% in estimating atom $\%^{15}$N and $\%^{13}$C.

The laboratory standards with their quoted and measured isotopic compositions, with the precision obtained during the present study are as listed in Table 2.1. Some examples of calibration plots, which were constructed to estimate the amount of nitrogen and carbon in the sample filters are shown in Figure 2.7. The mass spectrometer showed good stability during both the carbon and nitrogen measurements.

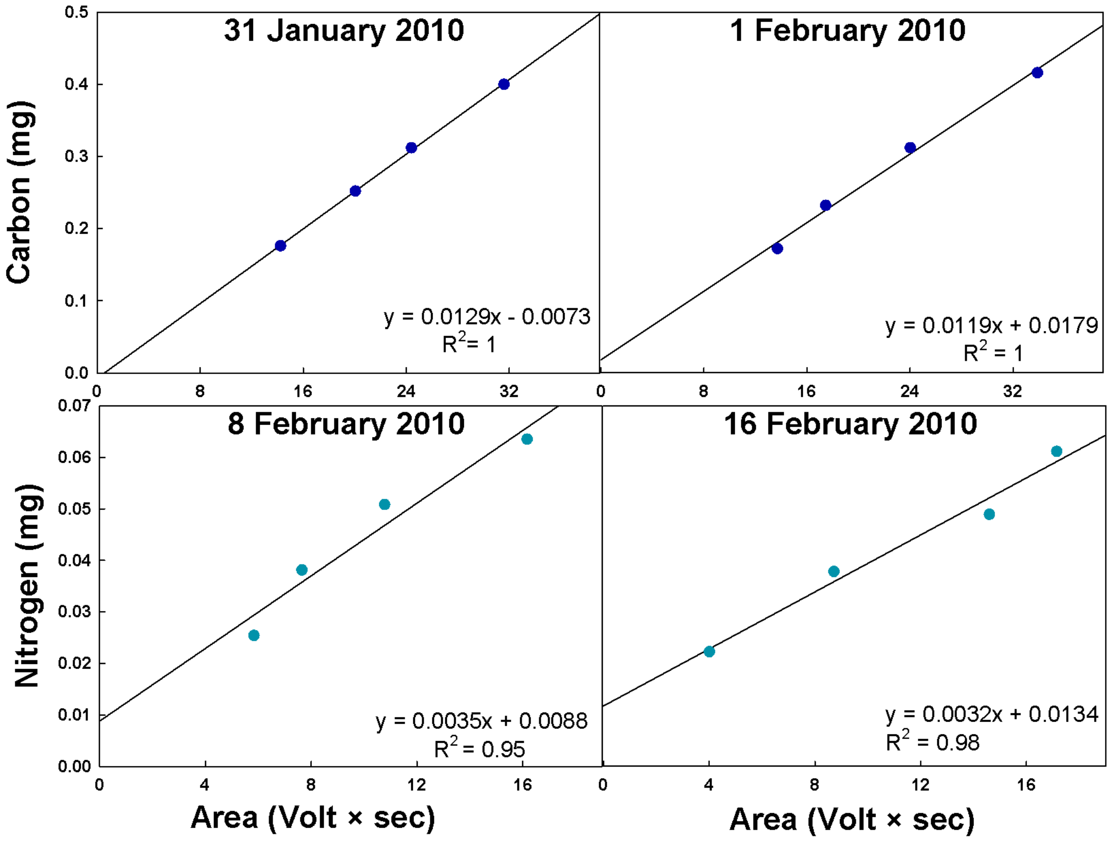

Figure 2.7: Examples of calibration plots for estimating the amount of nitrogen (or carbon) present in the sample filters

2.1.6 Nutrient measurements

An automated segmented flow analyzer was used to measure dissolved inorganic nutrients such as NO_3, NO_2, PO_4 and SiO_4 in sea water samples during all the cruises. 100 mL of sea water sample was separately collected for nutrient measurements from all the six depths at each sampling location. Standard techniques (*UNESCO*, 1994) for nutrient analysis in sea water were followed. Detection limits for NO_3, NO_2, PO_4, and SiO_4 were 0.1 μM, 0.02 μM, 0.01 μM, and 0.1 μM, respectively. Error in the nutrient measurements is less than 1 % for the concentrations >1 μM, while it reaches as high as 5 % for very low ambient values. Ambient NH_4 and urea could not be measured because of logistic reasons.

2.1.7 Experimental precautions

Precautions to avoid contamination during measurements are of utmost importance. Good quality polycarbonate bottles were filled directly from the Go-Flo/Niskin bottles, to avoid any trace metal contamination. Carboys were not used to store water samples. Bottles were thoroughly rinsed (atleast once) with the sample seawater before collection. Samples were covered with thick black cloth after the collection. New pipette tips were used for each tracer addition to bottles. The samples were kept in the dark before incubation; they were not exposed suddenly to light when taking out for incubation, to avoid possible light shock to phytoplankton. Filtration was also done in a near-dark environment. During the filtration, only the sample to be filtered was taken out and rest were kept in the ark. Different filtration cups and forceps were used for different tracers and for samples which monitored natural atom % ^{15}N and % ^{13}C. These cups were thoroughly rinsed with filtered seawater. GF/F filters were handled using clean and separate forceps for each tracer. Once the filtration was over, the polycarbonate bottles were cleaned with 5% HCl and three times with Milli-Q water before reaching the next sampling location. For the mass spectrometric analysis samples were packed in clean silver foils. Blanks of cleaned silver foils were found insignificant, as found by testing them in the mass spectrometer during every batch.

2.1.8 Uptake rate calculations

Nitrogen fixation

The concept of N_2 fixation equation is based on the isotopic mass balance at the end of the incubation. The number of ^{15}N atoms in final particulate nitrogen is equal to the sum of number of ^{15}N in the initial particulate nitrogen and number of ^{15}N atoms in the nitrogen taken up [*Montoya et al.*, 1996]. Nitrogen Specific uptake rate

$$V = \frac{(A_{PN_f} - A_{PN_0})}{(A_{N_2} - A_{PN_0}) \times T} \tag{2.1}$$

Volumetric rate of N_2 fixation

$$\rho = V \times [PN_f] \tag{2.2}$$

where,

A_{PN_f} = ^{15}N abundance of PON at the end of experiment,

A_{PN_0} = ^{15}N abundance of PON at the start of experiment,

A_{N_2} = ^{15}N abundance of N_2 available for fixation,

$[PN]_f$ = concentration of PON at the end of the experiment,

t = time of incubation (4 hrs for water and 6-11 hrs for sediment samples)

and A_{N_2} is defined as

$$A_{N_2} = \frac{^{15}N_{tracer} \times tracer\ conc + ^{15}N_{Natural} \times natural\ conc}{tracer\ conc + natural\ conc} \tag{2.3}$$

The following assumptions are made. During incubation,

(i) there exists only a single nitrogen source for ingestion by phytoplankton.

(ii) there is no excretion of nitrogen by phytoplankton.

(iii) Isotopic discrimination is negligible.

(iv) Atom % ^{15}N in the dissolved phase remains constant,

Equation (2.2) provides the most accurate estimate of uptake rate as a consequence of (ii) and (iii).

Carbon uptake rate

Similar to specific uptake rate of nitrogen, specific uptake rate of carbon can be calculated using the following relation:

$$V_C = \frac{^{13}C_{xs}}{(^{13}C_{enr} - ^{13}C_{natural}) \times T} \tag{2.4}$$

where ^{13}C$_{xs}$ is the excess atom % ^{13}C relative to the natural abundance of atom % ^{13}C in the particulate form, ^{13}C$_{enr}$ is the atom % ^{13}C in the initially labeled fraction in the dissolved form, ^{13}C$_{natural}$ is the abundance of (atom %) ^{13}C in the natural unlabeled fraction in the dissolved form, and T is the duration of incubation.

Also, carbon uptake rate in concentration units (mmol C m^{-3}d^{-1}) is calculated by multiplying the specific uptake rate and POC$_t$ particulate organic carbon (POC) at the end of incubation.

$$\rho_C = V_C \times POC_t \tag{2.5}$$

Depth integrated uptake rates (in the unit of mmol C m^{-2}d^{-1}) are calculated by trapezoidal integration. As in the case of nitrogen measurements, error in atom % ^{13}C measurements introduces <1 % error in the estimation of ρ_C and V$_C$. Usually the error in the dissolved inorganic carbon measurement is low (<1 %), which affects the $^{13}C_{enr}$ used in the denominator of the equation (2.4). Error in POC estimation is generally found to be <10 %, which only affects estimation of ρ_C. In general, error in the estimation of ρ_C and V$_C$ is found less than <10 % and <1 %, respectively.

Error analysis

Possible errors in the factors involved in the estimation of N_2 fixation estimation could be [*Montoya et al.*, 1996] -

1. Incubation time - $\pm(3-4\%)$
2. Isotopic composition of PON (A_{PN_0} and A_{PN_f}) - $\pm(0.2\%)$
3. A_{N_2} - $\pm 3\%$
4. PON concentration - $\pm 4\%$.

Hence, the maximum error in volumetric rate could be $\pm 6\%$.

2.1.9 Chlorophyll *a* measurements

1 L of water sample from each depth at each sampling location was collected for chlorophyll *a* measurement and filtered on 47 mm GF/F 0.7 μm pore size filters under low vacuum. Chlorophyll *a* was then extracted using 10 mL of 90% acetone (AR grade) and was measured using Turner Design fluorometer.

2.2 Methods to measure δ^{18}O of sea water samples

Surface and deeper water samples were collected during eight different cruises. Sampling stations were chosen to capture the typical pattern of spatial variation of δ^{18}O and salinity. All the samples were stored in tightly capped plastic bottles to prevent evaporation, and analyzed within one month of collection. The deviation in parts per mil of the sample ^{18}O/^{18}O ratio from that of standard Vienna Standard Mean Oceanic Water (VSMOW) is defined as

$$\delta^{18}O_{VSMOW}^{sample} = \left(\frac{R_{sample}}{R_{VSMOW}} - 1\right) \times 1000‰ \tag{2.6}$$

R is the ratio of the abundances of the heavier to lighter isotopic water molecules ($H_2^{18}O/H_2^{16}O$).

Surface water samples were collected from the Bay of Bengal during (i) August-

September 1988 (*Gaveshani* G-200) (ii) March-April 1991 (ORV *Sagar Kanya* SK-63) (iii) December 1991 (SK-70) (iv) September-October 2002 (SK-182) and (v) April-May 2003 (SK-191). Sample locations were roughly the same for SK-182 and SK-191. From the Arabian Sea, samples were collected during (i) December 1987 (SK-37) (ii) December 1988 (SK-47) and (iii) March 2009 (FORV *Sagar Sampada* SS-263) (Figure 2.8).

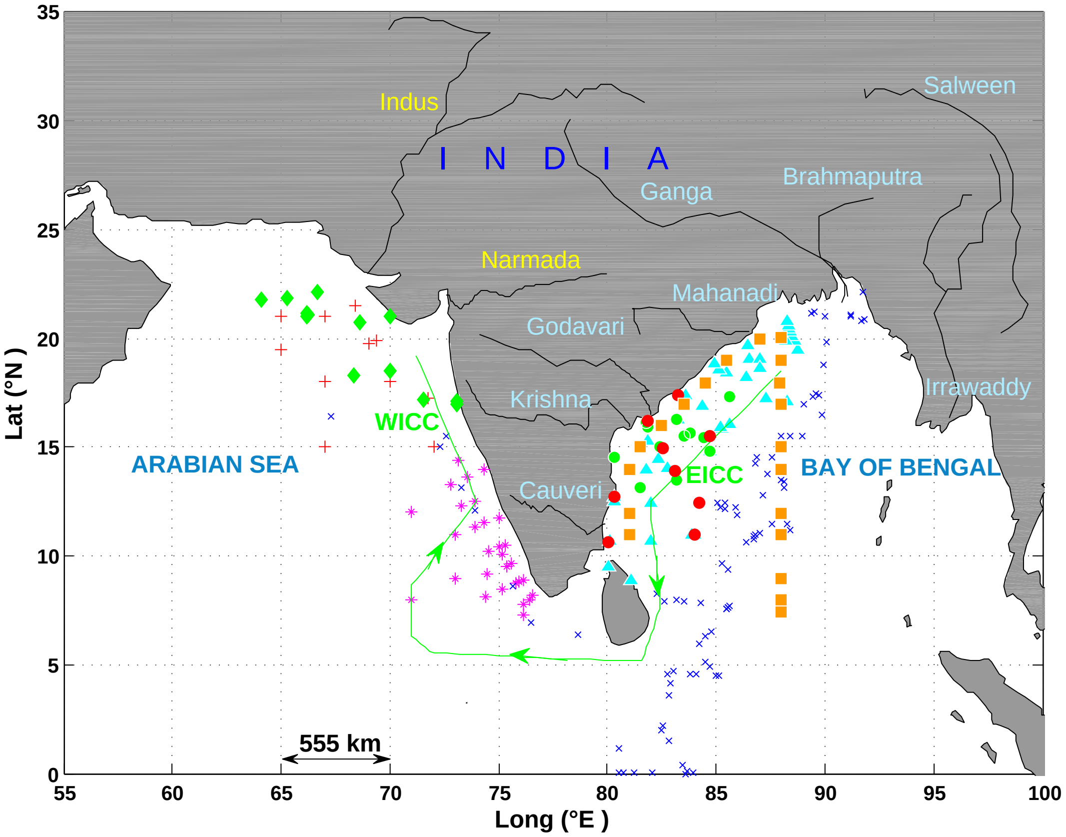

Figure 2.8: Sample locations in the northern Indian Ocean. Major rivers draining into the ocean are also shown. Legend: SK-37* (December 1987), G-200● (August-September 1988), SK-47+ (December 1988), SK-63▲ (March-April 1991), SK-70● (December 1991), SK-182■ (September-October 2002), SK-191■ (April-May 2003) and SS-263◆ (March 2009). × indicates the study area of *Delaygue et al.* [2001]. The same symbols are used for SK-182 and SK-191, as the locations were similar. The East India Coastal Current (EICC) and West India Coastal Current (WICC) of the peninsula are shown. Arrows depict direction of flow during winter. The direction reverses in summer [*Schott and McCreary*, 2001]

2.2.1 The CO_2 equilibration method

Measurement of the oxygen isotope composition in the water sample can be done by three different methods [*Gonfiantini*, 1981; *Brand et al.*, 1996]. In the first method, CO_2 gas (from any reference reservoir) is allowed to exchange oxygen isotopes with the water sample at constant temperature. This is known as the equilibration method. In the second method, oxygen of the water is extracted by reduction and converted into CO_2. The carbon dioxide is then introduced in the mass spectrometer. In the third method water vapour are directly let into the mass spectrometer. For practical reasons the equilibration method is simpler to follow in the automated machines.

In the present study, the CO_2 equilibration method [*Gonfiantini*, 1981] was followed. Equilibration was carried out on WES (Water Equilibration System) attached with the GEO 20-20 mass spectrometer. The operation of the of the WES is fully automated, controlled by software. A schematic diagram of the WES is shown in the Figures 2.9 and 2.10. Water sample (each 1mL) is filled in a 6.8 mL standard glass bottle. A threaded cap having a neoprene septum seals the bottle preventing any leakage. About 51 such bottles filled with water samples are kept in sequence in a rack. A secondary laboratory reference NARM (taken from the river Narmada) was also filled in similar glass bottles and one each placed after a batch of 10 samples. The measurement of oxygen isotopes was carried out in three steps.

Flushing of the air

A sharp needle with double holes (shown in the Figure 2.9 and 2.10) which can move up and down into the sample bottle, pierces the neoprene septum from the top of the cap so that both holes are inside the bottle. Carbon dioxide from a cylinder (obtained from Vadilal Gas Company and labeled as $VDCO_2$) is let into the sample bottle by opening the V-1. For 1 min duration the cylinder CO_2 flushes the air through a vent. After this, only pure CO_2 remains inside the sample bottles.

During flushing some water vapour may also be flushed out. But, this amount is too small to fractionate the sample significantly, and it is uniform for all samples and standards.

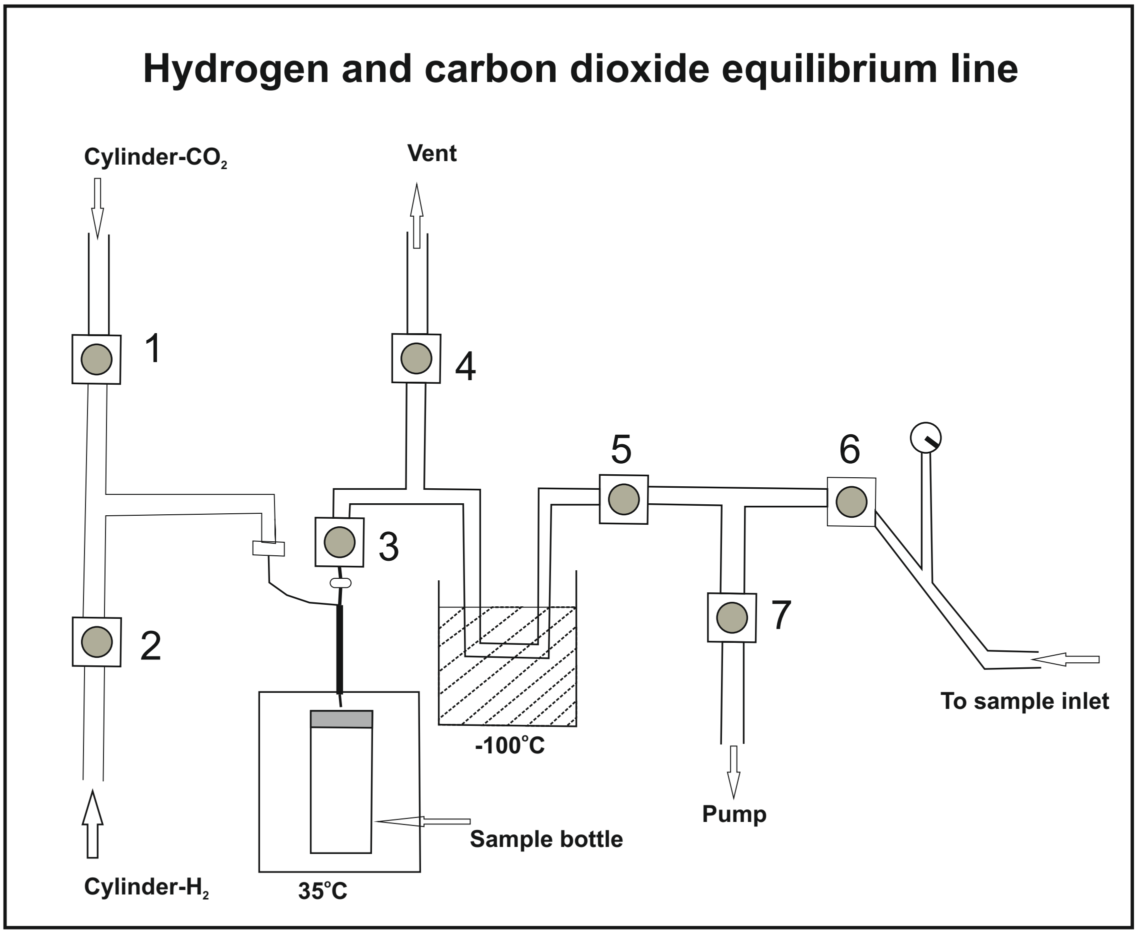

Figure 2.9: WES System: Hydrogen and carbon dioxide equilibration line of the GEO 20-20 mass spectrometer

CO_2 equilibration

The needle moves up and the holes in the neoprene septum get immediately closed because of its elastic nature. The carbon dioxide and water are left ∼8 hrs in the fully sealed and isolated condition for complete equilibration to occur. The rack carrying all the sample glass bottles is kept at 35 ℃ to enhance the isotopic exchange and to reduce the time taken for equilibration.

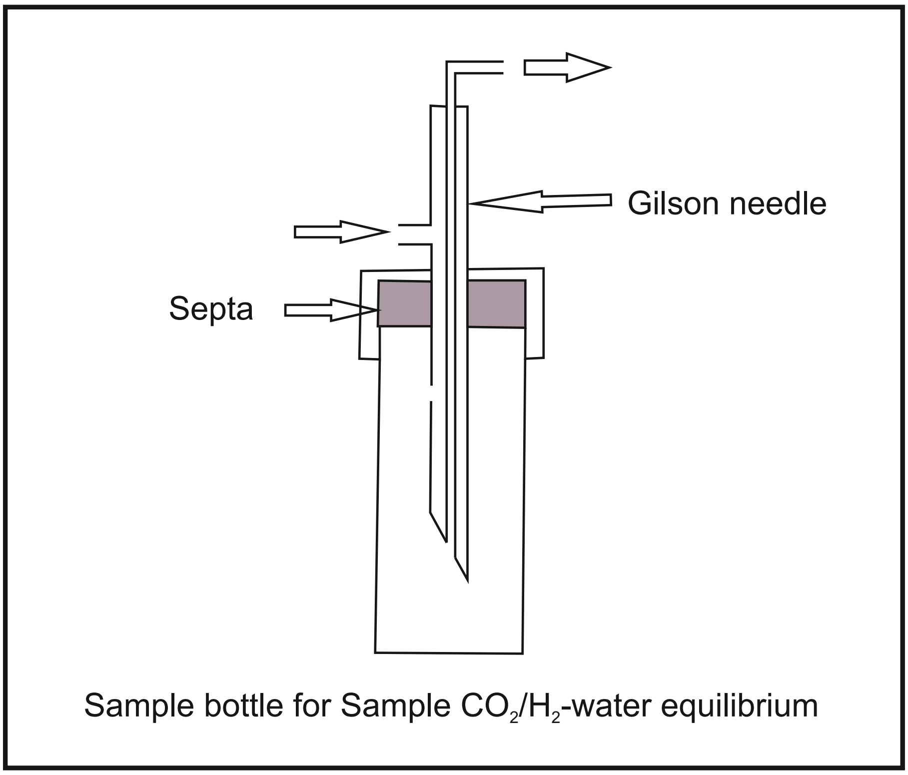

Figure 2.10: WES System: Sample bottle and Gilson needle

Isotopic exchange takes place due to the following reactions:

$$CO_2(g) \longleftrightarrow CO_2(aq) \tag{2.7}$$

$$CO_2(aq) + H_2O \longleftrightarrow HCO_3^- + H^+ \tag{2.8}$$

The isotopic exchange reaction is written as

$$C^{16}O_2 + H_2^{18}O \longleftrightarrow C^{16}O^{18}O + H_2^{16}O \tag{2.9}$$

After some time (e.g. 8 hrs at 35^0C in the present case) the reaction reaches equilibrium condition and the ratios ($^{18}O/^{16}O$) in the water and carbon dioxide is related by a temperature dependent fractionation factor α:

$$(^{18}O/^{16}O)_{CO_2} = \alpha(^{18}O/^{16}O)_{H_2O} \tag{2.10}$$

$$1000 + \delta^{18}O_{CO_2} = (1000 + \delta^{18}O_{H_2O})\alpha \qquad (2.11)$$

Value of α at 35^oC is 1.0393 [*Criss*, 1999].

Mass spectrometer inlet system in the GEO 20-20

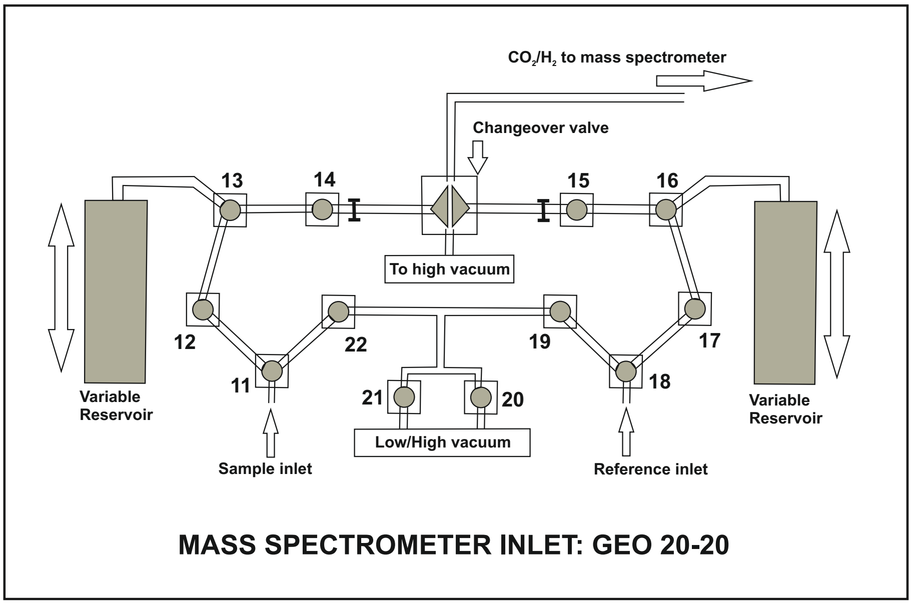

Figure 2.11: Inlet part of GEO $20 - 20$ mass spectrometer

A schematic diagram of inlet system of the GEO 20-20 mass spectrometer is shown in the Figure 2.11 (GEO 20-20 User's Manual 1999). The sample CO_2 is introduced through inlet near V-11, while V-22 and 14 are kept closed. The CO_2 is allowed to equilibrate for 1 min. duration after which V-12 is closed and V-14 was opened which allows the CO_2 to enter into the mass spectrometer. Reference CO_2 gas is taken in the reference reservoir through the inlet near V-18 . The procedures are exactly similar to those followed in the sample side. Through the change-over valve system, CO_2 either from the sample or reference side periodically enters into the mass spectrometer while the other is continuously being pumped and goes to waste. The variable volume reservoir was adjusted to provide major current (associated with mass 44) to be between 10 to 12 nA.

δ^{18}O measurement

The equilibrated CO_2 is passed through a moisture trap at -100 ℃ (before V-4) whereby all the water vapour is trapped and the pure CO_2 is passed into the sample reservoir of the mass spectrometer. The reference reservoir is filled with $VDCO_2$ gas. Inside the mass spectrometer the sample CO_2 is positively ionized by a heated electron source (generally thoriated tungsten or rhenium filament). By applying appropriate electric field the ions were collimated and are exposed to constant magnetic field in the perpendicular direction where they follow a circular orbit, the radius of which depends upon the mass of the singly charged ions.
In a triple collector type mass spectrometer simultaneous measurement of δ^{18}O and δ^{13}C is carried out in the same focussing condition. The ion beams corresponding to species 44, 45 and 46 are collected separately in three different collectors. The current ratios δ_{45} and δ_{46} are estimated by using appropriate electronic circuits. Here,

$$\delta_{45} = \left[(I_{45}/I_{44})_{sam} \,/\, (I_{45}/I_{44})_{ref} - 1 \right] \times 10^3 \tag{2.12}$$

$$\delta_{46} = \left[(I_{46}/I_{44})_{sam} \,/\, (I_{46}/I_{44})_{ref} - 1 \right] \times 10^3 \tag{2.13}$$

where, I_{44}, I_{45} and I_{46} are currents at the three collector due to ionic species $44, 45$ and 46 respectively. The current ratios were converted into the isotopic values δ^{13}C and δ^{18}O by applying following Craig corrections [*Craig*, 1957].

$$\delta^{13}C = 1.067675\delta_{45} - 0.033836\delta_{46} \tag{2.14}$$

$$\delta^{18}O = -0.00224\delta_{45} + 1.00107\delta_{46} \tag{2.15}$$

The flushing and measurements were carried out in automatic mode. The $\delta^{18}O^0_{CO_2}$ which is the oxygen isotope composition of the CO_2 gas equilibrated to the water sample assuming that the amount of water is infinite and hence it doesn't change the original isotope signature of water during equilibration is given [*Craig*, 1957; *Gonfiantini*, 1981] as:

$$\delta^{18}O^{0}_{CO_2} = (1 + \alpha(n/N))\delta^{18}O_{CO_2} - \alpha(n/N)\delta^{18}O^{i}_{CO_2} \tag{2.16}$$

where,

$\delta^{18}O_{CO_2}$ = oxygen isotope composition of the equilibrated CO_2

$\delta^{18}O^{i}_{CO_2}$ = initial oxygen isotope composition before equilibration, which is 0‰ as the same gas ($VDCO_2$) has been used as reference gas.

N = gram-atoms of oxygen present in the water sample and n in CO_2.

As the amount of oxygen in the CO_2 gas (5.8 mL at 1 atm pressure) in the 6.8 mL glass bottle is insignificant compared to that in the water phase (1 mL), hence, $\frac{n}{N} \approx 0$, this means that for practical purposes $\delta^{18}O^{0}_{CO_2}$ and $\delta^{18}O_{CO_2}$ are same and oxygen isotope composition of the water ($\delta^{18}O_w$) sample can be obtained with the help the of following expression -

$$(^{18}O/^{16}O)_{CO_2} = \alpha(^{18}O/^{16}O)_{H_2O}$$

During measurements NARM water, which is a secondary laboratory standard, is placed after each batch of 10 samples and is also equilibrated with the same CO_2 ($VDCO_2$). If the CO_2 measurements for NARM are represented as $\delta^{18}O_{NARM-VDCO_2}$ and for the sample as $\delta^{18}O_{SAM-VDCO_2}$ then oxygen isotope composition of the water sample relative to NARM water i.e. $\delta^{18}O_{SAM-NARM}$:

$$1000 + \delta^{18}O_{SAM-NARM} = \frac{1000 + \delta^{18}O_{SAM-VDCO_2}}{1000 + \delta^{18}O_{NARM-VDCO_2}} \tag{2.17}$$

As the temperature of equilibration for the water samples as well as the NARM standard is same (35 ℃), the value of α is same in both the cases and is cancelled out in the above expression.

Values with respect to VSMOW standard is given as:

$$\begin{aligned}\delta^{18}O_{SAM-VSMOW} &= \delta^{18}O_{SAM-NARM} + \delta^{18}O_{NARM-VSMOW} \\ &\quad + \delta^{18}O_{SAM-NARM} \times \delta^{18}O_{NARM-VSMOW} \times 10^{-3} \quad (2.18)\end{aligned}$$

Results of analysis on the NARM water and the associated precision are given in the Table 2.2. Routine measurements of δ^{18}O at the Physical Research Laboratory by the CO_2 equilibration method [*Epstein and Mayeda*, 1953; *Gonfiantini*, 1981], yield a long-term (over two decades) overall precision better than ±0.13 (1σ). The precision and accuracy of the measurements were routinely monitored by using an internal water standard (called NARM with a δ^{18}O of -4.4 ‰ relative to VSMOW, see *Yadava and Ramesh*, [1999]) along with samples in each batch, and frequent calibration with VSMOW. Salt correction to δ^{18}O values was found unnecessary, as the molalities of Mg, Ca and K were less than the values that call for significant correction [*Gonfiantini*, 1981].

Table 2.2: δ^{18}O values of lab standards

Sample Code	$\delta^{45}CO_2$ wrt WG*	$\delta^{46}CO_2$ wrt WG*	δ^{13}C Cr. Corr.•	δ^{18}O Cr. Corr.•
Std Run 2	13.07	16.31	13.41	16.30
Std Run 3	14.90	16.15	15.38	16.14
Std Run 21	14.92	16.25	15.39	16.24
Std Run 31	14.98	16.35	15.45	16.34
Std Run 41	14.94	16.20	15.42	16.19
Std Run 51	14.97	16.51	15.45	16.50
Std Run 59	15.02	16.45	15.49	16.44
			Average $(\delta^{18}O_{LS}^{NARM})$	16.30
			Average $(\delta^{18}O_{NARM}^{LS})$	-16.04
			σ	0.13
			Average $(\delta^{18}O_{VSMOW}^{NARM})$	-4.52 ± 0.13

*Working Gas, •Craig Correction.

We also participated in the international inter-comparison exercise of IAEA, which distributed 8 water samples in 1999 and 2002. The IAEA consensus values and our values are in agreement within 2σ uncertainty (Table 2.3), indicating that systematic errors are unlikely as far as water samples with δ^{18}O values in the range 0 to -15‰ are concerned.

Table 2.3: Comparison of δ^{18}O values of water samples distributed by IAEA for international inter-comparison in 1999 and 2002. The values recommended by IAEA (consensus values) and those measured at our laboratory (PRL) are shown

Sample Code	δ^{18}O (PRL)	δ^{18}O (IAEA)
OH-1*	-0.23	-0.05
OH-2*	-3.34	-3.28
OH-3*	-8.68	-8.65
OH-4*	-15.36	-15.28
OH-5$^\bullet$	-0.29	-0.02
OH-6$^\bullet$	-4.16	-4.17
OH-7$^\bullet$	-10.69	-10.65
OH-8$^\bullet$	-16.21	-16.2

*1991, $^\bullet$2002.

2.2.2 Salinity measurement

Salinity is a measure of dissolved salts in sea water. Unit of salinity is psu (Practical Salinity Unit), which is same as permil (‰). Salinity measurements for all the ocean surface water samples were performed on board by Autosal with an external precision of 0.001. IAPSO (International Association for the Physical Sciences of the Ocean standard seawater) of salinity 34.995, conductivity 1.997435 and conductivity ratio (K15) 0.99987 was used to check the accuracy [*Srivastava et al.*, 2007].

2.3 Role of Aerosol deposition and riverrine fluxes to new production

Significant amount of data on nitrogen in aerosols and rivers along with productivity have been made available in the literature over the years (Figures 2.12 and 2.13). This published data are used in the present study for assessing the role of atmospheric and river fluxes to the oceanic productivity.

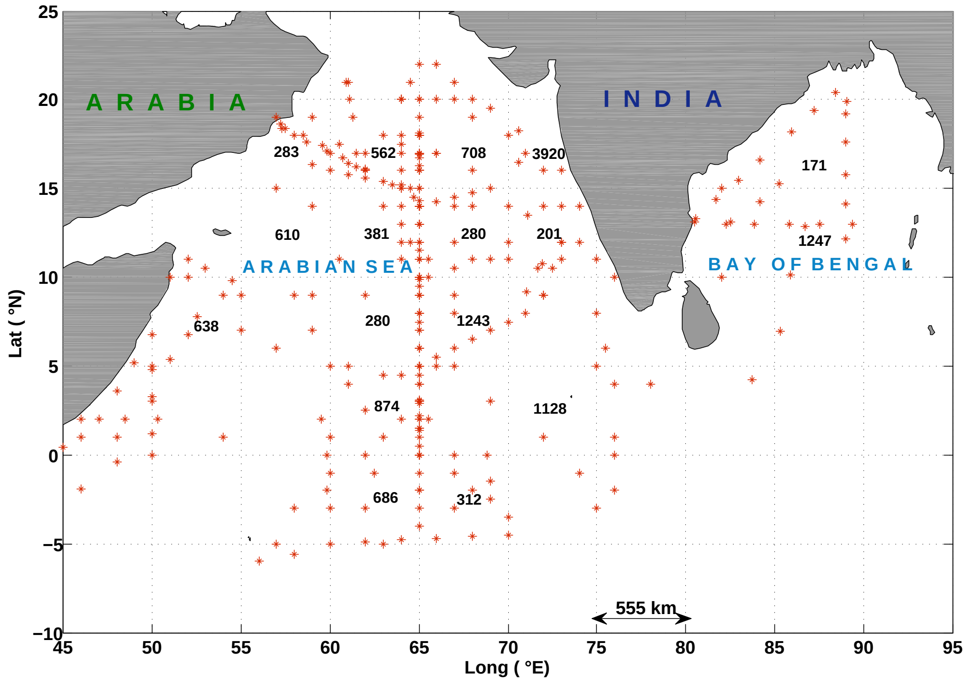

Figure 2.12: Locations of deposition flux measurements

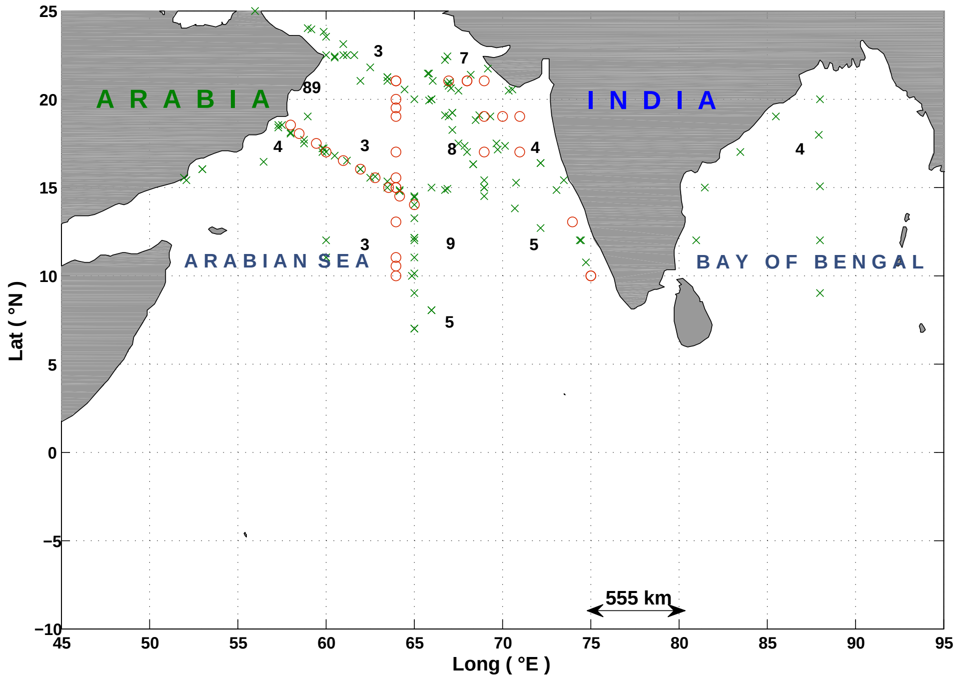

Figure 2.13: ○ and × represent ^{14}C and ^{15}N based productivity measurements, respectively.

The measured concentrations of nitrate, nitrite and ammonium in aerosols are converted into dry and wet deposition fluxes. Dry deposition occurs when particles settle under gravity while during wet deposition particles are scavenged by precipitation. Productivity is estimated on the basis of uptake rates of nitrate, nitrite and ammonium during photosynthesis. These are discussed in detail in the following subsections.

2.3.1 Calculation of dry and wet deposition fluxes

Nitrate, nitrite, and ammonia concentrations in aerosols collected over the Arabian Sea and the Bay of Bengal were obtained from the literature [*Savoie et al.*, 1987; *Rhoads et al.*, 1997; *Krishnamurti et al.*, 1998; *Johansen et al.*, 1999; *Gibb et al.*, 1999; *Sarin et al.*, 1999; *Bange et al.*, 2000; *Rengarajan and Sarin*, 2004; *Rastogi*, 2005; *Kumar et al.*, 2008]. Deposition of nitrogen occurs through gravitational settling (dry deposition) and precipitation (wet deposition). The dry deposition flux is given by $F_d = V_d \times C_d$; where C_d is the measured concentration of substance of interest in aerosol, and V_d the settling velocity of the particle which depends on complex interactions of various parameters such as wind speed, particle size, relative humidity, and sea surface roughness [*Duce et al.*, 1991], as a result V_d has large uncertainties. Thus, to simplify estimates of deposition fluxes, the mean values of V_d accounting for the aerosol size distribution, is frequently used. V_d of 1.5 cm s^{-1} for nitrate and 0.05 cm s^{-1} for ammonium are incorporated (because V_d varies with particle size so different rates are used for nitrate and ammonium) in these calculations [*Duce et al.*, 1991; *Schafer et al.*, 1993]. The wet deposition flux, F_w is given by $P\ S\ C_d\ \rho_a^{-1}\ \rho_w$, where P represents the rain rate, S the scavenging ratio and ρ_a (1.2 kg m^{-3}), ρ_w (103 kg m^{-3}), the densities of air and water, respectively. $S = C_r/\ C_d$, where C_r is the concentration of the substance of interest in rain. S is 330 and 200 for nitrate and ammonium, respectively [*Duce et al.*, 1991]. For the estimation of the seasonal wet deposition flux, *Bange et al.* [2000] used a constant P, (780 mm y^{-1} for the Arabian Sea, 2550 mm y^{-1} for the Bay of Bengal) taken from *Ramesh Kumar and Prasad* [1997]. High interannual and spatial variability of rainfall causes the large uncertainties in such wet deposition fluxes. To minimize these uncertainties, we estimated the wet deposition flux using TRMM (Tropical Rainfall Measuring Mission) rainfall data (http://disc2.nascom.nasa.gov/Giovanni/tovas/rain.GPCP.2.shtml) for each location at the corresponding time. For total deposition flux calculations, the areas of the Arabian Sea and the Bay of Bengal are taken to be 4.93×10^{12} m^2 and 2.93×10^{12} m^2, respectively [*Bange et al.*, 2000]. Figure 2.12 shows the aerosol sampling locations with annual mean of N_r deposition fluxes (in mg N m^{-2} y^{-1}) in $5^0 \times 5^0$ grid format. Aerosol measurements cover almost the entire the Arabian Sea, while a lesser area is covered in the Bay of Bengal. The overall uncertainty in the calculated nitrogen deposition flux is less than 20%, mainly caused by the spatiotemporal variability in rainfall over the oceanic regions (uncertainties in wet deposition flux due to rain are also discussed in *Baker et al.*, [2010]).

2.3.2 Calculation of new and primary production

Generally, the tracer used to measure oceanic primary productivity is ^{14}C, which provides an estimation of overall productivity i.e., total rate of carbon fixation. However, this tracer does not provide any information about the export/new production. The ^{15}N tracer technique [*Dugdale and Goering*, 1967], besides estimating the primary productivity, yields the new/export productivity as well (i.e. nitrate uptake). In this technique, primary productivity is calculated by sum of the uptake rates of nitrate, ammonia and urea integrated over the photic zone, and using the Redfield ratio (C:N:P: :106:16:1). Because of simultaneous microbial processes occurring in the sunlit layer of ocean, variation in Redfield ratio (C:N:P varies from 70:10:1 to 200:27:1) introduces some error in the productivity estimates [*Arrigo*, 2005 and references therein]. Since we compare only nitrogen uptake rates (based on ^{15}N tracer technique) with deposition fluxes, such errors are avoided here. More details of this technique are discussed by *Kumar and Ramesh* [2005].

^{15}N tracer technique based new and primary productivity data in the northern Indian Ocean have been obtained from several studies [*Owens et al.*, 1993; *McCarthy et al.*, 1999; *Watts et al.*, 1999; *Watts and Owens*, 1999; *Sambrotto*, 2001; *Kumar et al.*, 2004a; *Prakash et al.*, 2008; *Kumar et al.*, 2010; *Gandhi et al.*, 2010a]. ^{14}C tracer technique based primary productivity data are also available [*Ryther et al.*, 1966; *Qasim*, 1982; *Bhattathiri et al.*, 1996; *Madhupratap et al.*., 1996; *Barber et al.*, 2001; *Prasanna Kumar et al.*, 2001; *Jyothibabu et al.*, 2004; *Gauns et al.*, 2005] but not used here. Although ^{14}C and ^{15}N based productivity values are comparable [*Kumar and Ramesh*, 2005]; the incorporation of ^{14}C data might increase uncertainties in the nitrate uptake rate estimates while conversion from carbon to nitrogen uptake rates (using the variable Redfield ratio) and then assuming a constant fraction of the primary productivity as new productivity. Figure 2.13 shows the new and primary productivity locations where ^{14}C and ^{15}N tracer measurements were performed. Productivity measurements also cover almost entire the Arabian Sea (excluding south of 5^0N), while being spatially limited in the Bay of Bengal. The mean new productivity is also shown in 5°× 5°grid format in units of mmol N m^{-2} d^{-1}. These data in grid format may be useful for the validation of biogeochemical models as well [e.g., *Sharada et al.*, 2008]. The overall uncertainty in the productivity measurements is less than 10%. This is mostly due to patchiness of the particles and seasonal and inter-annual variations. Hence, our final analysis, based on productivity and atmospheric flux calculations, have less than 25% uncertainty.

2.3.3 Calculation of riverine fluxes

New production measured along the coastal area is used the present study for studying the role of river fluxes to the oceanic new productivity (Figure 2.14).

Subcontinent river system

Major Indian rivers are categorized into four (i) Himalayan, (ii) peninsular, (iii) coastal and (iv) inland. The two largest rivers in northern India i.e. the Ganga (also known as the Ganges) and the Brahmaputra, flowing towards east into the Bay of Bengal, originate in the Himalaya and rank the worlds third largest river in terms of discharge, after the Amazon and the Congo (Figure 2.14).

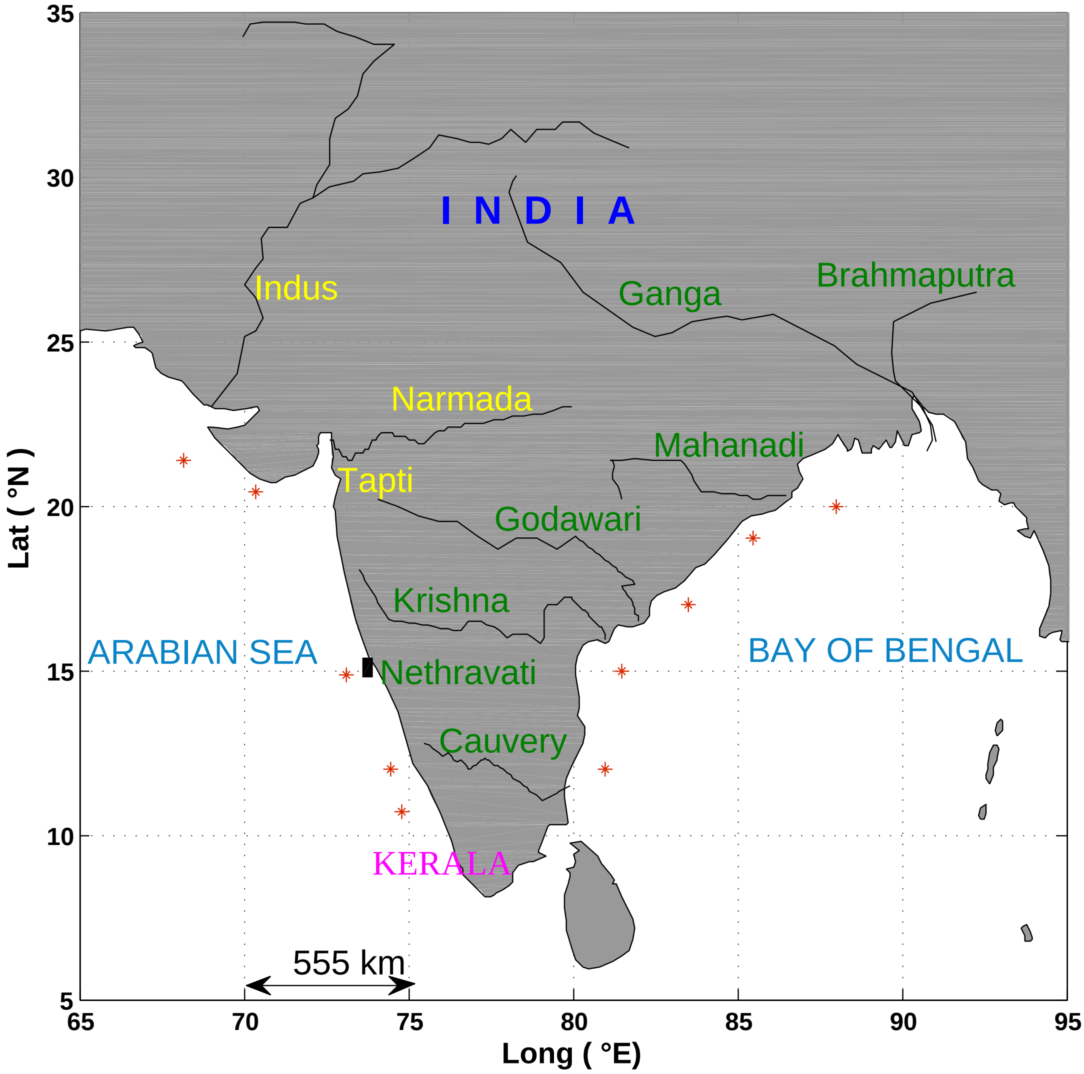

Figure 2.14: Locations of new productivity measurements.

The Indus, a major river that flows through Pakistan to the Arabian Sea also originates in the Himalaya (Tibet). In the south, east-bound peninsular rivers i.e. the Mahanadi, Godavari, Krishna and Cauvery; originate in the Deccan plateau and flow into the Bay of Bengal. Coastal rivers such as the Nethravati originate from the Western Ghats flow into the Arabian Sea. Rivers originating inland in central western India, such as the Narmada and the Tapti, discharge into the Arabian Sea [*Lambs et al.*, 2005].

Calculation of DIN flux

The DIN concentration (C) and water discharge (R) of rivers have been measured at several places on the river courses and estuaries/river mouths and the data are scattered in the literature [e.g., *Krupadam and Anjaneyulu*, 2000, *Sarin et al.*, 1992]. The areal influence (extension) of river discharge in the coastal ocean is assumed to be $1°\times 1°(\sim 1.2 \times 10^4\ \text{km}^2)$; a significant amount of DIN is unlikely to transported to the open ocean. Riverine DIN flux is derived as $F = CRA^{-1}$, where A = Area of influence. Nitrate measurements have a maximum error of 6 % [*Mukhopadhyay et al.*, 2006].

Chapter 3

N_2 fixation and Carbon uptake estimates in the sea water and sediments

Bio-available nitrogen (oxidized and reduced forms of nitrogen such as nitrate and ammonium) is an essential major nutrient for marine organisms, and its scarcity in surface waters limits the growth of phytoplankton in most ($\sim$ 80%) world oceans located between 30°N and 30°S [*Broecker*, 1974; *Eppley and Peterson*, 1979; *Longhurst*, 1998]. In such oceanic areas, the level of net biological activity is sustained by the upward mixing of nitrogen from the deeper ocean. This flux of new nitrogen into the euphotic zone supporting primary productivity is balanced by losses through sinking of organic nitrogen out of the upper ocean over annual time scales [*Eppley and Peterson*, 1979].

The triple bond strength between nitrogen atoms in N_2 makes it difficult for microbes to utilize it; however, diazotrophs such as *Trichodesmium*, present in the ocean surface are capable of adding 'new' nitrogen into the ocean through N_2 fixation, an exclusively prokaryotic metabolic process in which nitrogenase enzymes reduce dinitrogen to ammonium. *Trichodesmium* is a filamentous cyanobacterium that is found throughout warm oligotrophic oceans [*Capone et al.*, 1997]. N_2 fixation affects the C-N-P cycles in the ocean and also contributes to the removal of excess anthropogenic carbon dioxide from the atmosphere. In addition, diazotrophs release fixed nitrogen to the ocean water, which becomes available to the other non-diazotrophic primary producers [*Letelier and Karl*, 1996]. In contrast, bio-available nitrogen is lost from the oxygen depleted regions of the ocean through processes such as denitrification and anaerobic ammonium oxidation (anammox); these occur at depth, where ammonium and oxides of nitrogen get converted to molecular nitrogen, that eventually escapes to the atmosphere [e.g., *Naqvi*, 1987; *Kuypers et al.*, 2003].

Recently, an imbalance between the rates of nitrogen loss and gain has been suggested, indicating that other less well-studied or currently unknown processes could fix substantial amounts of N_2. The loss processes are rather well studied and the possibility of a decrease in the nitrogen loss term in the total nitrogen budget is less likely, while the gain processes are still poorly quantified [*Codispoti*, 2007]. Most earlier estimates of global N_2 fixation are based on the extrapolation of limited field measurements, and direct estimations of N_2 fixation using $^{15}N_2$ gas are quite limited. It has been recently found that denitrification and N_2 fixation may be closely coupled [*Deutsch et al.*, 2007] because nitrogenase (the enzyme involved in N_2 fixation) is extremely sensitive to oxygen [*Mulholland and Capone*, 2009 and references therein]. This intriguing enigma of nitrogen imbalance prompted us to study N_2 fixation in the water column of the Arabian Sea and sediments of the Wadden Sea.

3.1 N_2 fixation and Carbon uptake rates in the Arabian Sea

The Arabian Sea is one of three major open-ocean oxygen-minimum zones (OMZ) in the world oceans, others being the Eastern Tropical North Pacific and the Eastern Tropical South Pacific [*Codispoti*, 2007]. The climatology, hydrography and circulation of the Arabian Sea have been summarized by many authors [*Schott and McCreary*, 2001; *Rao and Sivakumar*, 2003; *Jyothibabu et al.*, 2010; *Singh et al.*, 2010]. In the following, we give a brief account of the monsoon circulation and biogeochemistry of the Arabian Sea and discuss the earlier work on nitrogen fluxes in some detail.

Biologically, the Arabian Sea is one of the most productive oceanic regions, mainly due to the seasonal input of nutrients to the surface [e.g., *Gandhi et al.*, 2010b]. Located east of the Arabian Desert and southwest of the Thar Desert, it experiences a seasonal reversal of winds twice a year. During the summer monsoon (June - August), intense southwesterly winds blow from the ocean to the land, causing nutrients to upwell from the deeper western Arabian Sea to the surface; on the other hand, during the winter monsoon (December - February), cool, dry winds from northeast induce convective mixing and increase productivity in the northeastern Arabian Sea [*Madhupratap et al.*, 1996; *Smith*, 2001; *Prakash and Ramesh*, 2007; *Kumar et al.*, 2010; *Padmakumar et al.*, 2010]. In addition, during spring and autumn inter-monsoons (mainly April-May and September-November), *Trichodesmium* blooms occur in the coastal and central Arabian Sea when the sea is calm and bio-available nitrogen relatively scarce at the surface [*Devassy et al.*, 1978; *Capone et al.*, 1998; *Parab et al.*, 2006]. Such blooms also lead to higher primary productivity under such oligotrophic (i.e., NO_3^- concentration below detection limit) conditions. However, only one earlier study reports N_2 fixation rate in the central Arabian Sea using the C_2H_2 reduction technique [*Capone et al.*, 1998]. In addition to *Trichodesmium* blooms, the presence of diazotrophic $\gamma-$proteobacteria in the Arabian Sea has also been reported [*Bird et al.*, 2005]. *Bange et al.* [2000] have estimated the N_2 fixation rate in the Arabian Sea to be 3.3 Tg N y^{-1}. Patchiness and temporal variability restrict the precise estimates of such rates; thus more measurements are needed for a better quantification of the marine nitrogen budget.

Higher productivity causes oxygen depletion in the deeper ocean and develops the largest open ocean OMZ in the Arabian Sea; this further leads to loss of bio-available nitrogen [*Bange et al.*, 2000]. Nitrogen gain does not reach the level of nitrogen loss (60 Tg N y^{-1}). About 20-40% of global oceanic bio-available nitrogen is lost by this region (only $\sim$ 2% of the global ocean area) through denitrification [*Bange et al.*, 2000; 2005]. Though the Arabian Sea is a well known region for N_2 fixation, the precise estimation of direct N_2 fixation is still lacking. It has already been suggested that direct N_2 fixation might be more important than realized previously [*Codispoti*, 2007]. This prompted us to make measurements of N_2 fixation by *Trichodesmium* along the eastern Arabian Sea using the $^{15}N_2$ gas technique to obtain an initial estimate of the new nitrogen input to the region. As primary productivity during the inter-monsoon periods is poorly constrained, and the measurements have large uncertainties, the ^{13}C tracer technique was also concurrently employed to estimate the total productivity.

3.1.1 Earlier results on N_2 fixation and primary productivity

Despite the reports of seasonal occurrence of the blooms of N_2 fixation organisms (*Trichodesmium*) in the Arabian Sea [*Devassy et al.*, 1978; *Capone et al.*, 1998; *Parab et al.*, 2006], no direct N_2 fixation estimates were made until this work. *Trichodesmium* blooms are observed in the Arabian Sea during November-February and March-May [*Parab et al.*, 2006]. Isotopic signature of nitrate (lower $\delta^{15}N$) above the OMZ in the Arabian Sea is attributed to N_2 fixation [*Brandes et al.*, 1998] with the conclusion that N_2 fixation is a significant process in the region [*Devol et al.*, 2006; *Devol*, 2008; *Naqvi*, 2008]. *Brandes et al.* [1998] suggested that 30-40% part of primary productivity was supported by N_2 fixation. Further, *Capone et al.* [1998] made an attempt to estimate the potential magnitude of N_2 fixation by *Trichodesmium erythraeum.* These indirect measurements were based on C_2H_2 reduction technique and represent a small region of the southern central Arabian Sea. In addition, based on nitrogen isotopic data of surface suspended particles, *Gandhi et al.* [2010a] recently showed that fixed nitrogen by *Trichodesmium* contributes as high as ∼79% of the nitrogen in surface suspended particles in the north-eastern Arabian Sea. In the absence of direct estimates, N_2 fixation in the Arabian Sea remains unconstrained.

On the other hand, new and primary productivity are studied extensively using ^{15}N and ^{14}C tracers in the Arabian Sea. The ^{15}N tracer technique has been used widely to understand the biogeochemistry of this region and to examine its role in carbon sequestration. ^{15}N based estimates were made under US JGOFS program in the western and central Arabian Sea. But in the eastern part of the Arabian Sea, such measurements were started in 2003 [*Kumar et al.*, 2010]. Spatiotemporal variation in the new productivity is observed. NO_3 uptake rate varied from 2.7 mmol N $m^{-2}d^{-1}$ in the central AS to 88.9 mmol N $m^{-2}d^{-1}$ in the coastal upwelling region during the fall 1986 [*Owens et al.*, 1993]. In the central Arabian Sea, N-uptake rates varied from 9.2 mmol N $m^{-2}d^{-1}$ to 40 mmol N $m^{-2}d^{-1}$ during the winter, and 3.9 mmol N $m^{-2}d^{-1}$ to 24 mmol N $m^{-2}d^{-1}$ during the late summer [*McCarthy et al.*, 1999]. On an average, N-uptake rate is significantly higher in winter (∼26 mmol N $m^{-2}d^{-1}$) than in late summer (11 mmol N $m^{-2}d^{-1}$). *Watts and Owens*, [1999] also reported large variations in the N-uptake rate, i.e. 1.1 mmol N $m^{-2}d^{-1}$ to 23.6 mmol N $m^{-2}d^{-1}$ in the north-western Arabian Sea during the early winter 1994. N-uptake rate ranged from 0.1 to 13 mmol N $m^{-2}d^{-1}$ during the spring inter-monsoon and the summer monsoon in the northern Arabian Sea [*Sambrotto*, 2001].

New productivity estimates in the eastern Arabian Sea are limited as measurements started only in the present decade. New productivity ranged from 1 to 4.3 mmol N $m^{-2}d^{-1}$, increasing from south to north in the north-eastern Arabian Sea during winter [*Kumar et al.*, 2010]. During late winter monsoon, new productivity was significantly higher in *Noctiluca* bloom (23 mmol N $m^{-2}d^{-1}$) than in the non-bloom (5.7 mmol N $m^{-2}d^{-1}$) regions. An increasing trend from south to north in N-uptake rates is also observed in the eastern Arabian Sea during this season [*Prakash et al.* 2008], attributed to the presence of different biogeochemical provinces. *Noctiluca miliaris* blooms develop in this season in the north-eastern Arabian Sea and make this region more productive than the southern Arabian Sea [*Prakash et al.*, 2008]. Winter mixing and its role in the formation of blooms have been studied [*Madhupratap et al.*, 1996; *Prasanna Kumar and Narvekar*, 2005]. *Gandhi et al.* [2010b] have broadened our understanding on the eastern Arabian Sea further by showing that N-uptake rates are similar in the coastal and open ocean during 2006. Rates were low and varied from 0.22 mmol N $m^{-2}d^{-1}$ to 1.29 mmol N $m^{-2}d^{-1}$. Such low rates are attributed to strong stratification.

Primary productivity varies seasonally in the Arabian Sea. Productivity is higher during the summer (600 mg C $m^{-2}d^{-1}$), moderate during the winter (300 mg C $m^{-2}d^{-1}$) and low (100 mg C $m^{-2}d^{-1}$) during the intermonsoon [*Bhattathiri et al.*, 1996; *Madhupratap et al.*, 1996]. In another study, primary productivity varied from 770 to 1782 mg C $m^{-2}d^{-1}$ during the summer 1996. This higher productivity is attributed to strong wind-driven turbulent mixing which leads to deepening of MLD (80 m) and cooling of SST (28 ℃) [*Prasanna Kumar et al.*, 2002]. *Gandhi* [2010] has used ^{13}C tracer for the first time in the Arabian Sea and showed that carbon uptake vary from 21 to 235 mg C $m^{-2}d^{-1}$ (with an average of 121.2 mg C $m^{-2}d^{-1}$) during the winter 2007. Their results were consistent with earlier estimates. Results from this study are discussed below.

3.1.2 Environmental conditions during spring 2009

Depth profiles of photosynthetically active radiation (PAR) are shown in Figure 3.1. Euphotic depth was less than 40 m at all the stations but NF3. The PAR values at sea surface varied from 826 to 1616 μmol m^{-2} s^{-1} (Table 3.1). The highest and the lowest PAR at surface were found at NF4 and NF3, respectively. Overall, average PAR at surface during the study period was 1272 μmol m^{-2} s^{-1}.

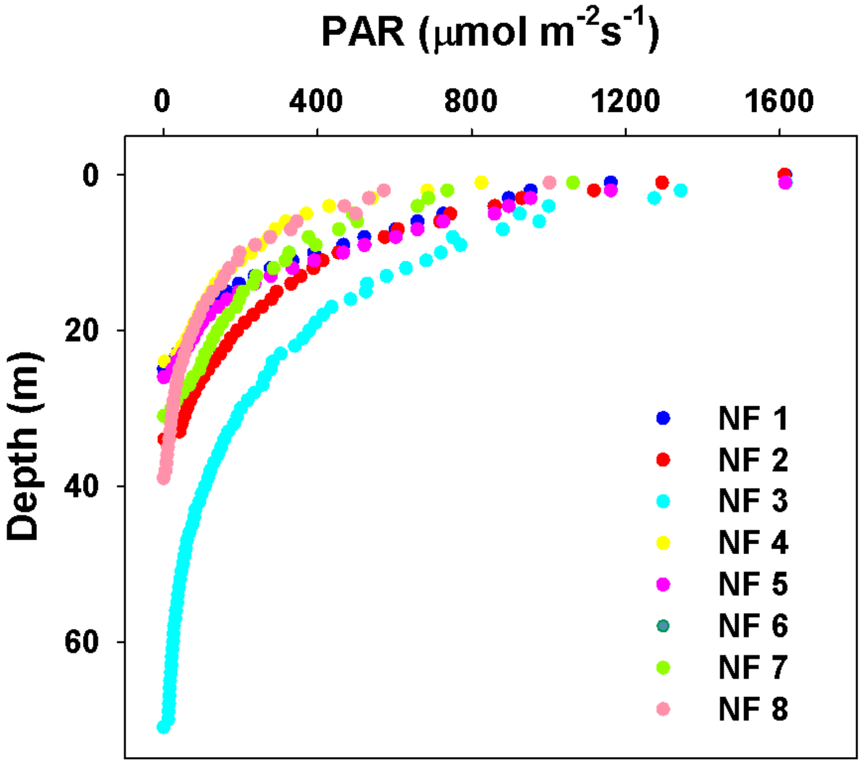

Figure 3.1: Depth profiles of Photosynthetically Active Radiation (PAR) at various stations

Table 3.1: Latitude (°N), Longitude (°E), Station Depth (m), Sea Surface Temperature (SST, ℃), Salinity (psu), Photosynthetically Active Radiation (PAR, μmol m^{-2} s^{-1}), Chlorophyll *a* (μg L^{-1}), and ratios of N/P and N/Si at the surface at the different stations

Station	Lat	Long	Station Depth	SST	Salinity	PAR	Chl *a*	N/P	N/Si
NF1	12°59.8’	74°28.4’	42	30.0	34.822	1384	0.32	2.6	0.1
NF2	12°59.7’	74°30.3’	42	30.5	34.997	1613	0.27	16.5	0.4
NF3	13°07.6’	74°27.6’	1362	30.0	34.824	1616	0.27	2.2	0.1
NF4	13°39.0’	74°29.2’	30	30.5	35.186	826	0.40	1.0	0.0
NF5	15°29.6’	73°36.5’	35	30.5	35.806	1615	0.33	1.6	0.1
NF6	17°09.1’	76°06.2’	38	29.0	35.793	1064	0.23	1.4	0.1
NF7	17°09.8’	73°09.3’	30	29.0	35.958	1064	2.55	8.3	0.3
NF8	15°27.2’	73°31.3’	47	30.0	35.605	1002	0.29	0.8	0.1

SST and salinity presented here are measured using a bucket thermometer and an Autosal, respectively; however, the values discussed in the text and Figures are collected using a CTD.

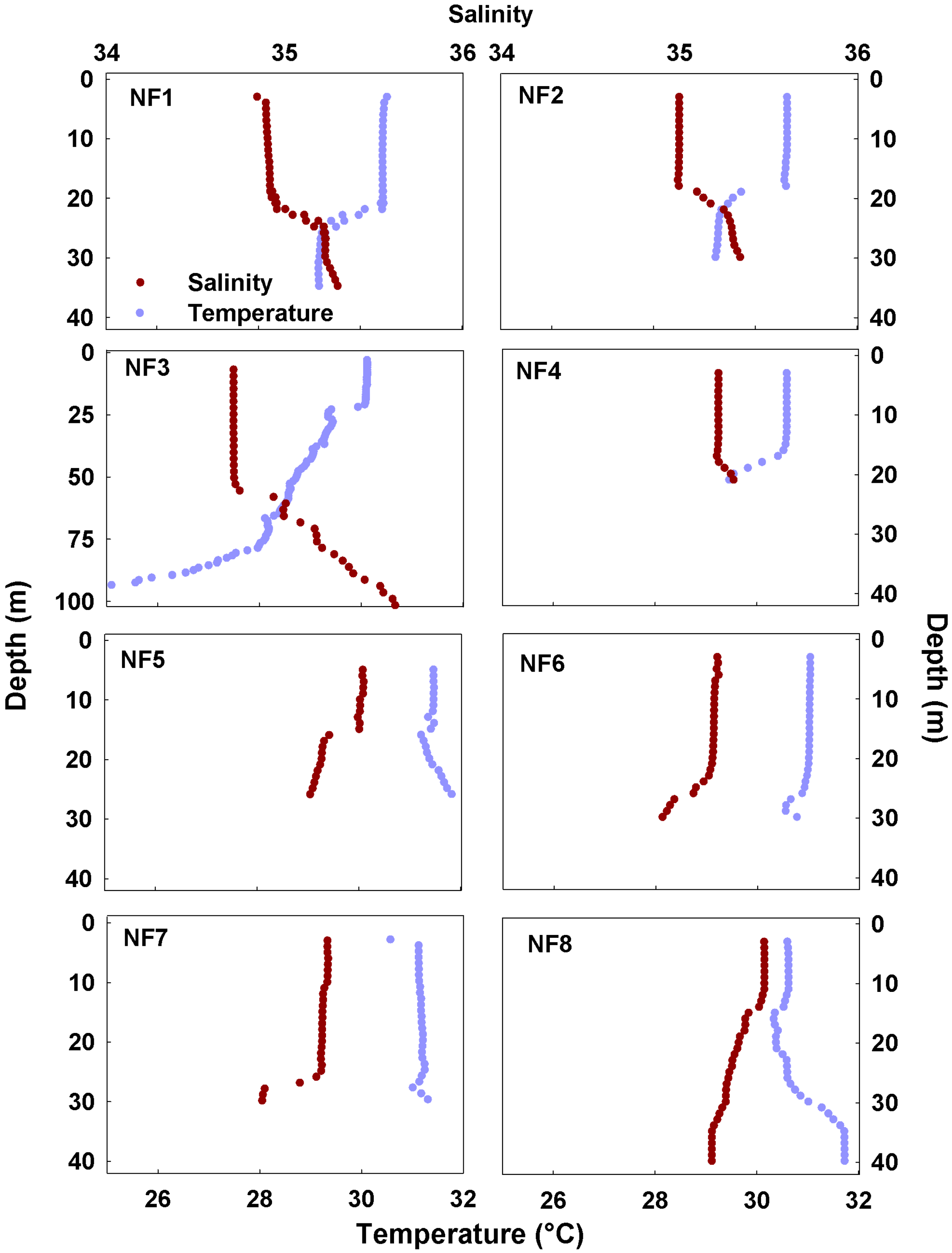

Figure 3.2: Depth profiles of salinity (psu) and Temperature (°C)

Figure 3.2 shows the temperature and salinity profiles of all the stations. Sea surface temperature (℃; SST) decreases significantly from the south to the north, varies from 29 to 30.6 ℃ with the highest value at NF2. In contrast, surface salinity shows the opposite trend, it increases from the south to the north, and is between 34.7 and 35.8, with the highest value at NF5. This north-south gradient in SST and salinity is a common feature of the Arabian Sea and has also been reported earlier [e.g., *Madhupratap et al.*, 1996; *Prasanna Kumar and Narvekar*, 2005; *Prakash and Ramesh*, 2007]. The depth where temperature decreases to 1 ℃ is termed as mixed layer depth (MLD), following *Prasanna Kumar and Narvekar* [2005]. MLD varies between 20 and 35 m at all the stations. During spring, winds are weaker and the strong surface light intensity promotes a strong stratification, which prevents the supply of nutrients from the deep to the surface.

3.1.3 Nutrients

Depth profiles of nutrients (NO_3, NO_2, PO_4 and SiO_4) are shown in Figure 3.3. Ratios of nitrate to phosphate (N:P) and nitrate to silicate (N:Si) observed in the surface waters are listed in Table 3.1. N:P varies from 0.8 to 16.5 in the region with the maximum at NF2 (Table 3.1). Except at NF2, the ratio remains lower (N:P $<$ 8) than the Redfield Ratio (C:N:P :: 106:16:1) at all the locations. Similar values are also found in the sub-surface layers. The ratio is as low as $<$0.1 between 3 and 6 m depth at NF8. In general, it remains between 0.01 and 8 throughout the euphotic zone at all the locations, except at the surface at NF8 and in sub-surface at NF1. At NF1, N:P is quite high as phosphate remains near detection limit in the sub-surface layers. Nitrogen to silicon ratio (N:Si) is also lower than the Redfield ratio; it varies from 0.02 to 0.3 in the surface layers. Like the N:P ratio, the sub-surface N:Si values are also lower than the Redfield ratio. N:P $<$ 10 and N:Si $<$ 1, observed here, are indicative of potential nitrogen limitation [*Harrison et al.*, 1977]. Such conditions, along with weaker winds, shallow MLD and a calm sea, favour the occurrence of *Trichodesmium*. Both *Trichodesmium erythraeum* and *Trichodesmium thibautii* are found in the region.

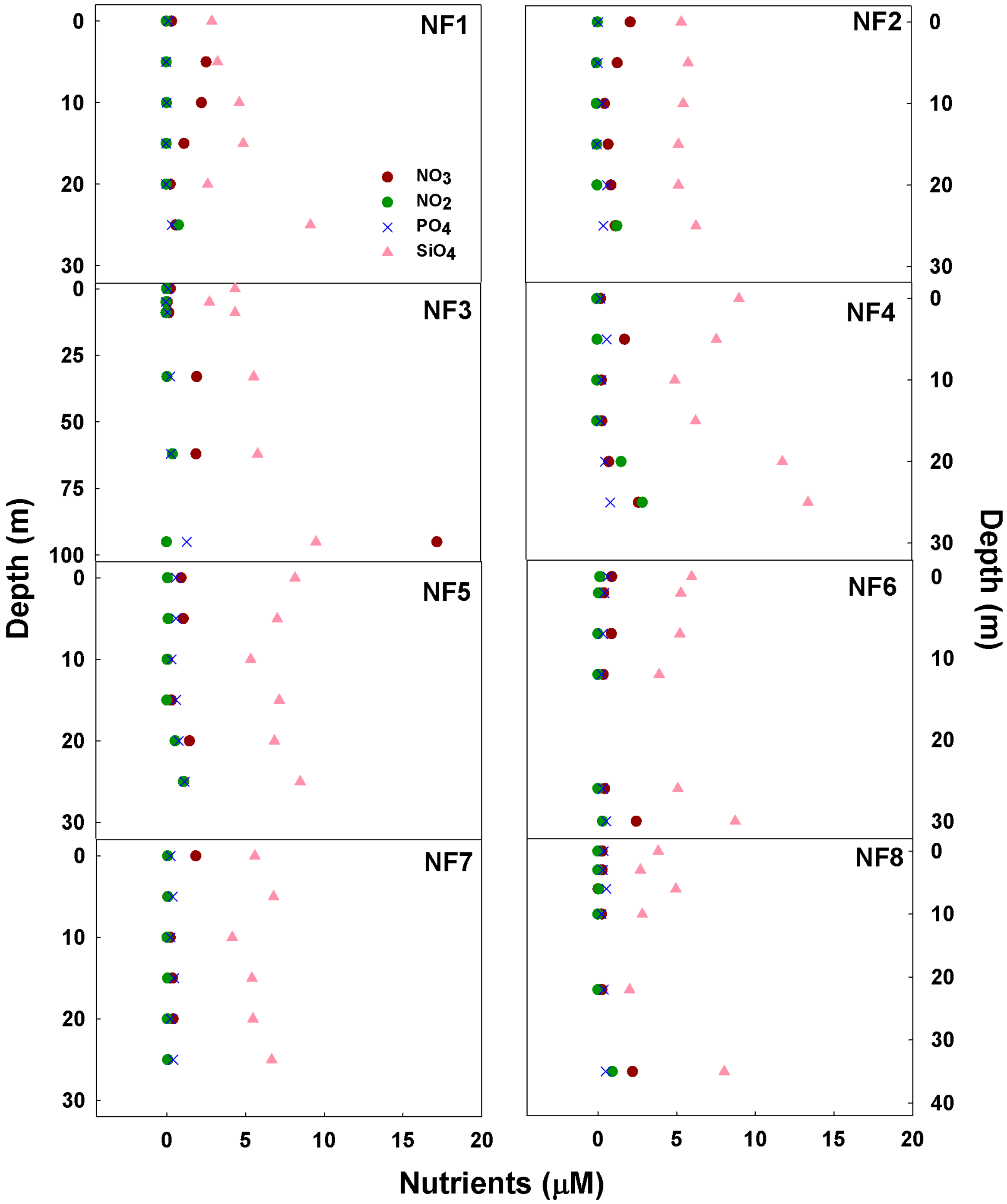

Figure 3.3: Depth profiles of different nutrients (NO_3, NO_2, PO_4 and SiO_4) at various stations

Iron and phosphorus control N_2 fixation [*Capone*, 2001]. There is no phosphate limitation since phosphate concentration was mostly more than 3 nM (concentration <3 nM is considered as phosphate-limited condition) here, unlike in the high iron-input regions [*Shiozaki et al.*, 2010]. This could be because parts of the Arabian Sea are considered to be iron-limited [*Naqvi et al.*, 2010a], despite the supply of iron from Arabia [e.g., *Krishnamurti et al.*, 1998]. Our data of phosphate concentration and N:P rules out phosphate-limited conditions (except at NF1).

3.1.4 Chlorophyll *a*

A large variation is seen in the surface chlorophyll *a* values, from <0.23 to as high as >2.55 μg L^{-1}, with the highest at NF7 (Table 3.1). The locations NF5-7 witness dense blooms of *Trichodesmium*, under such conditions, surface chlorophyll *a* concentration as high as >2000 μg L^{-1} has been reported during May 2003 [*Parab et al.*, 2006] and more than 100 μg L^{-1} during the springs of 1975 and 1977 [*Devassy et al.*, 1978]. Euphotic-depth-integrated chlorophyll *a* also shows a similar pattern, as that of surface chlorophyll *a*. The maximum euphotic-depth-integrated chlorophyll *a* is observed at NF7, with the lowest at NF6 (although this was one of the dense bloom stations). Overall, it varies between 8.2 and 71.3 mg m^{-2}. This variation is consistent with the intensity of *Trichodesmium* blooms observed and reported earlier from similar occurrences in the region by *Matondkar et al.* [2006]; however, more than 100 mg m^{-2} chlorophyll *a* values were reported earlier [*Desa et al.*, 2005].

3.1.5 N_2 fixation and carbon uptake rates

Figure 3.4 presents the depth profiles of N_2 fixation and carbon uptake rates. A large variation in surface N_2 fixation rate is observed; it varies from 0.1 to 450 nM N h^{-1}, with the highest rate at NF6; much higher range than reported by *Carpenter and Capone* [2008] (0 to 5.4 nM N h^{-1}). Except at NF6, the surface rates are less than 20 nM N h^{-1} (Figure 3.4).

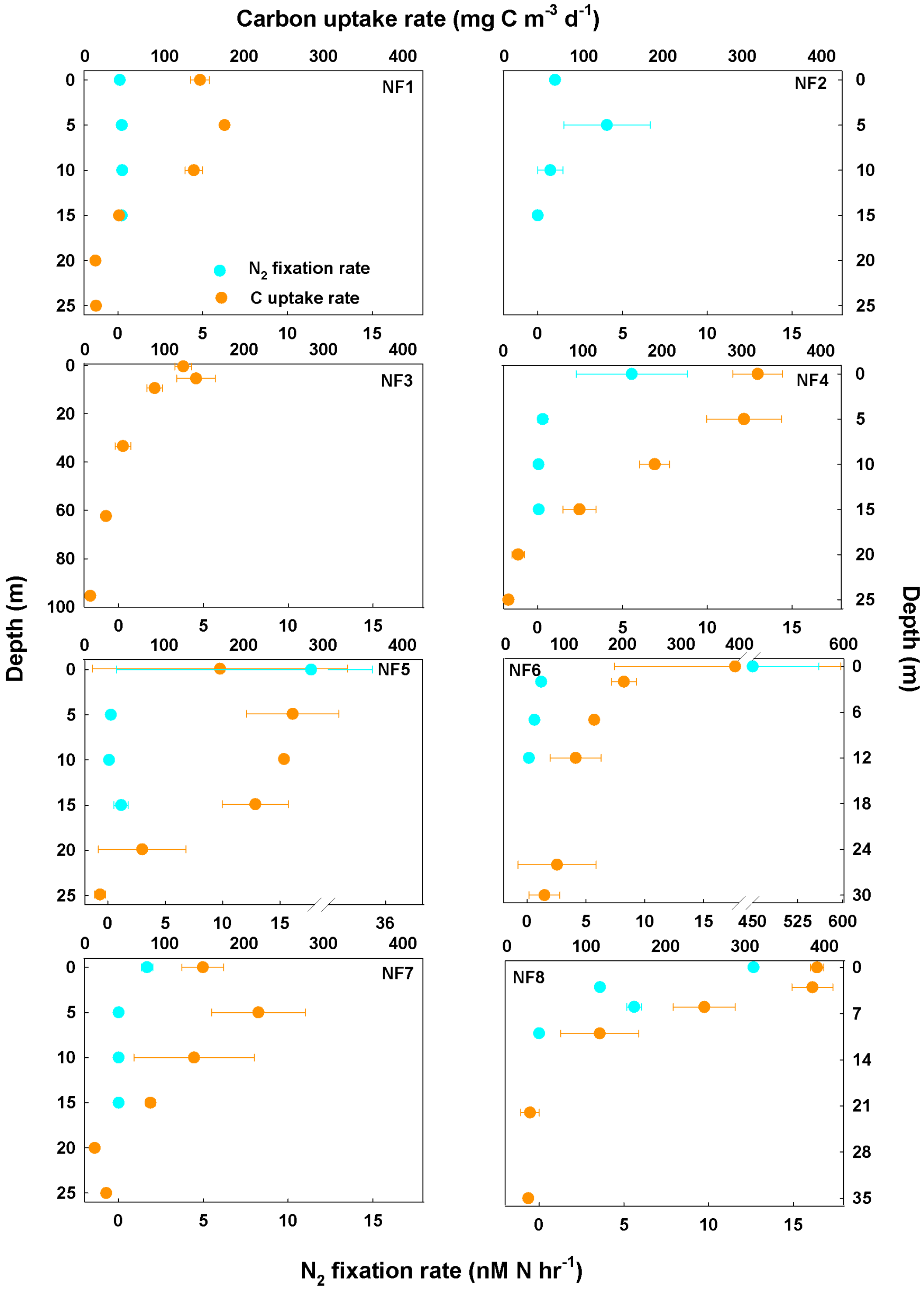

Figure 3.4: Depth profiles of N_2 fixation (nM N hr^{-1}) and primary productivity (mg C m^{-3} d^{-1}) using the $^{15}N_2$ and ^{13}C tracer techniques, respectively. Error bars are half the difference between duplicate measurements; some of these are less than the size of the symbol used

The arithmetic mean is ~6.5 nM N h^{-1}, excluding NF6; with the inclusion of NF6, the mean increases to ~70 nM N h^{-1}. As the variation is of three orders of magnitude, the geometric mean is a better statistic; this is 5.2 nM N h^{-1}. Surface values observed at three stations, NF5, NF6 and NF8, are significantly higher than those reported by *Capone et al.* [1998] and *Church et al.* [2009] in the central Arabian Sea and the North Pacific Ocean, respectively. *Capone et al.* [1998] used C_2H_2 reduction technique and estimated ~10 nM N h^{-1} in the top 0.5 m, similar to most of our values, but significantly less than those at NF5, NF6 and NF8. In the North Pacific Ocean, surface rates ranged from 0.5 to 11 nM N h^{-1} [*Church et al.*, 2009], also similar to values reported here, if our values are converted to daily rates by multiplying a factor of 12. At all the locations, surface values are much higher than the sub-surface values except at NF2, where NO_3 was present at the surface. N_2 fixation contributes ~50-90% to the total column N_2 fixation in the top 5 m; this is expected as positive buoyancy keeps *Trichodesmium* at the surface. *Capone et al.* [1998] also found about 3-fold higher N_2 fixation in the top 0.5 m than that occurring between 0.5 to 40 m. N_2 fixation increases from the surface to 5 m depth and then decreases up to 15 m at NF2; higher rate is observed at this station than at NF1, though these stations were nearby (Figure 2.13).

Depth profiles of carbon uptake rates are also shown in Figure 3.4. Primary productivity (carbon uptake rate) is not measured at NF2. It varies between 0.12 and 0.39 gC $m^{-3}d^{-1}$ (with an average of 0.24 gC $m^{-3}d^{-1}$). NF6 shows the highest surface productivity, comparable to that at NF8. The lowest surface productivity is seen at NF3, where surface chlorophyll *a* is also less.

Euphotic-depth-integrated carbon uptake rates are presented in Figure 3.5. Column productivity values range from 2.2 to as high as 4.4 gC $m^{-2}d^{-1}$, with the highest at NF5. The average productivity is 3.6 gC $m^{-2}d^{-1}$. *Ryther et al.* [1966] have reported a mean productivity of 2.23 g C $m^{-2}d^{-1}$ (ranging from 0.84-6.58 gC $m^{-2}d^{-1}$) for the Oman coastal upwelling zone (north of 18°N) compared to 3.08 gC $m^{-2}d^{-1}$ reported for the same region by *Savidge and Gilpin* [1999]. *Owens et* *al.* [1993] have reported primary productivity of ~0.5 gC $m^{-2}d^{-1}$ at the equator to 0.3 gC $m^{-2}d^{-1}$ in the oligotrophic gyre in the central Arabian Sea, and >2.5 gC $m^{-2}d^{-1}$ in the upwelling region off the coast of Oman during September-October 1986. *Qasim* [1982] reported a very wide range of primary productivity for the northern Arabian Sea (north of 15°N) varying from 0.01 to 6.01 gC $m^{-2}d^{-1}$ with an average value of 0.84 gC $m^{-2}d^{-1}$. He also found the coastal region to be more productive (average 1.33 gC $m^{-2}d^{-1}$) than the off-shore region (0.63 gC $m^{-2}d^{-1}$). The values reported here are much higher than that observed earlier during spring in the open ocean region of the Arabian Sea; However, they do confirm the mean value reported under similar bloom conditions earlier in the region by *Matondkar et al.* [2006], i.e., column productivity from 0.1 to as high as 17 gC $m^{-2}d^{-1}$ (with an average of ~2.7 gC $m^{-2}d^{-1}$).

The depth profiles of carbon uptake rate at NF1 and NF3 are similar. Despite the significant carbon uptake rate, NF1 shows no significant change in N_2 fixation with depth and the rates are small (<0.3 nM N h^{-1}). This indicates the dominance of non-diazotrophic plankton here, which contributes to carbon uptake but not to N_2 fixation. At NF1, nitrate is quite high except at the surface, while phosphate is near the detection limit. Silicate is also significantly higher here. All these conditions favour the non-diazotrophic plankton, which results in lower N_2 fixation rate with moderate carbon uptake rates. Variation in the N_2 fixation and carbon uptake rates with depth are similar at NF4. Stations NF5, 6 and 8 show nitrogen limiting conditions throughout the euphotic zone and witnessed dense blooms of *Trichodesmium*; however, NF7 (located near NF6) shows less N_2 fixation than NF5, 6 and 8. This could be due to the relatively higher N:P value at NF7.

Figure 3.5 presents the column-integrated N_2 fixation rates, primary productivity and chlorophyll *a* estimates. Column-integrated N_2 fixation rates vary from ~0.04 to 13.6 mmol N $m^{-2}d^{-1}$ (with an arithmetic average of 2.2 mmol N $m^{-2}d^{-1}$). The arithmetic average value decreases to ~0.30 mmol N $m^{-2}d^{-1}$, if we exclude NF6, the densest bloom station having the highest N_2 fixation rate.

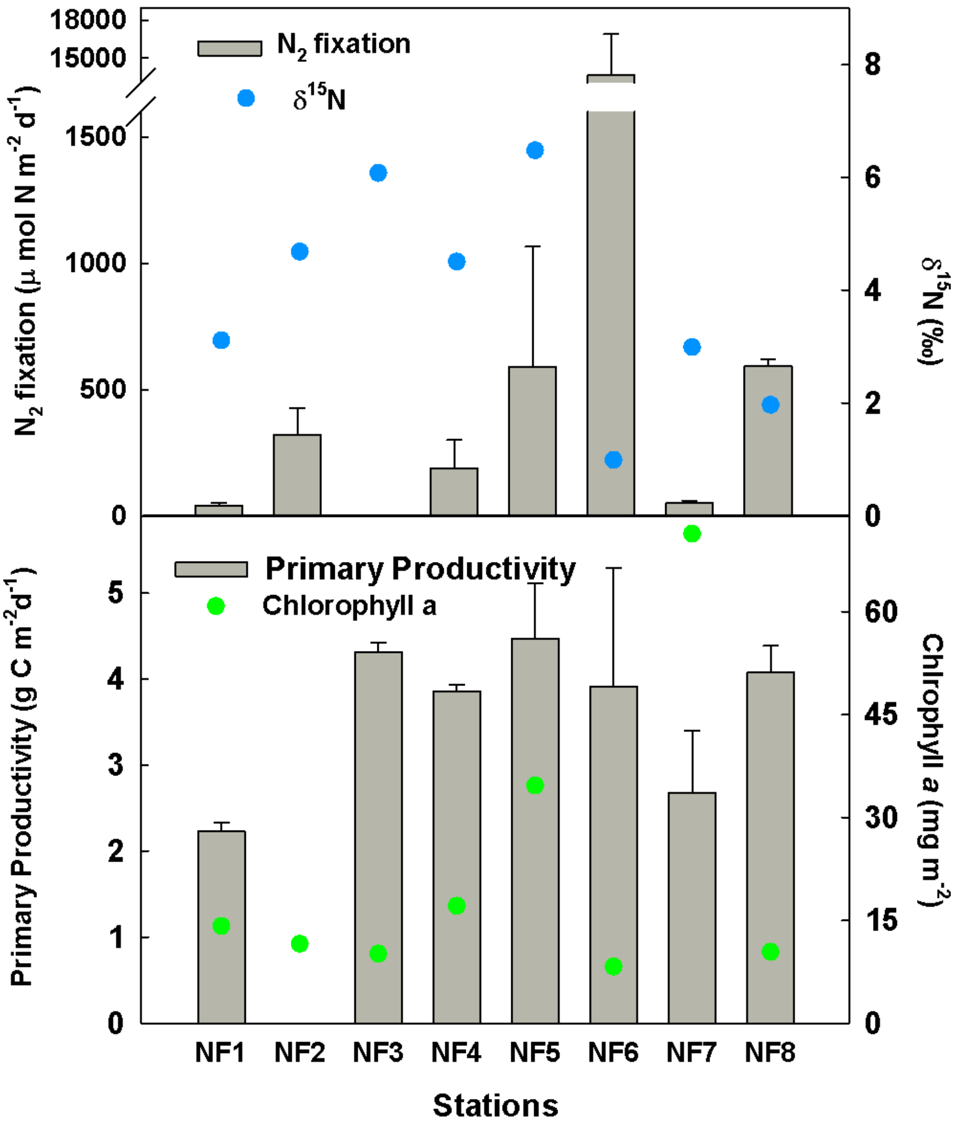

Figure 3.5: Depth integrated N_2 fixation (mol N m^{-2}d^{-1}) using the $^{15}N_2$ gas technique, $\delta^{15}N$ of surface natural samples (top panel); and primary productivity (gC m^{-3}d^{-1}) and chlorophyll *a* (mg m^{-2}) at various stations (bottom panel). Primary productivity at NF2 and N_2 fixation at NF3 are not measured. Error bars are half the difference between duplicate measurements. Note the break in scale in the Y axis

The geometric mean of all stations is 0.34 mmol N m^{-2}d^{-1}. Although chlorophyll *a* is higher at NF7, N_2 fixation here is lower than at NF6, probably due to the patchiness of diazotroph abundance. However, NF5 and 8 are near each other (~20 km) and show similar N_2 fixation rates. In the central Arabian Sea, the average column N_2 fixation was ~0.17 mmol N $m^{-2}d^{-1}$ [*Capone et al.*, 1998]. Average areal rates of N_2 fixation in the North Atlantic Ocean, covering different seasons and areas, ranged from about 0.06 to 0.90 mmol N $m^{-2}d^{-1}$ [*Capone at al.*, 2005]. *Chen et al.* [2008] reported seasonal variations in N_2 fixation rates in the upstream of Kuroshio and South China Sea. They observed N_2 fixation rates of 0.002 to 0.168 mmol N $m^{-2}d^{-1}$ and 0.001 to 0.013 mmol N $m^{-2}d^{-1}$ during different seasons in the Kuroshio and South China Sea, respectively. In both the basins, rates were found to be the highest during summer. N_2 fixation rates have been reported below the detection limit to 0.09 mmol N $m^{-2}d^{-1}$ along the 155°E meridian from the equator to 44°N in the western North Pacific Ocean during spring 2007 [*Shiozaki et al.*, 2010]. *Church et al.* [2009] found depth-integrated N_2 fixation rates between 0.02 and 0.31 mmol N $m^{-2}d^{-1}$ over a three year period in the North Pacific Ocean. N_2 fixation observed by us is higher than those observed elsewhere in the world oceans, except at the North Atlantic. This shows that the Arabian basin fixes a significant amount of atmospheric N_2 and hence provides new nitrogen to the ocean. The Arabian Sea is known for higher denitrification (nitrogen loss process) and the present results provide the first direct estimate of higher N_2 fixation rate (nitrogen gain process) in this basin. Therefore, more such measurements are needed to further constrain the nitrogen gain in the basin.

The average ratio of POC:PON of natural samples was near the *Redfield* ratio, but with a large variation i.e. 6.5 ± 5.0. This ratio was higher (9.4 ± 5.7) at non-bloom and less-dense bloom stations (NF1-4) stations than at the dense bloom stations i.e. 3.6 ± 1.0. In contrast, carbon to N_2 consumption ratio [*Takeda*, 1998] from the incubation experiments was 4994 (ranges from 6 to 27885), much higher than the Redfield Ratio. Similar to natural samples, consumption ratio was higher at NF1 and 4 (8256) than at NF5-8 (2818). These results indicate that, the presence of microbes that are incapable of fixing N_2, leads to higher consumption ratio.

3.1.6 Nitrogen isotopic composition (δ^{15}N) of natural surface samples

Nitrogen isotopic composition (δ^{15}N) is usually reported relative to atmospheric nitrogen.

$$\delta^{15}N = \left(\frac{(^{15}N/^{14}N)_{sample}}{(^{15}N/^{14}N)_{air}} - 1 \right) \times 1000‰ \tag{3.1}$$

This is a proxy which can indirectly reveal the existence of N_2 fixing microorganisms. Bacteria fix nitrogen from the dissolved form in the ocean with little fractionation and therefore (δ^{15}N) of a natural sample likely reflects that of the source of nitrogen [*Altabet and McCarthy*, 1985; *Kumar et al.*, 2004b; *Kumar et al.*, 2005; *Gandhi et al.*, 2010a]. Since the reference is air, the expected (δ^{15}N) of nitrogen fixing bacteria is likely to be close to 0‰. δ^{15}N values of surface PON at different stations are shown in the top panel of Figure 3.5. They vary between 1 and 6 with a minimum value corresponding to the sites with maximum N_2 fixation rates i.e. at sampling station at NF6. This confirms that the source of new nitrogen here is dissolved air.

δ^{15}N of organic matter is a mixture of various nitrogen sources. *Capone et al.* [1998] used a simple mass balance equation to estimate the contribution of recently fixed nitrogen to the surface pool of suspended particles. They assumed it to be a two component mixing and took the nitrogen isotopic composition of *Trichodesmium* as δ^{15}N = 0‰ and that of the nitrate below mixed layer as δ^{15}N = 10‰. Using the same approach, our isotopic data on PON of surface natural samples suggest that recently fixed nitrogen contributes 40 to 90% (with an average of 60%) of the nitrogen in the surface PON. If so, the fraction of primary productivity due to *Trichodesmium* (depth profiles up to 15 m) can be estimated; we find that the carbon to N_2 consumption ratio is accordingly revised downwards to an average of 2031 (varies from 7 to 5988).

3.1.7 Revising the nitrogen budget

A synthesis of the previous and recent estimates of nitrogen fluxes in the Arabian Sea and in the global ocean is presented in Table 3.2.

Table 3.2: Developments in the N-Cycle of the Arabian Sea, global fluxes are also presented: Results from earlier, recent and the present study (nitrogen fluxes in Tg N y^{-1})

Process	Arabian Sea				Global	
	Latest Estimates	Reference	Earlier Estimates	Reference	Earlier Estimates	Reference
Atmospheric deposition	1.2 ± 0.2	1	1.6	2	67	3
N_2 fixation	6.2 ± 0.6	This study	3.3	2	135	4
Riverine fluxes	0.1 ± 0.02	5	1.2	2	50-80	3
Denitrification	-60	6	-33	2	>400	4
Anammox	-60*	7	–	–	–	–

*This is an indirect estimate suggested by *Lam et al.* [2009], that nitrogen loss through anammox can be equal to that through denitrification. 1. *Singh et al.* [2011], 2. *Bange et al.* [2000], 3. *Duce et al.* [2008], 4. *Codispoti* [2007], 5. *Singh and Ramesh* [2011],6. *Bange et al.* [2005], 7. *Lam et al.* [2009].

Gandhi et al. [2010a] reported N_2 fixation 0.002 to 0.54 mmol N m^{-2} d^{-1} associated with *Trichodesmium* estimated from the abundance of *Trichodesmium* and specific N_2 fixation rates of 1.5 pmol N $trichome^{-1}$ h^{-1} for spring 2006. Using these data with taking the total surface area covered by blooms (more than 20% of the area of the Arabian Sea [*Capone et al.*, 1998]) and their persistence (more than 30% of the time [*Westberry and Siegel*, 2006]) with the estimated N_2 fixation rates can be used to extrapolate the nitrogen input by *Trichodesmium* blooms for the whole region. The estimated annual nitrogen gain for the region by such blooms is ∼0.9 Tg N y^{-1} in good agreement with that reported by *Capone et al.* [1998] (∼1 Tg N y^{-1}). However, in the present study, fixation rate at NF6 is ∼50 times higher than at the other stations (Figure 3.5). For calculating the average rate we take the arithmetic mean of data except from NF6, and then take the geometric mean of this value and the data from NF6; we estimate that 2.01 mmol N m^{-2} d^{-1} is likely fixed in the Arabian Sea during a bloom. After extrapolating the results into the area of bloom occurrence and its duration we have estimated that 6.2 Tg y^{-1} (arithmetic mean of all results in 6.7 Tg N y^{-1}, which is the same within the error; however, geometric mean of all the data suggests 1.1 Tg N y^{-1}) nitrogen is fixed in the Arabian Sea, which is ∼5% of global nitrogen fixation in the 2% of the global ocean area. In addition, dry and wet deposition aerosols supply 1.2 ± 0.2 Tg N y^{-1} in the Arabian Sea and much lesser amount through rivers i.e. 0.1 ± 0.02 Tg N y^{-1} [*Singh et al.*, 2011; *Singh and Ramesh*, 2011]. A simple calculation suggests that ∼85% of new nitrogen is gained through N_2 fixation.

The Arabian Sea loses 60 Tg N y^{-1} through denitrification [*Bange et al.*, 2005]. In addition, it has been suggested that biological production of N_2 in the Arabian Sea may exceed estimates based on canonical stoichiometries for denitrification [*Devol et al.*, 2006]. If suggestions from *Lam et al.* [2009] are to be taken seriously, then the same amount of nitrogen could be additionally lost through anammox.

A mystery about missing nitrogen still remains and suggests that there may be significant nitrogen fixation over the Arabian Sea not limited to spring and fall seasons alone. We believe that *Trichodesmium* may not be the only species which fixes N_2, as the presence of another diazotropth, i.e. γ-proteobacteria, is also reported in the Arabian Sea [*Bird et al.*, 2005] even in the presence of bio-available nitrogen. In addition, *Montoya et al.*, [2004] reported substantial N_2 fixation by smaller microbes. Heterotrophic diazotrophs may also contribute significantly to N_2 fixation in and outside the euphotic zone [*Mulholland and Capone*, 2009 and reference therein]. To address these issues, more measurements are required during different seasons, possibly including other diazotrophs.

3.2 N_2 fixation and carbon uptake rates in the Janssand Flat

It is recognized recently that heterotrophic bacteria present in the sediments can fix atmospheric N_2 and hence introduce 'new reactive nitrogen' to the system [*Dekas et al.*, 2009]. Sometimes nitrogen fixation can be associated with methane oxidation [*Dekas et al.*, 2009]. Even in the presence of ammonium, these bacteria

(ANME-2/DSS consortia) fix N_2. Because of dense and tightly packed organic matter, ammonium is not accessible to the bacteria and this constrained the bacteria to fix N_2.

Janssand Flat, a tidal-sandy flat located in the German Wadden Sea, is characterized by semi-diurnal tides with a tidal range of 2.6 m [*Flemming and Davis*, 1994]. It is exposed to the atmosphere for 6-7 hr each day depending upon the properties of the tides. It remains covered by 1-2 m during high tides. This is one of the biologically active regions. Aerobic denitrification ($\geq$ 0.19 mmol N m^{-2} h^{-1}) is reported in this region [*Gao et al.*, 2010]. On the basis of previous studies on this Flat we hypothesize that the loss of reactive nitrogen could be compensated by N_2 fixation. Although sandy flats cover a large area in the continental margins but a little is known about such flats' role in the nitrogen cycle. N_2 fixation, along with carbon uptake, is investigated in the present study using four combinations of labelling to understand the role of other compounds, i.e. (a) $^{15}N_2$+^{13}C - for estimating of natural N_2 fixation and carbon uptake (b) $^{15}N_2$+^{13}C+Glucose - to prove/disprove the hypothesis of heterotrophic N_2 fixation (c) $^{15}N_2$+^{13}Glucose - for estimating the Glucose uptake rates along with N_2 fixation, and (d) $^{15}N_2$+$^{13}CH_4$ - to understand the role of methane in the N_2 fixation; motivation to add methane came from study by *Dekas et al.* [2009].

3.2.1 N_2 fixation rates

N_2 fixation rates are shown in the Figure 3.6. Samples were incubated in light as well as in dark in triplicates and the standard deviation is shown as error bars. Some error bars are large because of the heterogeneity in sample amount. It was difficult to implant equal amount of sediments in each bottle.

Significant N_2 fixation is observed in the samples labelled with $^{15}N_2$+^{13}C (Figure 3.6a). N_2 fixation increases with depth during incubation in the light except at sediment from the 0-5 cm depth, however, it remains constant (within the error) with the depth during dark incubation. This disproves the hypothesis of heterotrophic

N_2 fixation to a small extent.

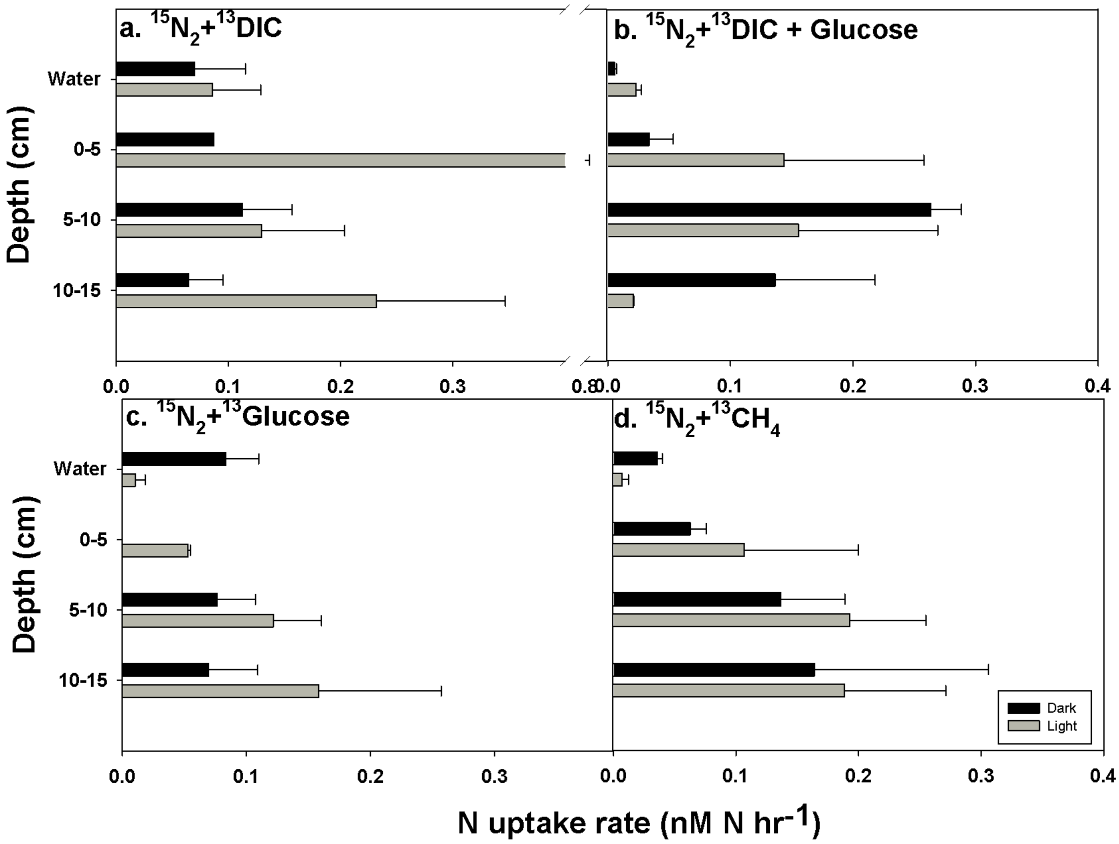

Figure 3.6: Nitrogen fixation rates (a) $^{15}N_2$+^{13}C (b) $^{15}N_2$+^{13}C+Glucose (c) $^{15}N_2$+^{13}Glucose and (d) $^{15}N_2$+^{13}CH$_4$. Grey and black bars show light and dark incubations respectively. Error bars are the standard deviation of triplicates. Note the break axis at 0.4-0.8 in (a)

In the treatments with un-labelled glucose (Figure 3.6b), N_2 fixation increases with depth upto (10 cm) during incubation in the light and dark both and then decreases at the deeper depth. N_2 fixation rates in treatment with $^{15}N_2$+^{13}C are not significantly different to that in treatment with $^{15}N_2$+^{13}C+Glucose, except at 0-5 cm depth. This indicates that glucose could not stimulate the N_2 fixation. This also rejects the heterotrophic N_2 fixation hypothesis to a certain extent.

In treatments with labelled glucose, rates in the light incubation increases significantly with depth, however, no such trend is observed in the dark incubation.

A clear increasing trend in N_2 fixation rates is observed in both the light and dark incubations when samples were labelled with $^{15}N_2$+$^{13}CH_4$ (Figure 3.6d). Incubation done under the light shows higher rates than those in dark, except in the water sample. However, these rates (with treatment d) are not significantly different with compare to other treatments (a, b, c). This suggests that N_2 fixation is not associated with methane oxidation.

Overall, A large variation in N_2 fixation rates is observed; it varies from 0.01 to 0.50 ± 0.32 nM N h^{-1}, with the maximum rate at 0-5 cm depth during the incubation in the light. In most of the treatments, rates at deeper depths (10-15 cm) are significantly higher than the surface values except in treatment (a), where highest rate (0.50 ± 0.32 nM N h^{-1}) is found at 0-5 cm (Figure 3.6). N_2 fixation in the overlying water is always less than that in the sediments (Figure 3.6a-d). On one side where treatments with glucose rules out the possibility of heterotrophic N_2 fixation, increase in the rates with depths still suggests heterotrophic N_2 fixation. Nevertheless, incubation under the light suggests that autotrophic N_2 fixation does take place significantly in the sediments and the overlying water of the Janssand Flat.

3.2.2 Carbon uptake rates

Carbon uptake rates are shown in the Figure 3.7. Carbon uptake and N_2 fixation rates are measured on the same samples. Significant carbon uptake rates are observed in the samples labelled with $^{15}N_2$+^{13}C (Figure 3.7a). Carbon uptake rate increases with depth during the incubation in both the light and dark incubations. In the treatments with un-labelled glucose (Figure 3.7b), carbon uptake rate increases with depth during incubation in both the light and dark. Rates of carbon uptake in dark are higher than the light which show a heterotrophic nature of the bacteria. Carbon uptake rates in treatment with $^{15}N_2$+^{13}C are not significantly different to that in treatment with $^{15}N_2$+^{13}C+Glucose. This indicates that like the N_2 fixation, glucose do not affect carbon uptake rates either which is in contradiction to the earlier statement stating the presence of heterotrophic bacteria.

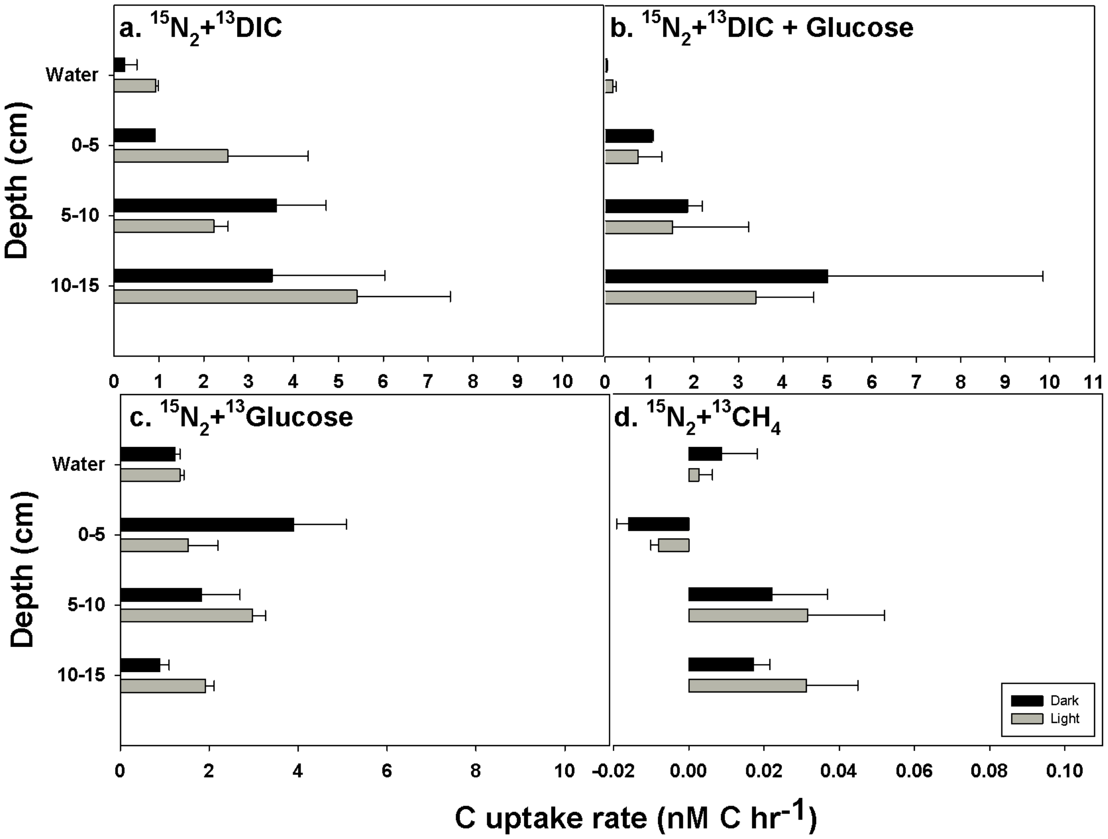

Figure 3.7: Carbon uptake rates (a) $^{15}N_2$+^{13}C (b) $^{15}N_2$+^{13}C+Glucose (c) $^{15}N_2$+^{13}Glucose and (d) $^{15}N_2$+$^{13}CH_4$. Grey and black bars show light and dark incubations respectively. Error bars are the standard deviation of triplicates. Note the change in the scale of the x-axis in (d)

In treatments with labelled glucose, no trends in the carbon uptake rate is observed. It confirms the results obtained in the treatments (a) $^{15}N_2$+^{13}C and (b) $^{15}N_2$+^{13}C+Glucose.

Results from the incubations with $^{15}N_2$+$^{13}CH_4$ are surprising (Figure 3.7d). Carbon uptake rates are an order of magnitude less than with the other treatments (note the change in the scale of the x-axis in the Figure 3.7d. Samples incubated from 0-5 cm depth show negative carbon uptake rates, this is just mathematical artifact and indicates that bacteria oxidize methane but do not assimilate it. No trend is seen in either the light or dark incubations when samples were labelled with $^{15}N_2$+$^{13}CH_4$ (Figure 3.7d).

Incubation done under the light is insignificantly different from those done in the dark. As in the case of N_2 fixation, carbon uptake in the overlying water is also always less than that in the sediments (Figure 3.7a-d).

3.2.3 Integrated rates

Significant N_2 fixation and carbon uptake rates are observed (Table 3.3). N_2 fixation varies from 63-141 μmol N m^{-2} y^{-1} (on an average 97 μmol N m^{-2} y^{-1}) while carbon uptake varies in a wide range i.e. 9.8-2121 μmol C m^{-2} y^{-1} (on an average 1337 μmol C m^{-2} y^{-1}). Rates are not as higher as hypothesized though these rates are comparable to those observed in the many oligotrophic regions; e.g. N_2 fixation in Gulf of California ranged from 20-250 μmol N m^{-2} y^{-1} (on an average 106 μmol N m^{-2} y^{-1}) [*White et al.*, 2007].

Table 3.3: Depth integrated N_2 fixation (μmol N m^{-2} y^{-1}) and carbon uptake rates (μmol C m^{-2} y^{-1})

Treatments	N_2 fixation	Carbon uptake
$^{15}N_2$+^{13}C	141	2121
$^{15}N_2$+^{13}C+Glucose	86	1510
$^{15}N_2$+^{13}Glucose	63	1709
$^{15}N_2$+$^{13}CH_4$	98	9.8

3.3 Conclusion

We report the first results of direct measurements of N_2 fixation in the Arabian Sea, useful to constrain the regional nitrogen budget. N_2 fixation by *Trichodesmium* occurs mainly in the upper 10 m of the ocean surface, while carbon uptake happens throughout the euphotic zone. Our results suggest that significant dinitrogen is fixed (∼5% of the global N_2 fixation) during a *Trichodesmium* bloom in the Arabian Sea. Our estimate shows that previously N_2 fixation rates were considerably underestimated, however, the revised value for the fixed nitrogen (6.2 Tg N y^{-1})

is still far less than the estimated nitrogen loss (~120 Tg N y^{-1}) through denitrification, assuming an equal rate of nitrogen loss through anammox. N_2 fixation is the most important process among all the nitrogen gain processes and the Arabian Sea gains ~85% of its 'new' nitrogen through this process. Lower values of $\delta^{15}N$ of PON associated with higher fixation rates confirm the presence of N_2 fixing bacteria. Higher N_2 fixation rates are consistent with higher carbon uptake rates. The presence of microbes that are incapable of fixing N_2, leads to higher consumption ratios.

Nitrogen and carbon fixation experiments with different labelling treatments were carried out in the Wadden Sea sediment (Janssand Flat). N_2 fixation was observed in the Wadden Sea sediments, fixation rates were not as high as hypothesized. A large variation in these rates is observed due to the heterogeneity in the samples. Lower fixation rates could be possible if N_2 fixation varies seasonally. Most of the measurements show that the uptake rates are higher under light than in the dark (Figure 3.6). With methane treatments, rates increase significantly with depth. Glucose does not seem to play any significant role. In addition, higher rates of carbon fixation were observed with different treatments of carbon (^{13}C, ^{13}Glucose); and treatment with $^{13}CH_4$ does not support higher carbon fixation. These results may be taken in to account to understand the marine nitrogen cycle better. To understand this process better in the sediments a further study during summer is required. The present study is the first attempt to quantify the N_2 fixation rates in the Wadden Sea sediments using $^{15}N_2$ tracer technique which may provide a better understanding of N_2 fixation (beyond the traditional N_2 fixers). The technique developed here for measuring N_2 fixation in the sediments can be used to measure the same in sediments from the northern Indian Ocean.

Chapter 4

Simulating nitrogen loss in the ocean and its application in other processes

Extending the use of stable isotopes further, an attempt is made here to understand nitrogen loss process in the Arabian Sea theoretically and verify it using data available in the literature. This model is further applied to understand other some oceanographic processes as well.

Stable isotopic evolution of a reservoir from which material is continuously removed with isotopic fractionation is generally described by the Rayleigh equation [*Dansgaard*, 1964], widely used in geochemical research to describe two-component systems [*Rayleigh*, 1902; *Broecker and Oversby*, 1971; *Hoefs*, 1980; *Gat and Gonfiantini*, 1981; *Faure*, 1986; *Clark and Fritz*, 1997; *Criss*, 1999; *Mook*, 2006; *Sharp*, 2007]. It has been extended to the case of multi-component sources as well [*Ray and Ramesh*, 2000]. Here we present an equation describing isotopic fractionation in open systems, wherefrom material is not only removed with isotopic fractionation, but fresh material of a different isotopic composition is added from an external source, at a given rate, and some examples where this equation is applicable.

4.1 Deriving the equation

Let R be the (non-radiogenic) stable isotopic ratio under consideration (e.g. $^{18}O/^{16}O$, D/H, $^{13}C/^{12}C$, $^{15}N/^{14}N$, etc.), denoted by N^*/N, where N^* and N are respectively the number of molecules containing the heavier and lighter isotopes of a given mass of the same element (e.g. oxygen; $H_2{}^{18}O$ and $H_2{}^{16}O$; $N^* << N$; typical values in the ocean are 2000 and 106, respectively, in $\sim 3 \times 10^{-17}$ g of water). Taking the logarithm and differentiating, we obtain

$$\frac{\mathrm{d}R}{R} = \frac{\mathrm{d}N^*}{N^*} - \frac{\mathrm{d}N}{N} = \frac{\mathrm{d}N^*}{RN} - \frac{\mathrm{d}N}{N} \tag{4.1}$$

At any instant $\mathrm{d}N_e^*$ and $\mathrm{d}N_e$ of the isotopically heavier and lighter molecules, respectively, are being removed by some physical process (e.g. evaporation from a lake) during an infinitesimal time interval $\triangle$t. Isotopic fractionation implies that $\mathrm{d}N_e^*$ is not equal to $\mathrm{d}N_e$. In such a case, we define a fractionation factor between the material leaving (e.g. vapour) and the material left behind (e.g. water) as $\alpha = [\mathrm{d}N_e^*/\mathrm{d}N_e]/R$. In per mil units (‰), this fractionation factor is represented by $\epsilon = (\alpha - 1) \times 10^3$. We restrict our consideration to isothermal processes where α and ϵ are constants. As in the case of Rayleigh fractionation, we assume that the reservoir remains isotopically homogeneous and has no isotopic gradients within, at any time. Let $\mathrm{d}N_r^*$ and $\mathrm{d}N_r$ of the heavier and lighter molecules be added to the reservoir during the interval $\triangle$t, but without fractionation (i.e. $\mathrm{d}N_r^*/\mathrm{d}N_r$ is the same as N_r^*/N_r, the isotopic composition of the contributing source, which remains a constant $R_r \neq \alpha$R). Therefore, the net changes in the numbers of heavier and lighter isotopic molecules during $\triangle$t are $\mathrm{d}N^* = \mathrm{d}N_r^*$ - $\mathrm{d}N_e^*$ and $\mathrm{d}N = \mathrm{d}N_r$ - $\mathrm{d}N_e$ respectively, and their ratio,

$$\frac{\mathrm{d}N^*}{\mathrm{d}N} = \frac{\beta R_r - \alpha R}{\beta - 1} \tag{4.2}$$

where β is $\mathrm{d}N_r/\mathrm{d}N_e$, the ratio of the amount of material added to that lost (the case $\beta = 1$ causes a singularity in eq. (4.2) and is discussed as a special case later). Integrating eq. (4.2) using eq. (4.1), with initial value of R as R_0, we obtain (see Appendix 1 for details in *Ramesh and Singh*, [2010]):

$$R = R_0 f^{\rho} + \frac{\beta R_r}{\alpha + \beta - 1}(1 - f^{\rho}), \text{when } \beta \neq 1 \tag{4.3}$$

Here f is the fraction of the material left in the reservoir relative to its initial amount, i.e. $(N^* + N)/(N_0^* + N_0)$, approximated as (N/N_0), and $\rho = \alpha/(1 - \beta) - 1$. When $\beta = 0$, i.e., when these are only loss of material and no addition, this reduces to $R = R_0\ f^{\alpha-1}$, the classical Rayleigh fractionation equation. Using the δ notation for isotope ratios, taking the initial composition R_0 of the reservoir to be the reference value relative to which all other δ values are expressed, we have $\delta = (R/R_0 - 1)\times10^3$ ‰ and $\delta_r = (R_r/R_0 - 1)\times10^3$ ‰. With this standard notation eq. (4.3) becomes

$$\delta = (1 - f^{\rho})\frac{\beta\delta_r - \epsilon}{\alpha + \beta - 1}, \text{when } \beta \neq 1 \tag{4.4}$$

For the case where $\beta = 1$, we cannot express the isotopic ratio of the reservoir as a function of f because it remains constant at unity (i.e. N remains as N_0), as the amount of material lost is compensated exactly by the incoming material from the source. A different approach is therefore necessary. The change in the number of heavier molecules is given, as before, by $\mathrm{d}N^* = \mathrm{d}N_r^* - \mathrm{d}N_e^*$, while the change in the number of lighter molecules is $\mathrm{d}N = \mathrm{d}N_r - \mathrm{d}N_e = 0$, as $\beta = \mathrm{d}N_r/\mathrm{d}N_e = 1$. Therefore, the change in the isotopic ratio of the reservoir is $\mathrm{d}R = R_r(\mathrm{d}N_r/N) - \alpha\ R(\mathrm{d}N_e/N)$ (mass balance is used: $R\mathrm{d}N = 0$ as $\mathrm{d}N = 0$). This can be rewritten as

$$\frac{\mathrm{d}R}{R_r - \alpha R} = \frac{\mathrm{d}N_r}{N_0} \tag{4.5}$$

Integrating this with initial value of R as R_0, we get

$$R = R_0 e^{-\alpha N_r/N_0} + \frac{R_r}{\alpha}(1 - e^{-\alpha N_r/N_0}) \tag{4.6}$$

Here N_r indicates the total number of lighter isotopic molecules added thus far. In the δ notation, eq. (4.6) becomes:

$$\delta = \frac{(\delta_r - \epsilon)}{\alpha}(1 - e^{-\alpha N_r/N_0}) \tag{4.7}$$

It is clear that for large mixing (i.e. $N_r >> N_0$), the reservoir isotopic composition (δ) saturates to (δ_r - ϵ)/α, rather than δ_r expected in the case of simple mixing, as here both mixing and removal by fractionation occur simultaneously. However, when α is small (e.g. close to unity), thus δ reaches δ_r - ϵ. We note that eq. (4.4) was derived in another form by *Mook* [2006]. The case of alteration of radiogenic stable isotopes undergoing isotopic exchange with meteoric water was treated similarly by *Albarede* [1995]. On the other extreme, when $N_r << N_0$, $\delta \approx$ (δ_r - ϵ)(N_r/N_0).

Figure 4.1 shows an example of the isotopic (δ) evolution of a reservoir as a function of the fraction (f) left of the initial amount. The fractionation factor α has been taken as 1.01 (i.e. ϵ = 10‰) and isotopic composition of the source contributing to the reservoir, as -10‰. As the material lost from the reservoir is isotopically heavier in this example (i.e. $\alpha > 1$), the isotopic composition of the remaining material rapidly decreases and reaches close to -46‰ (from a value of 0), when f becomes small ($\sim$0.01); this is the Rayleigh case where no material is added to the reservoir ($\beta = 0$ in Figure 4.1). As β values increase, the reservoir δ value is brought up higher and higher, as the source steadily contributes material with a constant isotopic composition (δ_r) of -10‰. The saturation value is δ_r - ϵ = -10-10 = -20‰, as expected from eq. (4.7).

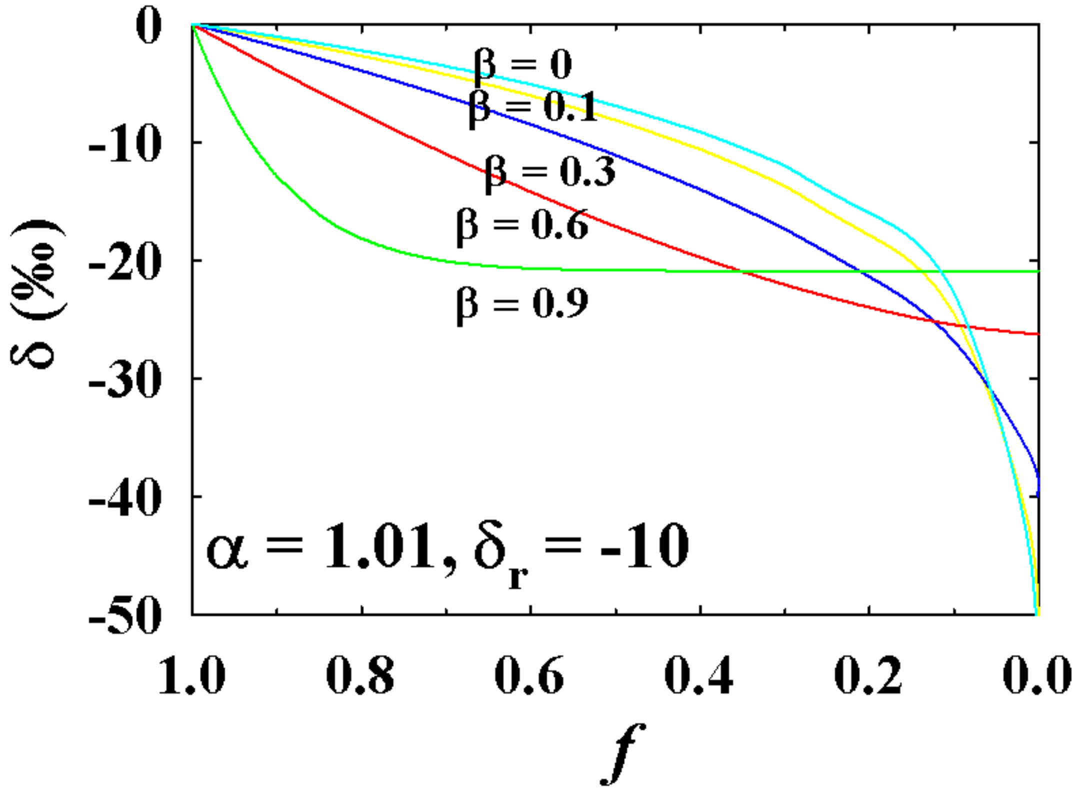

Figure 4.1: An example of the evolution of the isotopic composition (δ) of a reservoir as a function of the fraction (f) of the original material left, for different values of β, the ratio of instantaneous amount added to that lost ($\beta \neq 1$). The isotopic composition of the external source is taken as -10‰ and the fractionation factor, 1.01

Figure 4.2 shows another example where fractionation factor has been taken as 0.99 (ϵ = -10‰) and isotopic composition of the source contributing to the reservoir, as -10‰. As the material lost from the reservoir is isotopically lighter in this example (i.e. $\alpha < 1$), the isotopic composition of the remaining material rapidly increases and reaches close to +47 ‰(from a value of 0), when f becomes small (~0.01); this is the Rayleigh case where no material is added to the reservoir (closed system, $\beta = 0$ in Figure 4.2). As β increases, the reservoir δ value is lowered further and further, as the source steadily contributes material with a constant isotopic composition (δ_r) of -10‰. The saturation value is δ_r - ϵ = -10-(-10) =

0‰, as expected from eq. (4.7).

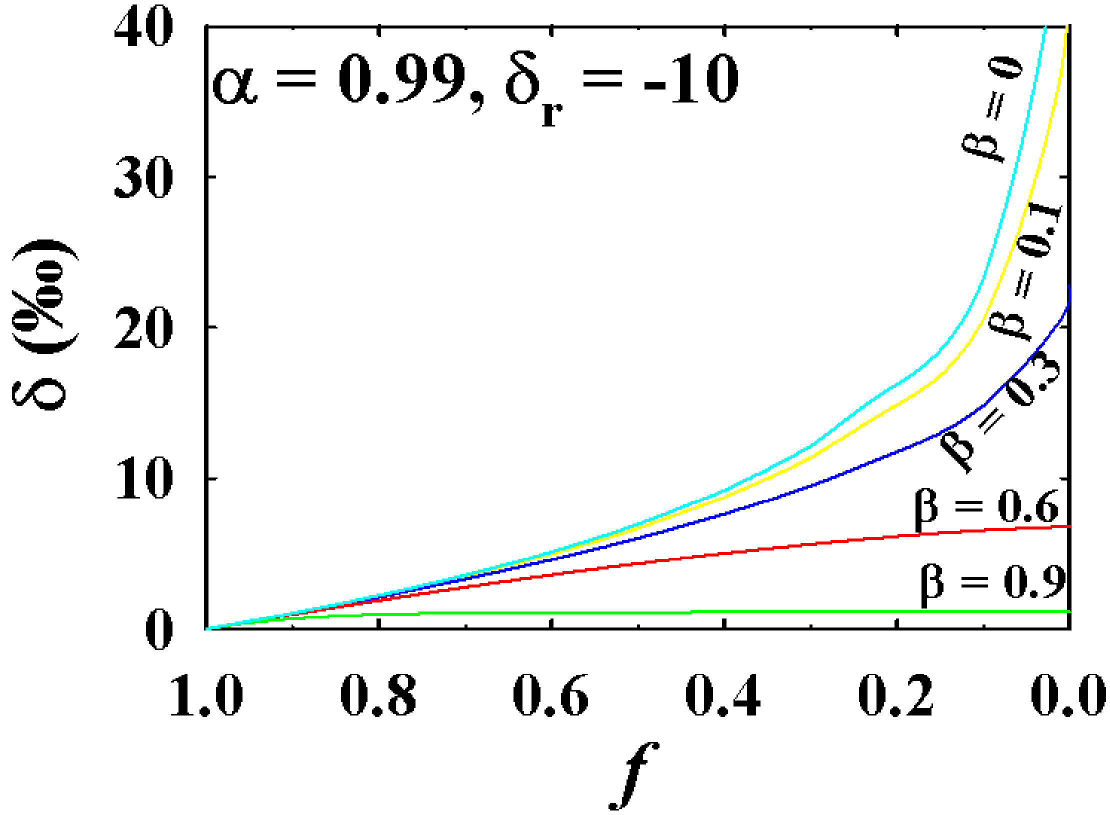

Figure 4.2: An example of the evolution of the isotopic composition (δ) of a reservoir as a function of the fraction (f) of the original material left, for different values of β, the ratio of instantaneous amount added to that lost ($\beta \neq 1$). The isotopic composition of the external source is taken as -10‰ and the fractionation factor, 0.99

We further discuss a general example for a special case of $\beta = 1$, i.e. the rates of addition and removal of material remain same at any instant. Figure 4.3 shows the isotopic (δ) evolution of a reservoir as a function of N_r/N_0 (ratio of lighter isotopic molecules being added by some source to the number of initial lighter isotopic molecules of the reservoir) for different combinations of enrichment factor (ϵ) and isotopic composition of material being added (δ_r). Initial isotopic composition of the reservoir is taken 5‰ . The enrichment factor ϵ has been taken as -25‰ and -22‰ and δ_r as 10‰ and 5‰ . Keeping δ_r constant, δ in the case of more negative ϵ increases faster than in the case of less negative ϵ. While keeping ϵ constant, δ in the case of higher δ_r increases faster than that in the case of lower δ_r.

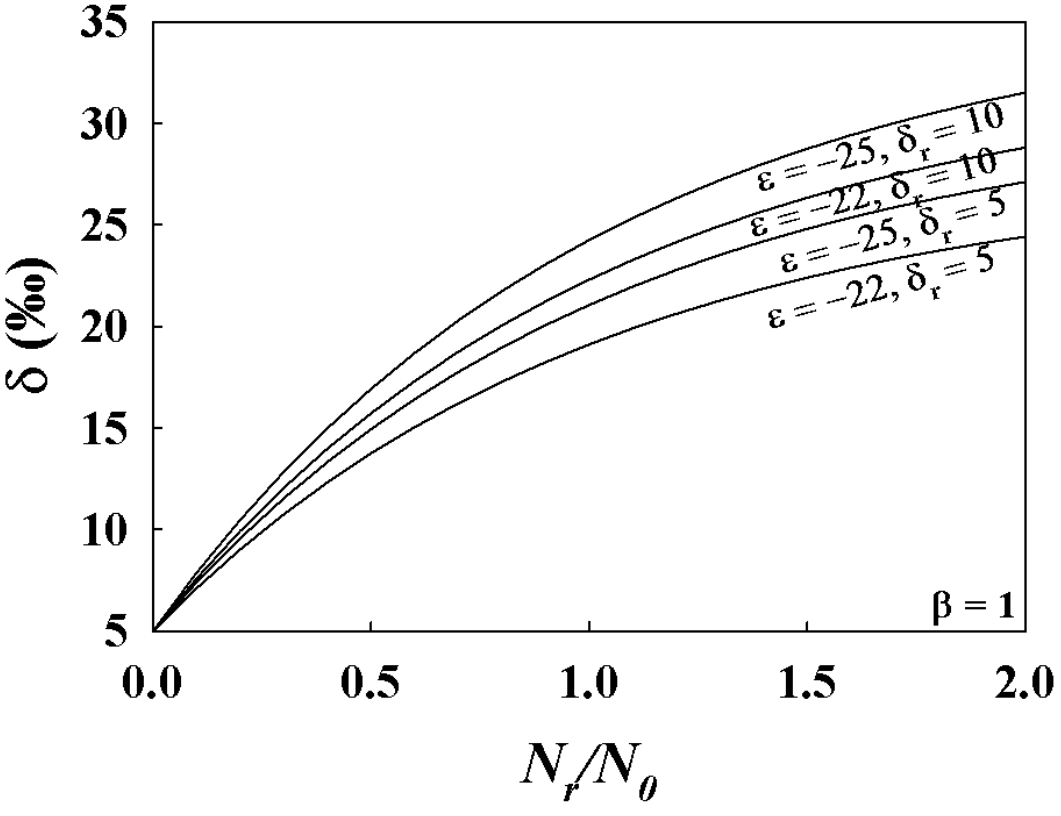

Figure 4.3: An example (for $\beta = 1$, i.e. the rate at which material is being added is equal to the removal rate) of the evolution of the isotopic composition (δ) of a reservoir as a function of N_r/N_0 (ratio of the total number of lighter isotopic molecules being added from an external source to the number of initial lighter isotopic molecules of the reservoir) for different combinations of ϵ and δ_r.

We now discuss some examples where the given equations are applicable: ocean denitrification and soil organic matter decomposition. Data on both processes are limited. We extracted the data on isotopic composition (δ) and f values from the literature using the 'origin' package.

4.2 Simulating denitrification in the Arabian Sea

Primary productivity in surface ocean is generally limited due to unavailability of nutrients. However, some parts of the world oceans are highly productive due to nutrient inputs by upwelling, riverine inputs, etc. Decomposition of organic matter in these regions at intermediate ocean depths (∼500 m) leads to oxygen deficiency at these depths. In such regions microorganisms use nitrate as an oxidant to decompose organic matter and produce N_2O and N_2 gases ($NO_3^- \rightarrow NO_2^- \rightarrow NO \rightarrow N_2O \rightarrow N_2$). This microbially catalysed multi-step process is known as denitrification [*Richards*, 1965; *Payne*, 1973]. Ocean loses bioavailable nitrogen (NO_3^-) through this process. Denitrification occurs in oxygen minimum zones (OMZ) of the world oceans, e.g. the eastern tropical North Pacific and the Arabian Sea [*Cline and Richards*, 1972; *Naqvi*, 1987]. During denitrification, the nitrate concentration, $[NO_3^-]$, in OMZ (generally 150-1000 m depth) decreases, i.e. f decreases. Denitrifying bacteria reduce lighter nitrate ($^{14}NO_3$) preferentially; hence the remaining NO_3^- gets enriched in heavier isotopes (^{15}N). At the same time, NO_3^- is being added by settling organic matter from above, by decay. If this is unaccounted for, the isotopic composition of the NO_3^- reservoir can be significantly different from that expected from a simple Rayleigh model. Unlike earlier studies, we apply eq. (4.4), which takes this effect into account, to understand the isotopic evolution of nitrate in the OMZ of the Arabian Sea using literature data.

Brandes et al. [1998] obtained values for the enrichment factor (ϵ) and initial isotopic composition of nitrate (δ_0) of -22‰ and 6‰, respectively, in the Arabian Sea using a simple Rayleigh model and the measured $\delta^{15}N$ values of dissolved NO_3^-. We know that organic matter steadily rains down to the deeper ocean and therefore treating this system with a simple Rayleigh equation may lead to an incorrect estimation of the fractionation factor. This is borne out by laboratory derived ϵ values, which show large variations -17‰ to -29‰ [*Delwiche and Steyn*, 1970; *Mariotti et al.*, 1981; *Barford et al.*, 1999].

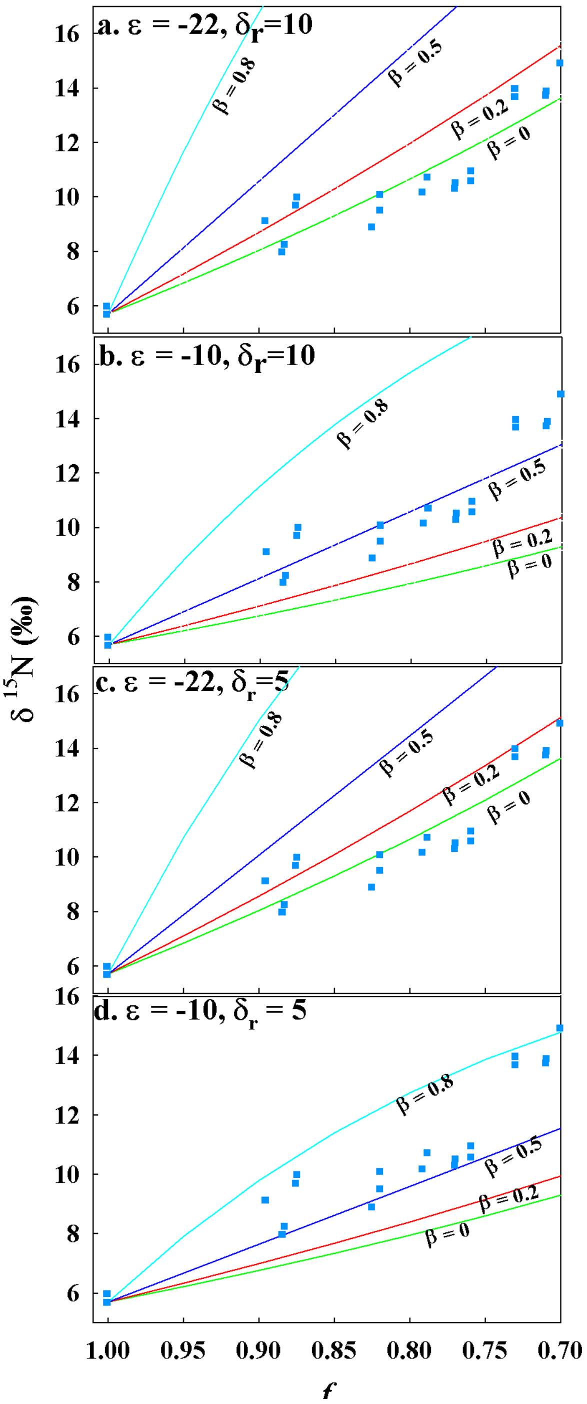

Figure 4.4: An example of denitrification in the sea: open squares in all the plots show the variation of δ^{15}N of dissolved NO_3^- with f (fraction of NO_3^- remaining) from experimental data [*Brandes et al.*, 1998]. Initial isotopic value of nitrate (δ_0) is 5.7‰ and β values are taken as 0, 0.2, 0.5 and 0.8. Dotted and solid lines are plotted using eq. (4.4) for different β values. a, ϵ = -22‰ and δ_r = 10‰; b, ϵ = -10‰ and δ_r = 10‰; c, ϵ = -22‰ and δ_r = 5‰; d, ϵ = -10‰ and δ_r = 5‰.

We use different combinations of ϵ (-22‰ and -10‰) and δ_r values (5‰ and 10‰) to understand the isotopic evolution of nitrate and estimate the fraction of material added. β values are taken as 0, 0.2, 0.5 and 0.8. As the data are from *Brandes et al.* [1998], for ϵ = -22‰, it shows no addition from an external source (Figure 4.4a), even by changing the δ_r value 10‰ to 5‰ as f decreases from 1 to 0.75 (Figure 4.4a and c). But when f decreases further (0.75-0.70), ~20% contribution from external source is observed. In Figure 4.4b and d, when ϵ value is -10‰, results show that ~50% of the nitrate that is lost during denitrification is compensated by organic matter raining from above, for a small initial decrease in f; if f decreases further, this contribution rises to ~80%. Thus by fixing β, the ratio of the rates of nitrate release due to fresh organic matter getting oxidized and the in situ denitrification, we can constrain the fractionation factor better with the eq. (4.4). In this special case $\delta_r = \delta_0$.

4.3 Soil organic matter decomposition

Now we discuss another example where soil organic matter (SOM) is decomposed by bacteria up to 100 cm depth. Similar to oceanic denitrification, these decomposing organisms also preferentially release lighter isotopic molecules (^{12}C) for respiration and hence remaining SOM enriched in heavier isotopes (^{13}C) [*Blair et al.*, 1985; *Cleixner et al.*, 1993]. Decrease in the total carbon content and increase in δ^{13}C are signatures of fractionation during decomposition of SOM. There is a supply of organic matter from above by diffusion/leaching, so eq. (4.4) is suitable to characterize this process. Surface isotopic composition of SOM is taken as initial isotopic composition (δ_0; freshly deposited organic matter). The remaining fraction f of SOM is calculated as the ratio of carbon content at a particular depth and the surface [*Accoe et al.*, 2002].

Accoe et al. [2002] have estimated an ϵ value -2.3‰ using the simple Rayleigh model. We use four different combinations of ϵ (-2.3‰ and -1‰) and δ_r (-25‰ and -30‰) values in eq. (4.4) to analyse the same data.

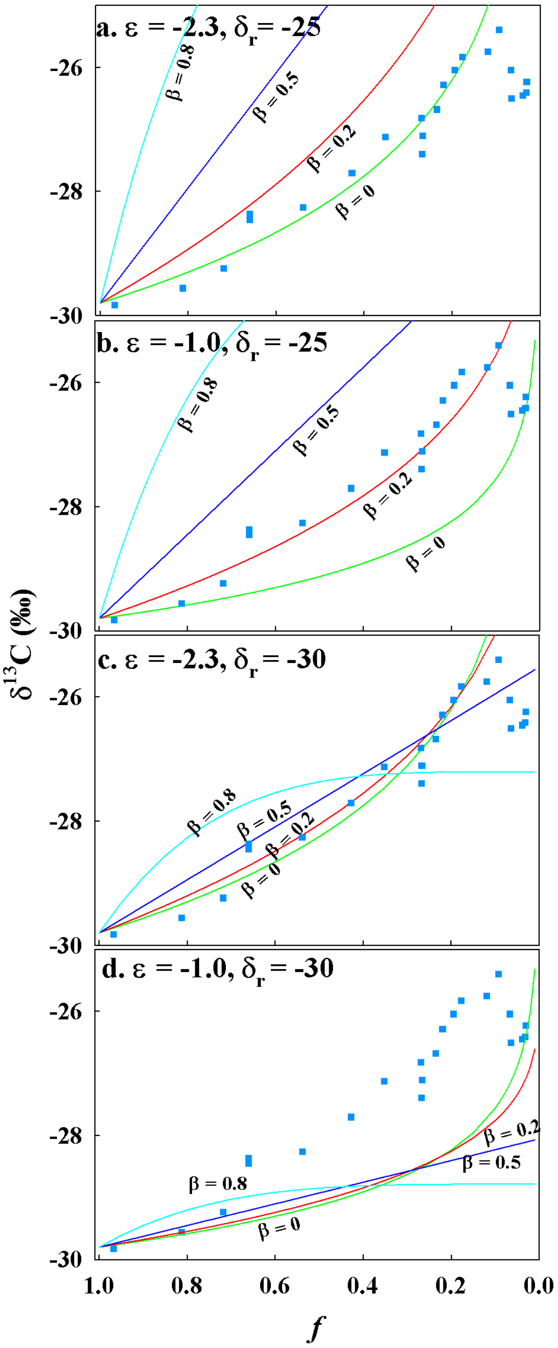

Figure 4.5: Example where soil organic matter (SOM) is decomposed by microorganisms: open squares in all the plots show the variation of δ^{13}C of SOM variation with f (fraction of SOM remaining) from experimental data [*Accoe et al.*, 2002]. Initial isotopic value of SOM (δ_0) is -29.8‰ and β values are taken as 0, 0.2, 0.5 and 0.8. Dotted and solid lines are derived using eq. (4.4) for different β values. a, ϵ = -2.3‰ and δ_r = -25‰; b, ϵ = -1‰ and δ_r = -25‰; c, ϵ = -2.3‰ and δ_r = -30‰; d, ϵ = -1‰ and δ_r = -30‰.

In Figure 4.5a and b, when δ_r remains constant (-25‰), an increase in enrichment factor shows that contribution of SOM from above increases (i.e. β value increases). In Figure 4.5c, when f decreases from 1 to 0.7, no external contribution ($\beta = 0$) is seen. Further decrease in f shows $\beta = 0.2$. When ϵ = -1‰ and δ_r = -30‰ (Figure 4.4d), data points are difficult to explain especially when f decreases from 0.7 to 0.0. This happens because unlike all other cases, here value of the external source is less than the initial reservoir value. While increasing β, isotopic com- position of the resultant SOM cannot be increased, therefore it saturates. This can be used as an indication of absence of carbon percolation from above.

4.4 δ^{18}O-salinity relation in the northern Indian Ocean

Oxygen isotopic composition (δ^{18}O) and salinity (S) of surface ocean water are important tools for tracing water masses and paleoclimatic reconstruction using foraminiferal δ^{18}O in sediment cores [*Duplessy et al.*, 1981; *Rostek et al.*, 1993; *Paul et al.*, 1999; *Tiwari et al.*, 2005; 2009]. δ^{18}O and salinity are known to covary linearly in the surface ocean [e.g. *Criss*, 1999; *Bigg and Rohling*, 2000]. As δ^{18}O of certain foraminiferal shells faithfully represents the sea water δ^{18}O, the slope of the δ^{18}O-S relation is used to reconstruct paleosalinity, assuming it to be time invariant [e.g. *Rostek et al.*, 1993]. In reality, the slope may vary seasonally and spatially depending on environmental conditions [*Rohling and Bigg*, 1998; *Benway and Mix*, 2004; *Austin et al.*, 2006]. Evaporation (E), precipitation (P), continental run-off (R), upwelling/advection, and eddy diffusion are the major physical processes that determine δ^{18}O-S relation [*Ferronsky and Brezgunov*, 1989]. Here present a new data set for the northern Indian Ocean and address the spatiotemporal variability of this relation and its implication.

Unlike other oceans, the northern Indian Ocean being bounded by the Asian land mass to its north suffers a strong seasonal change in the wind direction, known as the monsoon circulation. During June-September (Southwest or summer monsoon), strong winds blow from ocean towards land resulting in higher evaporation in the northwestern Indian Ocean (Arabian Sea) relative to the northeastern Indian Ocean (Bay of Bengal). The highest rainfall occurs along the west coast and northeastern regions of Indian peninsula during this season [*Gadgil*, 2003]. During December-February (Northeast or winter monsoon), cool and dry air from the Himalaya enhances evaporation in the northeastern Arabian Sea causing convective mixing, while there is little rainfall over most of India. The Arabian Sea and the Bay of Bengal, located at similar latitudes (Figure 2.8), significantly differ in some aspects: e.g. the former loses ~1 m y^{-1} fresh water through evaporation, while the latter receives ~2 m y^{-1} by intense precipitation [*Prasad*, 1997]. Additionally, the Bay receives a large river discharge from the Ganga, Brahmaputra, Mahanadi, Godavari and Krishna (Figure 2.8) rivers, particularly in the north (1.6×10^{12} m^3 y^{-1} compared to 0.3×10^{12} m^3 y^{-1} to the Arabian Sea from rivers Narmada, Tapti, Nethravati and Indus, *Subramanian*, [1993]). The mean δ^{18}O value of the river discharge to the Arabian Sea is likely to be higher than that to the Bay [*Lambs et al.*, 2005], as the major runoff to the Bay is from rivers of Himalayan origin. Maximum seasonal variations in salinity of 2 and 8 psu are observed in the Arabian Sea and the Bay of Bengal, respectively [*Delaygue et al.*, 2001; *Rao and Sivakumar*, 2003]. The East India Coastal Current (EICC) during the winter, transports low salinity water from the Bay to the southeastern Arabian Sea (Figure 2.8). The West India Coastal Current (WICC) carries this water northward [*Shetye, 1999*; *Schott and McCreary*, 2001], and decreases the surface salinity of the eastern Arabian Sea. In contrast, during summer, the eastward flowing Indian Monsoon Current carries high salinity water from the Arabian Sea to the Bay of Bengal [*Prasanna Kumar and Prasad*, 1999; *Vinayachandran et al.*, 1999]. Thus both basins experience significance changes in salinity and δ^{18}O through the exchange of surface waters.

At present in the northern Indian Ocean, evaporation, precipitation and continental run-off dominate over other processes, the relative contributions of these processes being very different in the Arabian Sea and the Bay of Bengal. The northwestern Arabian Sea experiences a large E-P flux (excess of evaporation over precipitation) decreasing towards the southeastern part of the Arabian Sea where intense rainfall results into higher P-E. Because of the geography of the Indian sub-continent, surface water of the Bay is more diluted by river run-off than that of the Arabian Sea [*Rohling and Bigg*, 1998; *Rao and Sivakumar*, 2003], decreasing the surface salinity of the Bay by ~2 psu relative to the southern Indian Ocean [*Delaygue et al.*, 2001]. In oceanic surface waters, salinity and δ^{18}O (1) increase due to evaporation, (2) decrease due to precipitation and continental run-off, (3) vary due to mixing by advection and diffusion, and generally, show a linear relation, the slope of which might vary seasonally and geographically, as the controlling processes are season, climate and location dependent [*Craig and Gordan*, 1965; *Rohling and Bigg*, 1998; *Delaygue et al., 2001*; *Clark and Fritz*, 1997; *Schmidt et al.*, 2007]. Published δ^{18}O data pertaining to the northern Indian Ocean are limited; here we report additional data from eight different cruises during 1987-2009, and discuss the seasonal and spatial variations of the δ^{18}O-S relation in the northern Indian Ocean.

4.4.1 Results

Surface water samples were collected from the Bay of Bengal (Table 4.1; Figure 2.8) during (i) August-September, 1988 (*Gaveshani* G-200) (ii) March-April, 1991 (ORV *Sagar Kanya* SK-63) (iii) December 1991 (SK-70) (iv) September-October 2002 (SK-182) and (v) April-May 2003 (SK-191). Sample locations were the same for SK-182 and SK-191. From the Arabian Sea, samples were collected during (i) December, 1987 (SK-37) (ii) December, 1988 (SK-47) and (iii) March, 2009 (FORV *Sagar Sampada* SS-263).

In the Bay of Bengal, surface salinity ranged between 31 and 34 psu (mean value, μ = 32.6±0.8) and δ^{18}O from -1 to 0.5‰ (μ = -0.23±0.48) during March-April, 1991. For Apr-May, 2003 data are presented for two regions i.e. coastal and

Table 4.1: Mean and standard deviations of salinity and δ^{18}O, and their linear regression parameters in the northern Indian Ocean. Some published data also are included with appropriate references

Date	Cruise	Region	No. of samples	Mean Salinity $\pm \sigma_v^a$	Mean δ^{18}O $\pm \sigma_v^a$	Slope $\pm \sigma^b$	Intercept $\pm \sigma^b$	Correlation coefficient	References
Mar-Apr 1991	SK-63	Bay Of Bengal	39^c	32.6 ± 0.8	-0.23 ± 0.48	0.27± 0.04	-9.0± 1.3	0.77	This study
December 1991	SK-70	Coastal Bay Of Bengal	9	30.8 ± 2.8	-1.65 ± 0.60	0.17± 0.05	-7.0± 1.4	0.82	This study
Jan-Feb 1994	SK-93	Central Bay Of Bengal	78	33.3 ± 2.1	-0.11 ± 0.40	0.18± 0.01	-5.9± 0.2	0.97	*Delaygue et al.* [2001]
Apr-May 2003	SK-191	Coastal Bay Of Bengal	12	33.6 ± 0.5	0.15 ± 0.07	0.10± 0.04	-3.4± 1.2	0.69	This study
Apr-May 2003	SK-191	Central Bay Of Bengal	11	33.0 ± 0.5	0.24 ± 0.11	0.17± 0.05	-5.4± 1.7	0.74	This study
Aug-Sep 1988	G-200	Coastal Bay Of Bengal	12	33.4 ± 0.4	-0.17 ± 0.41	0.51± 0.3	-17.2± 10.0	0.47	This study
Sep-Oct 2002	SK-182	Bay Of Bengal	20	30.7 ± 4.2	-0.38 ± 0.96	0.21± 0.02	-6.9± 0.7	0.92	This study
-	-	Bay Of Bengal	22^d	-	-	0.45	-15.2	0.87	*Rostek et al.* [1993]
May-Jun 1977	OMD13	Southeastern Arabian Sea	5	35.6 ± 0.5	0.52 ± 0.12	0.23± 10^{-3}	-7.8± 0.1	1	*Duplessy et al.* [1981]
Jun-July 1976	OMD10	Southeastern Arabian Sea	9	35.5 ± 0.5	0.50 ± 0.14	0.25± 0.04	-8.3± 1.4	0.93	*Duplessy et al.* [1981]
December 1987	SK-37	Southeastern Arabian Sea	27	35.2 ± 0.4	0.91 ± 0.32	e	e	e	This study
December 1988	SK-47	Northeastern Arabian Sea	9	36.4 ± 0.5	0.62 ± 0.37	e	e	e	This study
March 2009	SS-263	Northeastern Arabian Sea	13	36.1 ± 0.5	0.56 ± 0.30	0.45± 0.12	-15.5± 4.4	0.74	This study
1977-1993	-	Northeastern Arabian Sea	112	-	-	0.26± 0.02	-8.9± 0.7	0.79	*Delaygue et al.* [2001]
-	-	Arabian Sea	52	-	-	0.28	-9.2	0.87	*Rostek et al.* [1993]
1987-2009	-	Northern Indian Ocean	152	33.4 ± 2.5	0.06 ± 0.80	0.26± 0.02	-8.6± 0.5	0.80	This study
Salinity and δ^{18}O in surface waters (50-500 m)									
Aug-Sep 1988	G-200	Coastal Bay Of Bengal	14	34.1 ± 0.5	-0.13 ± 0.30	0.42± 0.15	-14.4± 5.1	0.63	This study
December 1987	SK-37	Southeastern Arabian Sea	29	35.5 ± 0.4	0.99 ± 0.43	0.55± 0.16	-18.5± 5.6	0.56	This study
December 1987	SK-47	Northeastern Arabian Sea	16	35.6 ± 0.2	0.30 ± 0.35	e	e	e	This study

[a] σ_v is the standard deviation of observed data (not the uncertainty)

[b] σ represents uncertainty in the slope/intercept

[c] 5 data points encircled in the Figure 4.6(a) are excluded in the best fit line as these were sampled closer to the river-mouths

[d] δ^{18}O values of surface waters derived from δ^{18}O of foraminifera shells, assuming their precipitation under isotopic equilibrium

[e] Data show scatter

central Bay of Bengal. Most of the salinity values were ~33 psu in both the regions, while δ^{18}O values were similar (μ = 0.24±0.11 in central Bay and μ = 0.15±0.07 in the coastal Bay). Salinity and δ^{18}O variations were observed to lie between 33 to 34 psu (μ = 33.4 ±0.4) and -0.8 to 0.55‰ (μ = -0.17±0.41), respectively, during the summer monsoon (August-September) 1988. Although samples were collected from the same locations during SK-191 and SK-182, salinity and δ^{18}O ranged between 21 and 35 psu (μ = 30.7±4.2) and -2.4 and -0.5‰ (μ = -0.38±0.96), respectively during SK-182. In December 1991, salinity was observed to be between 27 and 34 psu (μ = 30.8±2.8) and all δ^{18}O values from -2.45 to -0.76 (μ = -1.65±0.60), as five of the samples were from river mouths (Mahanadi, Krishna, Cauveri and Godavari).

In the Arabian Sea, salinity ranged between 34.5 and 36 psu (μ = 35.3±0.4) in December, 1987 and 35 to 37 psu (μ = 36.4±0.5) in December 1988. δ^{18}O varied between 0.4 and 1.7‰ (μ = 0.90±0.32) in December, 1987 and 0.06 to 1‰ (μ = 0.62±0.37) in December, 1988. In the recent (March, 2009) data, salinity varied from 35.1 to 36.6 psu (μ = 36.1±0.5) while δ^{18}O varied between 0.04 and 0.99‰ (μ = 0.56±0.30). Higher values of δ^{18}O and salinity in the Arabian Sea than in the Bay of Bengal attest to the well known effects of evaporation in the former and run-off in the latter.

Mean values of salinity and δ^{18}O with standard deviations from all the cruises are listed in Table 4.1. Five data points having the lower salinity are excluded from the linear regression as these came from too close to the river mouths (Figure 4.6a). Salinity and δ^{18}O are linearly correlated, both for winter, pre monsoon and summer monsoon periods in the Bay (Figure 4.6a, b, c). In the Arabian Sea, significant slope could be derived only for SS-263 data; the rest of the data, from SK-37 and SK-47, data show scatter (Figure 4.6d). The best fit slopes and intercepts of the S-δ^{18}O relation for all data sets are shown in Table 4.1. The δ^{18}O-salinity relation for the sub-surface northern Indian Ocean (50 to 500 m water depths) is also shown in Table 1 (Figure 4.8). *Delaygue et al.* [2001] reported slopes of 0.18 and 0.26

in the Bay of Bengal and the Arabian Sea, respectively, while *Rostek et al.* [1993] observed slopes of 0.45 and 0.28, respectively.

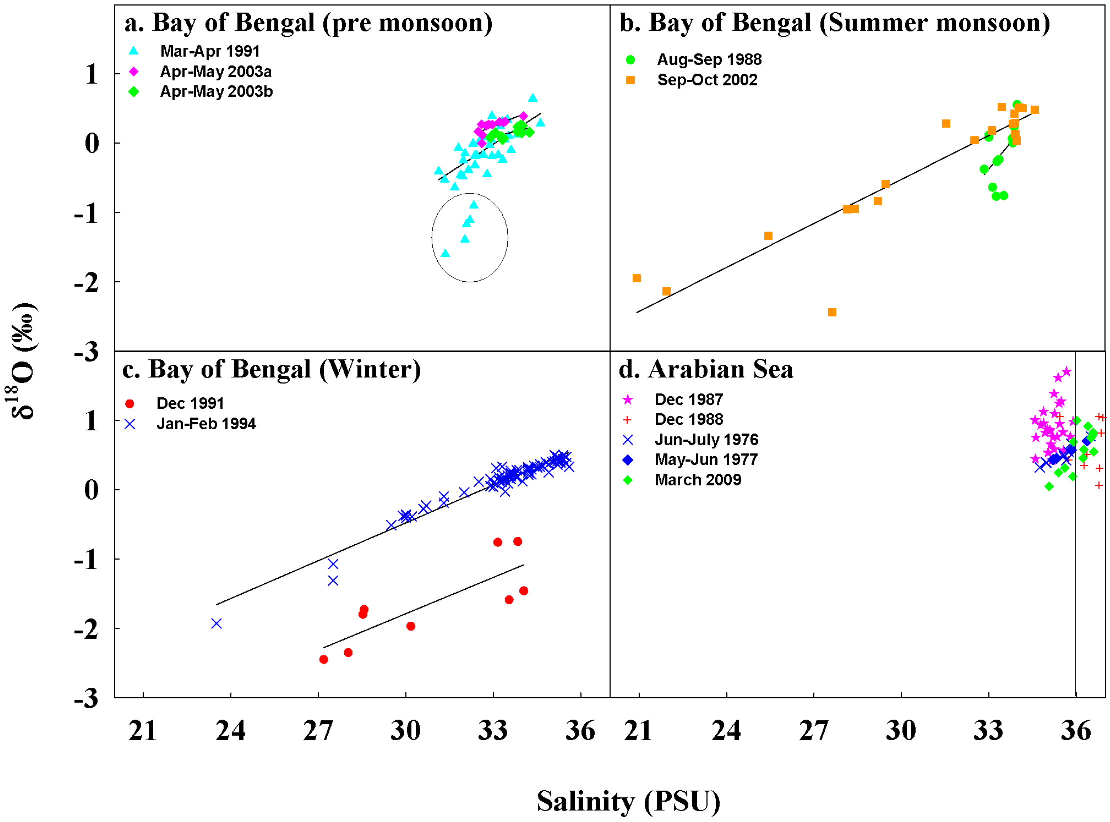

Figure 4.6: δ^{18}O-salinity relation for the Bay of Bengal: (a) pre-monsoon SK-63▲ (March-April 1991, slope m = 0.27, after excluding 5 data points shown in a circle, as these were from river-mouths, if included slope is 0.40); and SK-191 (April-May 2003, m = 0.10 for the coastal samples◆, m = 0.17 for the open ocean samples◆) (b) southwest monsoon - G-200● (August-September 1988, m = 0.51), SK-182■ (September-October 2002, m = 0.21) (c) winter- SK-70● (December 1991, m = 0.17), *Delaygue et al.* [2001]×, (January-February 1994, m = 0.18). For the Arabian Sea : (d) SK-37* (December 1987, insignificant slope), SK-47+ (December 1988, data points form a cluster), SS-263◆ (March 2009, m = 0.45), Duplessy et al. (1981)× (June-July,1976 m = 0.25) and ◆ (May-June,1977 m = 0.23), vertical line is drawn to differentiate higher salinity in the northeastern (>15° N) than in the southeastern (<15° N) Arabian Sea.

Error Analysis

Linear regression between δ^{18}O ('y' variable) and salinity ('x' variable) was done using the method of least squares (e.g., *Topping*, [1962]; *Chao*, [1974]); best fit lines are drawn for the data obtained from the cruises undertaken in the Bay of Bengal (Figure 4.6a, b, c). Though no line is shown for the Arabian Sea data because of the scatter (Figure 4.6d), the calculated slopes for a few such data are included in Table 4.1. Best fit lines are drawn only for the data corresponding to the upper 50 m; data of waters deeper than 50 m show scatter (Figure 4.8). Likewise, linear regression is also performed for the calculated slopes (and intercepts) against the annual rainfall over India, obtained from the India Meteorological Department (Figure 4.9).

The uncertainties on the calculated slopes (m) and intercepts (c) of the best fit lines (in the form of $y = mx + c$) are calculated following *Topping* [1962]. The standard error in slope (σ_m) is given by $\pm\sqrt{(\frac{n}{n-2})\frac{\sum d^2}{n\sum x^2-(\sum x)^2}}$, where n is the number of data pairs, d is the residual (defined as $mx + c$ - $y_{observed}$) and x refers to salinity. The standard error in intercept (σ_c) is given by $\pm\sigma_m\sqrt{\frac{\sum x^2}{n}}$. The goodness of fit is ascertained by Student's 't' test.

Often the scatter in the data precludes finding differences in the parameters m and c between different regions/seasons. The statistical significance of such differences is tested following *Chao* [1974]. If the first data set of n_1 samples has an error of σ_1 in the slope (or intercept) and the second data set of n_2 samples has an error of σ_2, the slopes (or intercepts) are significantly different if the difference between their means exceeds or equals 1.645 $\sqrt{\frac{\sigma_1^2}{n_1} + \frac{\sigma_2^2}{n_2}}$. Claims made in this study have more than 95% confidence level.

4.4.2 Discussion

Attempts were made earlier to explain the observed slopes in the δ^{18}O-S relation in the northern Indian Ocean using the multi-box and General Circulation Models [*Delaygue et al.*, 2001]. Here we use set of equations derived using isotopic mass balance by *Ramesh and Singh* [2010] for interpreting salinity-oxygen isotope data from the mixing of isotopically depleted water to and simultaneous evaporation of fresh water from the ocean.

The Model

The oxygen isotope ratio R (=^{18}O/^{16}O) of a water body (with an initial oxygen isotopic ratio R_0) evolves as two competing processes take place, i.e., evaporation and addition of fresh water (of oxygen isotopic ratio R_r, assumed to be constant for the sake of simplicity) by surface runoff, as given by eqs. 4.3 and 4.4 [*Ramesh and Singh*, 2010]. Evaporating water leaves the salt behind and addition of runoff does not add salt. Thus the salinity changes only a function of the amount of net water removed, and therefore is a function only of f

$$S = \frac{S_0}{f} \tag{4.8}$$

Using eqs. (4.4) and (4.8), the δ^{18}O-S relation is obtained as

$$\delta = \delta_0(\frac{S_0}{S})^{\rho} + \frac{\beta\delta_r - \epsilon}{\alpha + \beta - 1} \tag{4.9}$$

We may assume the initial isotopic composition of the ocean δ_0 to be zero. For relatively small changes in salinity, i.e., $|(\mathrm{S} - \mathrm{S}_0)/\mathrm{S}_0| << 1$, the above equation could be linearised as:

$$\delta = \frac{\epsilon - \beta\delta_r}{1 - \beta} + \frac{\beta\delta_r - \epsilon}{1 - \beta}\frac{S}{S_0} \tag{4.10}$$

This equation is valid for all non-negative values of β except unity (when it is unity, the amount lost by evaporation is exactly balanced by runoff and the salinity remains constant and only the isotopic composition changes, and this is rare to occur in nature).

The rate of variation of the intercept with respect to β for constant values of ϵ and δ_r is given by $\frac{\epsilon - \delta_r}{(1-\beta)^2}$. As ϵ is negative (~-5‰) and δ_r is less negative (~-4‰), this derivative is negative as long as $|\delta_r| < |\epsilon|$, indicating that the intercept decreases with increasing proportion of runoff. Likewise, the rate of variation of the slope with respect to β for constant values of ϵ and δ_r is given by $\frac{\delta_r-\epsilon}{S_0(1-\beta)^2}$, positive provided $|\delta_r| < |\epsilon|$. Therefore higher proportion of runoff results in higher slope. We also note that the intercept is more sensitive than the slope to changes in the runoff. The sensitivity is quite high, when β is close to unity.

Isotopic fractionation during evaporation is a non-equilibrium process, the vapour is always 2-5‰ more enriched than expected from equilibrium fractionation [*Craig and Gordan*, 1965; *Merlivat and Jouzel*, 1979; *Jouzel and Koster*, 1996]. We have adopted ϵ (isotopic fractionation factor between vapor and liquid for oxygen expressed in per mil units) to be -5‰. $S_0 = 34.6$ psu, the mean salinity of the deep oceanic reservoir [*Clark and Fritz*, 1997; *Delaygue et al.*, 2001], is considered as initial salinity (S_0). Eq. (4.10) is used to plot δ^{18}O-S in Figure 4.7, for different combinations of β and δ_r. Hereafter δ_r is used to denote $\delta^{18}O_r$ and referred as oxygen isotopic composition of external source (i.e. runoff and/or precipitation) and is taken to be -4‰ (constant) in Figure 4.7a, as this is mean value of the Indian rivers debouch into the Bay of Bengal [*Somayajulu et al.*, 2002; *Lambs et al.*, 2005]; Isotopic composition of precipitation over Kolkata taken from Global Network on Isotopes in Precipitation (GNIP) suggests $\delta^{18}O_r$ to be -6‰ (IAEA/WMO, 2006). β is allowed to vary between 1.5 and 3 in steps of 0.5. As β progresses from 0 to 1 (evaporation flux is increasingly compensated by runoff and precipitation), slope increases and intercept decreases, according to the the model.

In the other case, taking $\beta(=2)$ to be constant, when $\delta^{18}O_r$ decreases, slope increases and intercept decreases. In this model, overhead oceanic precipitation is not considered directly. δ^{18}O values of precipitation over the Bay of Bengal and the Arabian Sea are -4.5‰ and -3.5‰ (most likely over the open ocean), respectively, with a seasonal variation of ±1‰ [*Delaygue et al.*, 2001], which is similar to $\delta^{18}O_r$. Estimated δ^{18}O and salinity using the above equations are plotted in Figure 4.7. Table 4.2 shows the slopes and intercepts calculated using linear regression analysis of data generated by the model.

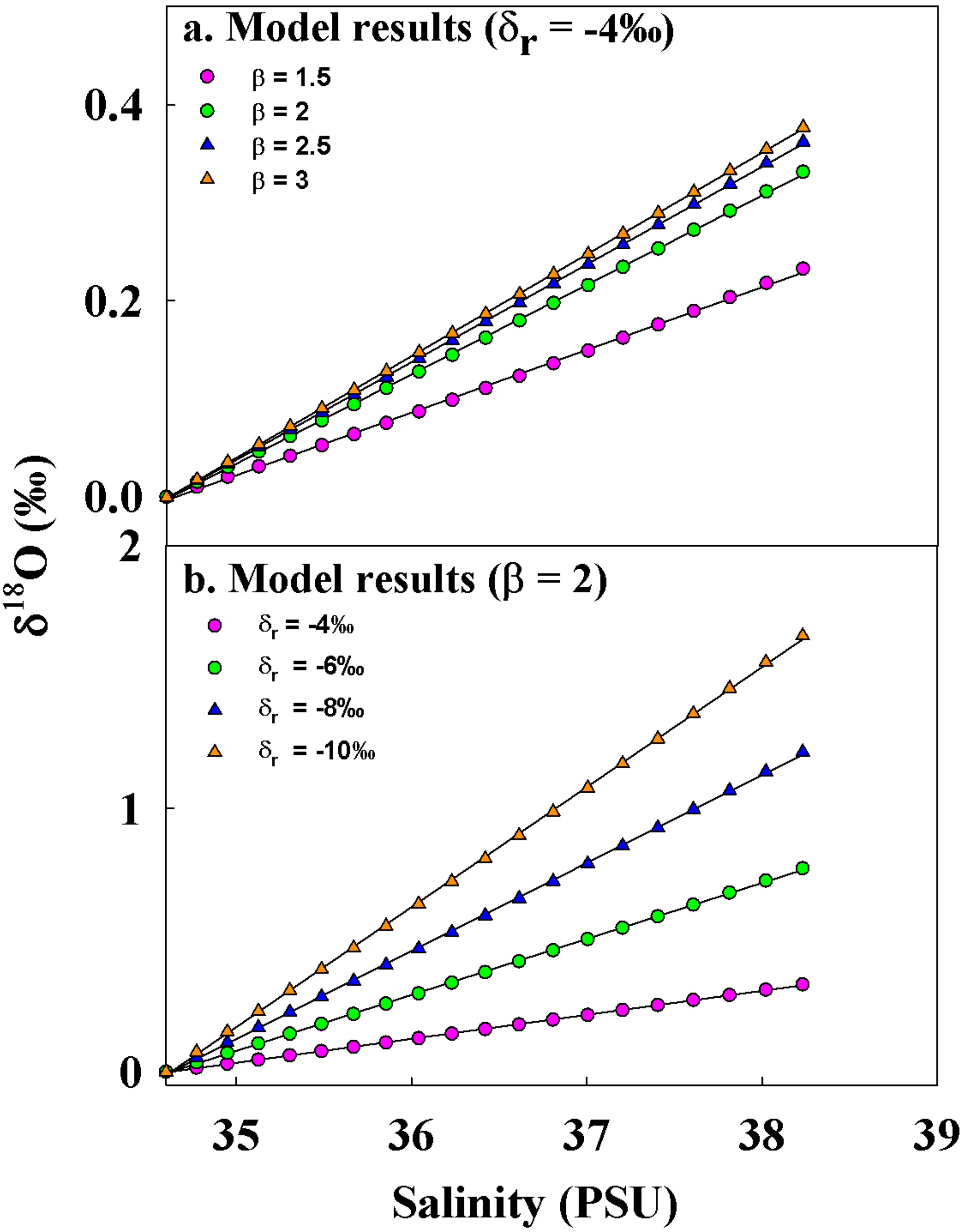

Figure 4.7: Linear regression of simulated δ^{18}O and salinity values for (a) mixing of constant δ^{18}O (-4‰) runoff with different fluxes; m = 0.06, 0.09, 0.10 and 0.10, respectively, for β = 1.5, 2, 2.5 and 3 and (b) constant runoff (twice of the evaporative loss) with different mean δ^{18}O values; m = 0.09, 0.21, 0.33 and 0.46, respectively, for δ^{18}O values of -4‰, -6‰, -8‰, -10‰.

Table 4.2: Model results from the mixing of isotopically ($\delta^{18}O_r$) different water masses into the ocean with various runoff fluxes (β)

Constant $\delta^{18}O_r$ (-4‰) with different continental run-off fluxes		
Runoff/$\delta^{18}O_r$	Slope	Intercept
$\beta = 1.5$	0.06	-2.2
$\beta = 2$	0.09	-3.2
$\beta = 2.5$	0.10	-3.4
$\beta = 3$	0.10	-3.6
Constant runoff ($\beta = 2$ with different $\delta^{18}O_r$)		
$\delta^{18}O_r$ = -4	0.09	-3.2
$\delta^{18}O_r$ = -6	0.21	-7.4
$\delta^{18}O_r$ = -8	0.33	-11.6
$\delta^{18}O_r$ = -10	0.46	-15.8

Interpretation of the results

A significant variation in slope is observed during different seasons and locations in the Bay of Bengal (Table 4.1). During the pre-monsoon (March-May), a significant spatiotemporal variation in the slope is observed (Figure 4.6a). The model slope agrees with the observed slope (0.27) during March-April 1991, when $\delta^{18}O_r$ value is ~-7‰ and $\beta = 2$. These values are reasonable as isotopically depleted water from melting of ice/snow of the Himalayan glaciers contributes to runoff during spring [*Ramesh and Sarin*, 1992]. During April-May 2003, lower slope (0.10) is observed in the coastal and the open ocean (0.17) in the Bay of Bengal, a clear indication of reduced monsoon runoff (by ~25%, see Figure 4.9) and also possible reduced contribution of Himalayan snow-melt during the intervening decade. The model gives these slopes for $\delta^{18}O_r$ ~-4‰ and $\beta = 2$. Slope obtained for March-April by us is higher than that reported by *Delaygue et al.* [2001], for January-February because our observations were more towards the coastal Bay, where rivers of Himalayan origin discharge waters highly depleted in ^{18}O [*Ramesh and Sarin*, 1992; *Rao*, 2006]. In addition eastbound peninsular rivers bring ^{18}O depleted water from northeast monsoon rains [*IAEA/WMO*, 2006]. During summer monsoon (July-October), the slope is significantly higher (Figure 4.6b). In August-September 1988, the observed higher slope (0.51) indicates a good monsoon, whereas in a failed monsoon year (Sep-Oct 2002), the observed slope (0.21) was significantly less. The higher slope during monsoon is in agreement with the estimate of *Rostek et al.* [1993] of 0.45 for the Bay. Although the sample locations for SK-182 and SK-191 cruises are the same; the slopes are different, as they pertain to different seasons. During winter (Figure 4.6c), the slope (0.17) and intercept (-9) observed by us are statistically indistinguishable from those reported by *Delaygue et al.* [2001]. These observations and the model strongly suggest that slope varies seasonally in the Bay. These observations and model together suggest that δ^{18}O of river run-off and rainfall over the Indian region governs the slope of the δ^{18}O-S relation in the Bay of Bengal.

The Arabian Sea is known to be dominated by evaporation. The strong southwest monsoon causes intense upwelling in the western Arabian Sea during summer, while in winter surface cooling in the north results in enhanced vertical mixing [*Madhupratap et al.*, 1996, *Prakash and Ramesh*, 2007]. Salinity is higher in the northeastern Arabian Sea than in the southeast, indicating greater evaporation during winter in the former and higher rainfall above the Deccan Mountains during summer in the latter [*Duplessy*, 1982]. No significant slopes could be derived from the data of December, 1987 and December, 1988, possibly due to vertical mixing which generally occurs in the northeastern Arabian Sea during the winter [*Prakash and Ramesh*, 2007]. *Duplessy et al.* [1981] and *Rostek et al.* [1993] reported slopes of ~0.26 for other seasons in the Arabian Sea, which can be simulated when $\delta^{18}O_r$ = -7‰ (discharge from the Indus river mainly, depleted values are reported by *Rozanski et al.*, [2001]) and $\beta = 2$. In contrast, March 2009 data show slope and intercept of 0.45 and -15.5, respectively, attributable to the transportation of the Bay of Bengal water ($\delta^{18}O_r$ = -10‰ and $\beta = 2$) to the Arabian Sea through EICC and WICC during winter. It is difficult to infer temporal variation in the slope in this region due to the paucity of data for other seasons.

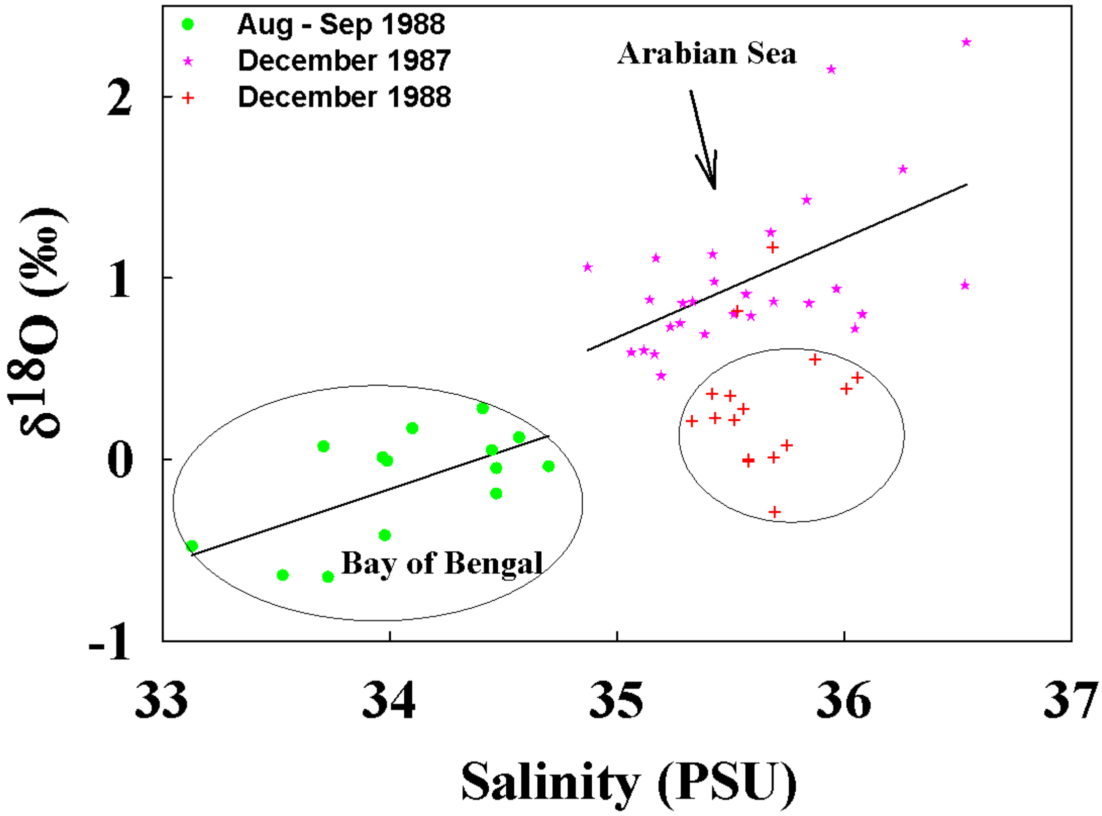

Figure 4.8: δ^{18}O-salinity relation in the sub-surface northern Indian Ocean (depths from 50 to 500 m). The same symbols are used as in Figures 2.8 and 4.6. Data points in the left ellipse (shown as ●) are from the Bay of Bengal. Ones on the right ellipse (shown as +) are from the northeastern Arabian Sea, which do not show a significant correlation.

Significant correlation in the δ^{18}O-S relation is observed at 50 m depth over the Bay of Bengal, the slope and intercept being similar to the surface values observed during the same cruise (Figure 4.8). It appears that mixing in the Bay of Bengal could be vigorous up to at least 50 m in some years either due to eddies or due to cyclones. Samples at 50 m depth from the eastern Arabian Sea in Dec 1987 show a significant δ^{18}O-S relation, and the high slope and low intercept are similar to the values observed in March 2009 (Figure 4.8, Table 4.1). It is known that during December to March, this region receives low salinity water from the Bay of Bengal [*Wyrtki*, 1973; *Schott and McCreary*, 2001; *Prakash and Ramesh*, 2007]. Added to this may be the north-east monsoon precipitation and associated runoff in southern India. These could explain the significantly higher slope and lower intercept.

LeGrande and Schmidt [2006] reported a slope of 0.16 for the northern Indian Ocean, while our results suggest a value of 0.26. Their locations are concentrated mainly in the Bay of Bengal during the winter, whereas our data set includes a large number of samples from the Arabian Sea as well.

Effect of monsoon runoff on the δ^{18}O-salinity relation

We have observed large variation in the slope (0.10-0.51) and intercept (-3.4 to -17.2) during 1987-2009 in the northern Indian Ocean; rainfall varied from ∼900 to 1200 mm y^{-1} for the corresponding period over India. The magnitude of the interannual variation (∼10%) in the monsoon rainfall is significantly less than that of its seasonal and geographical variations [*Gadgil*, 2003]. Nevertheless, our analysis suggests that monsoon runoff is capable of changing the δ^{18}O-S relation in the northern Indian Ocean (Figure 4.9). Data of annual rainfall over India (ftp://www.tropmet.res.in/pub/data/rain/iitm-regionrf.txt), roughly a measure of runoff, are plotted against slope and intercepts of the δ^{18}O-S relation for surface waters for the corresponding years (e.g., slope and intercept obtained for June-July 1976 data are plotted against rainfall of the preceding 12 months, i.e., during June 1975 to May 1976). Significant increase in slopes and decrease in intercepts are caused by higher rainfall (Figure 4.9). Monsoon runoff mainly debouches into the Bay of Bengal through eastbound rivers; besides, we have included the slopes from the Arabian Sea data as well, wherever a significant relation was obtained (Figure 4.9). This is appropriate as they pertain mainly to the eastern Arabian Sea, where a dilution effect is observable through advection and runoff.

^{18}O-depleted runoff could also result from the 'amount effect': higher rainfall is associated with lower δ^{18}O [*Dansgaard*, 1964; *Araguas-Araguas et al.*, 1998; *Yadava and Ramesh*, 2005]. Thus stronger monsoon rainfall, more depleted in ^{18}O, could also increase the slope and decrease the intercept.

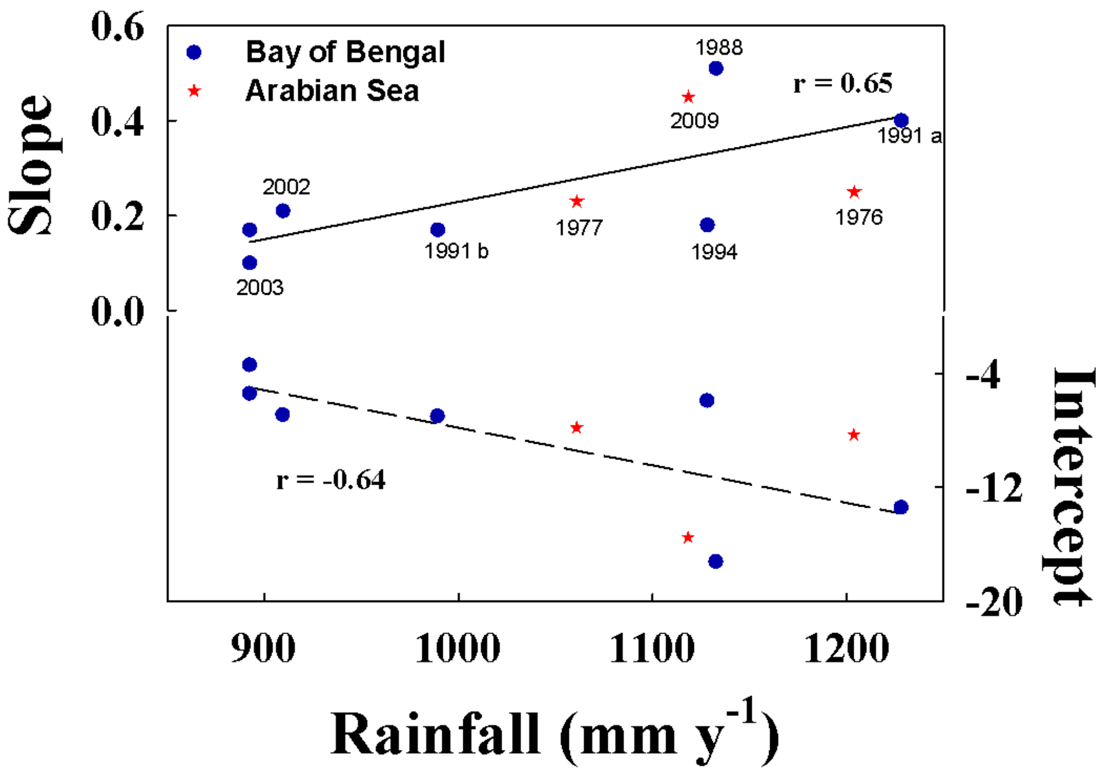

Figure 4.9: Slopes and intercepts of the δ^{18}O-salinity relation of various datasets are plotted against the corresponding annual rainfall over India, which is a rough measure of river discharge. Numbers near the symbols correspond to years of observations; 1991a and 1991b refer to the periods March 1990-February 1991 and December 1990-November 1991, respectively

Implications for paleosalinity reconstructions

A number of paleoclimatic/paleoceanographic studies have been carried out in the northern Indian Ocean (see for a recent review, *Tiwari et al.*, [2009]) using δ^{18}O of foraminifera in marine sediments. As high resolution paleoclimate studies are likely to use coastal cores with higher sedimentation rates, interpretation of the δ^{18}O of foraminifera must be done with caution. The glacial-interglacial change in δ^{18}O in the eastern Arabian Sea and in the Bay of Bengal (either assumed to be due mostly to surface salinity change (e.g., *Duplessy*, 1982), or after correcting for temperature change by using alkenones and Mg/Ca [*Rostek et al.*, 1993; *Rashid et al.*, 2007]), over and above the change attributable to global sea-level rise, is generally interpreted as a reduced monsoon and runoff. The estimate of the extent of reduction assumes a constant δ^{18}O-S relation observed at present. If indeed the monsoon runoff had decreased during the glacial period, the slope of the relation would have significantly reduced (Figure 4.9), thus the extent of monsoon reduction would be significantly underestimated by the assumption of time- invariant slope. Care should also be taken in interpreting the δ^{18}O values of foraminifera whose abundance peaks in different seasons: a higher slope would be applicable to post-monsoon ones and a lower to pre-monsoon ones. Also, the observed significant spatial variation in the δ^{18}O-S relation (coastal versus open ocean) must be considered.

4.5 Conclusions

The Rayleigh equation is revised for a reservoir wherefrom material is not only removed with isotopic fractionation, but fresh material of a different but constant isotopic composition is added from an external source, at a given rate. Our results show that ~50% of the nitrate that is lost during denitrification could be compensated by organic matter raining from above. In another application to SOM decomposition, ~20% of the organic matter is compensated by an appropriate choice of $\delta^{18}O_r$ and ϵ.

The equation is further extended to understand the observed variations in the δ^{18}O-S relation of sea surface water in the northern Indian Ocean. This is the first study to assess the spatiotemporal variations of this relation in the northern Indian Ocean using a new data set that can help to decrease the uncertainty in paleosalinity estimates for this region. A significant spatiotemporal variation in the δ^{18}O-S relation has been observed in the Bay of Bengal. A mass balance model predicts a higher slope when river discharge depleted in ^{18}O is added to the Bay of Bengal surface waters, as also reflected by the data. Significant fresh water resulting from the summer monsoon rains over the hinterland increases the slope relative to the pre/post monsoon in the Bay of Bengal. In the southeastern Arabian Sea most data suggest little variation in the slope (∼0.26) during the summer, as reproduced by the model where evaporation dominates over other processes. During late winter a higher slope of 0.45 is observed in the northeastern Arabian Sea than the southeastern Arabian Sea, caused possibly by the mixing of water transported from Indian coastal currents or river inputs to this region. In contrast, limited data obtained during the two cruises in the southeastern Arabian Sea form a cluster, possibly because of small differences between evaporation and precipitation. The mass balance model presented can be useful to quantify the relative importance of runoff sources from different processes such as rain snow-melt and rain over land.

Chapter 5

An assessment of the contribution of atmospheric and riverine fluxes to new productivity in the northern Indian Ocean

5.1 Contribution of atmospheric deposition to new productivity

As discussed in the previous chapters, marine biological productivity (rate of carbon fixation, measured in mg C m^{-2} d^{-1}) is one of the major sinks of atmospheric carbon dioxide, thus an important regulator of Earth's climate [*Sabine et al.*, 2004]. The rate of transfer of fixed carbon from the sunlit layers of the ocean (i.e., the top ∼100 m) to the darker, deeper layers, is termed as export productivity. This is approximately equal to 'new productivity', the fraction of the productivity sustained by the input of new nutrients into the photic zone, over annual time scales [*Eppley and Peterson*, 1979]. The availability of nutrients, especially reactive nitrogen N_r, is known to limit the biological productivity in the surface ocean in many regions

[*Broecker*, 1974]. Nitrogen is an essential nutrient for the growth of marine biota and understanding the role of atmospheric deposition of nitrogen on marine productivity is the main focus of this section. Regionally atmospheric deposition may have significant impacts on marine biogeochemistry and support up to 25% of the new productivity. On the other hand, atmospheric Si and P inputs may have only minimal impacts on regional new productivity as these inputs are smaller relative to the flux from below the sunlight layer [*Krishnamurthy et al.*, 2010].

Nitrogen enters the surface ocean through a number of processes related to the marine nitrogen cycle; e.g., N_2 fixation, upwelling/eddy diffusion, fertilizer use on land and waste discharge, and atmospheric deposition by aerosols [*Galloway et al.*, 2004]. Molecular nitrogen (N_2) is most abundant in the Earth's atmosphere, but can only be utilized by a specific group of marine microorganisms (diazotrophs such as *Trichodesmium*). Most other organisms prefer oxidized or reduced forms of nitrogen, i.e., reactive nitrogen (e.g., NO_3^-, NH_4^+ etc.). Upwelling is an important process through which new nitrogen is brought up from deeper ocean to the surface, but this occurs in limited and specific regions of the ocean, e.g., in the western Arabian Sea during summer [*Madhupratap et al.*, 1996]. Nitrogen inputs from fertilizer use on land and waste discharge are limited to the coastal region [*Seitzinger et al.*, 2006].

Nitrogen is lost from the ocean through denitrification and anaerobic ammonium oxidation (anammox) to the atmosphere, and burial of organic matter in the deep [e.g., *Kuypers et al.*, 2003]. Recently, an imbalance between the nitrogen loss and gain rates has been observed, which suggests that other less well-studied or currently unknown processes may exist and fix substantial amounts of N_2 [*Codispoti*, 2007]. This prompted us to study one of the gain processes, i.e. atmospheric deposition to the ocean; as the possibility of decrease in the nitrogen loss have been ruled out [*Codispoti*, 2007].

As a consequence of increasing anthropogenic activity such as deforestation, fossil fuel burning and industrialization, the global nitrogen emissions have increased since the preindustrial era [*Galloway et al.*, 2004; *Duce et al.*, 2008]. *Mulitza et al.* [2010] reported that a considerable increase in African dust emissions occurred with the onset of agricultural irrigation about two centuries ago. Therefore it becomes important to assess the impact of continental aerosols over oceanic productivity. Wet and dry deposition of N_r (mainly nitrate and ammonia) can stimulate phytoplankton productivity and change the phytoplankton community structure and composition, when not limited by other nutrients such as iron [*Mills et al.*, 2004; *Baker et al.*, 2007]. The western Arabian Sea, however, appears to be at least seasonally iron limited, i.e. a high-nutrient, low-chlorophyll (HNLC), region [*Naqvi et al.*, 2010a]; despite the supply of iron to this region through Arabian dust deposition [e.g., *Krishnamurti et al.*, 1998]. The present study primarily focuses on the nitrogen inputs (through aerosols) and its contribution to new productivity in the northern Indian Ocean.

The Arabian Sea and the Bay of Bengal, the two northern Indian Ocean basins located in similar latitudes, are significantly different in many aspects: strong winds during summer monsoon produce intense upwelling in the northwestern Arabian Sea. Nutrients brought up though upwelling enhance surface productivity. Cooler winds during the winter monsoon, lead to convective mixing in the northeastern the Arabian Sea, which brings up nutrients from the deep, thus increasing surface productivity. In addition, the Arabian Sea receives nutrients in the form of dust from Arabia in the west and the Thar in the east. These processes make the Arabian Sea one of the most productive regions in the world [*Madhupratap et al.*, 1996; *Smith*, 2001; *Prasanna Kumar et al.*, 2002; *Kumar et al.*, 2004a, 2010;*Prakash and Ramesh*, 2007; *Prakash et al.*, 2008; *Gandhi et al.*, 2010a]. On the other hand, a large influx of fresh water stratifies the Bay of Bengal surface, limiting surface productivity [*Kumar et al.*, 2004a; *Singh et al.*, 2010]. The sources of atmospheric nitrogen deposition at these two sites may be quite different, but are believed to be mainly from the industrial nations, India and China [*Galloway et al.*, 2004]. Hence, these two basins of the northern Indian Ocean provide an ideal marine environment to study the impact of atmospheric deposition on the surface ocean biogeochemistry. The hydrography, circulation and winds of the northern Indian Ocean have been discussed by many authors including *Thadathil et al.* [2007] and *Jyothibabu et al.* [2010].

The role of atmospheric nitrogen deposition in new productivity is poorly understood. *Patra et al.* [2007] discussed the relative significance of atmospheric deposition over vertical mixing in maintaining chlorophyll abundances in the northern Indian Ocean. Since atmospheric input is at best comparable to new productivity because productivity is fuelled mostly by recycled nutrients [*Eppley and Peterson*, 1979]; comparing total chlorophyll with atmospheric deposition might lead to large uncertainties. *Spokes et al.* [2000] reported that up to 30% of the new productivity in the oligotrophic waters of the northeast Atlantic could be supported by atmospheric inputs in spring. The highly productive northern Indian Ocean lacks such an estimate. For example, systematic surface productivity measurements in the Bay of Bengal became available only during the last decade. In the open ocean, oligotrophic waters such as in the Bay of Bengal [*Wiggert et al.*, 2006], where the supply of nutrients through riverine influx and upwelling is not significant, atmospheric deposition could be an important cause for productivity in addition to vertical mixing by eddies *Kumar et al.* [2004a], based on preliminary data, suggested that a significant part of new productivity in the Bay of Bengal could be due to atmospheric deposition. Since then more data have been generated both on new productivity and the atmospheric deposition in various parts of the northern Indian Ocean [*Rastogi*, 2005; *Prakash*, 2008; *Gandhi*, 2010]. Here we assess the role of atmospheric nitrogen deposition in contributing to new productivity in the northern Indian Ocean.

5.1.1 Classification of Zones

We analyze the data into two ways. First (case A), we consider the Arabian Sea and the Bay of Bengal as two different basins and list the results in Table 5.1.

Second (case B), the northern Indian Ocean is divided into four different zones (i) Western Arabian Sea, 45°-60°E (ii) Central Arabian Sea, 60°-70°E and (iii) Eastern Arabian Sea, 70°-78°E, and (iv) Bay of Bengal, 78°-95°E, and the results are presented in Table 5.2. This division is based on the differences in biogeochemistry among these basins; for example, the western Arabian Sea gets nutrients through upwelling during the summer monsoon, while the eastern Arabian Sea, by convective vertical mixing in the winter [*Madhupratap et al.*, 1996; *Prakash and Ramesh*, 2007].

Data from some simultaneous and nearly co-located measurements for new productivity and aerosol concentrations are available in both the basins (Figures 2.13 and 2.12); but these were sampled during different cruises. Exactly simultaneous and co-located measurements of aerosol and ocean productivity are not possible since the standard protocols for measurements of the two are quite different: aerosol samples are mostly collected while ship is moving (by pumping air over a large area to increase the collected mass) and productivity measurements need the ship to be stationary, and are done over a limited area. Even if done simultaneously, the aerosols collected may not represent any effect on the ocean because (i) they may be transported from elsewhere and (ii) their timescales of interaction are different. These unavoidable limitations need to be borne in mind. Nevertheless, the orders of spatiotemporal variations in deposition flux and productivity could be less than the observed ranges. As far as possible, we match the data of corresponding areas for deposition flux, primary and new productivity. Figures 5.1 and 5.2 show the seasonal new productivity and nitrogen deposition, respectively, in different years, over the different zones of the Arabian Sea.

5.1.2 Seasonal variations in new productivity and atmospheric deposition flux

In the first case A, the aerosol deposition flux, new and total primary productivity (in mmol N m^{-2} d^{-1}) of the Arabian Sea and the Bay of Bengal are listed in

Table 5.1. Seasons are classified as winter (December-February), spring (March-May), summer (Jun-August), and fall (September-November). Aerosol data are not available for the fall inter monsoon in the Arabian Sea while in the Bay of Bengal, only the winter monsoon and spring inter monsoon data are available. New and total primary productivity estimations based on ^{15}N tracer technique are available for all the seasons in the Arabian Sea, while they are missing for the winter monsoon and summer monsoon in the Bay of Bengal.

Table 5.1: Nitrogen deposition flux (dry+wet), new and total productivity in the northern Indian Ocean (Data of new and primary productivity, and atmospheric deposition are obtained from the various sources discussed in the Chapter 2)

Season[a]	Region	NP[b]	PP[c]	TAD[d]	%Cont.[e]
WM	Arabian Sea	5.8	17.0	0.08	1.4
SIM	Arabian Sea	2.6	16.2	0.04	1.5
SM	Arabian Sea	5.3	34.3	0.01	0.2
FIM	Arabian Sea	33.0	49.5	ND	-
WM	Bay of Bengal	ND	ND	0.06	-
SIM	Bay of Bengal	5.4	7.2	0.01	0.2
SM	Bay of Bengal	ND	ND	ND	-
FIM	Bay of Bengal	2.6	4.0	ND	-

ND- no data available, [a]WM - Winter monsoon, SIM - Spring Inter monsoon, SM - Summer monsoon and FIM - Fall Inter monsoon, [b]NP is new productivity in mmol N m^{-2} d^{-1}, [c]PP is primary (new + regenerated) prodution in mmol N m^{-2} d^{-1}, [d]TAD is total (wet + dry) atmospheric nitrogen deposition flux in mmol N m^{-2} d^{-1}, [e]Cont. is % contribution of aerosol to NP, i.e. (TAD/NP)×100%.

New and total productivity (33 and 49.5 mmol N m^{-2} d^{-1}, respectively) were maximum in the Arabian Sea during the fall inter monsoon; minimum (2.6 and 4 mmol N m^{-2} d^{-1}) during the same season (the fall inter monsoon) in the Bay of Bengal. This new productivity is around six fold higher than the second highest productivity observed during the winter monsoon. On the other hand, atmospheric nitrogen deposition (0.08 mmol N m^{-2} d^{-1}) was maximum during the winter and minimum (0.01 mmol N m^{-2} d^{-1}) in the spring inter monsoon over the Bay of Bengal. Such higher deposition during the winter monsoon could be possible due to episodic events which were reported in some places in the ocean as well [*Owens et al.*, 1992].

In the second case B, when the Arabian Sea is divided into three different zones, a significant seasonal variation in new productivity is observed during 1995 in the western Arabian Sea (Figure 5.2). Higher new productivity in the summer monsoon, suggests the importance of intense upwelling that occurs during the summer monsoon in the western Arabian Sea.

Table 5.2: Nitrogen deposition flux (dry + wet), new productivity after dividing the northern Indian Ocean into four zones (Data of new productivity and atmospheric deposition are obtained from the various sources discussed in the Chapter 2). Units and other details are the same as those in Table 5.1

Season	Region	NP	TAD	%Cont.
WM	Eastern Arabian Sea	8.9	0.22	2.5
WM	Central Arabian Sea	2.4	0.05	2.1
WM	Western Arabian Sea	3.2	0.05	1.6
WM	Bay of Bengal	ND	0.06	-
SIM	Eastern Arabian Sea	2.1	0.02	1.0
SIM	Central Arabian Sea	3.3	0.04	1.2
SIM	Western Arabian Sea	3.1	ND	-
SIM	Bay of Bengal	5.4	0.01	0.2
SM	Eastern Arabian Sea	6.6	ND	-
SM	Central Arabian Sea	4.3	0.01	0.2
SM	Western Arabian Sea	4.8	0.01	0.2
SM	Bay of Bengal	ND	ND	-
FIM	Eastern Arabian Sea	ND	ND	-
FIM	Central Arabian Sea	5.0	ND	-
FIM	Western Arabian Sea	89.0	ND	1.0
FIM	Bay of Bengal	2.6	ND	-

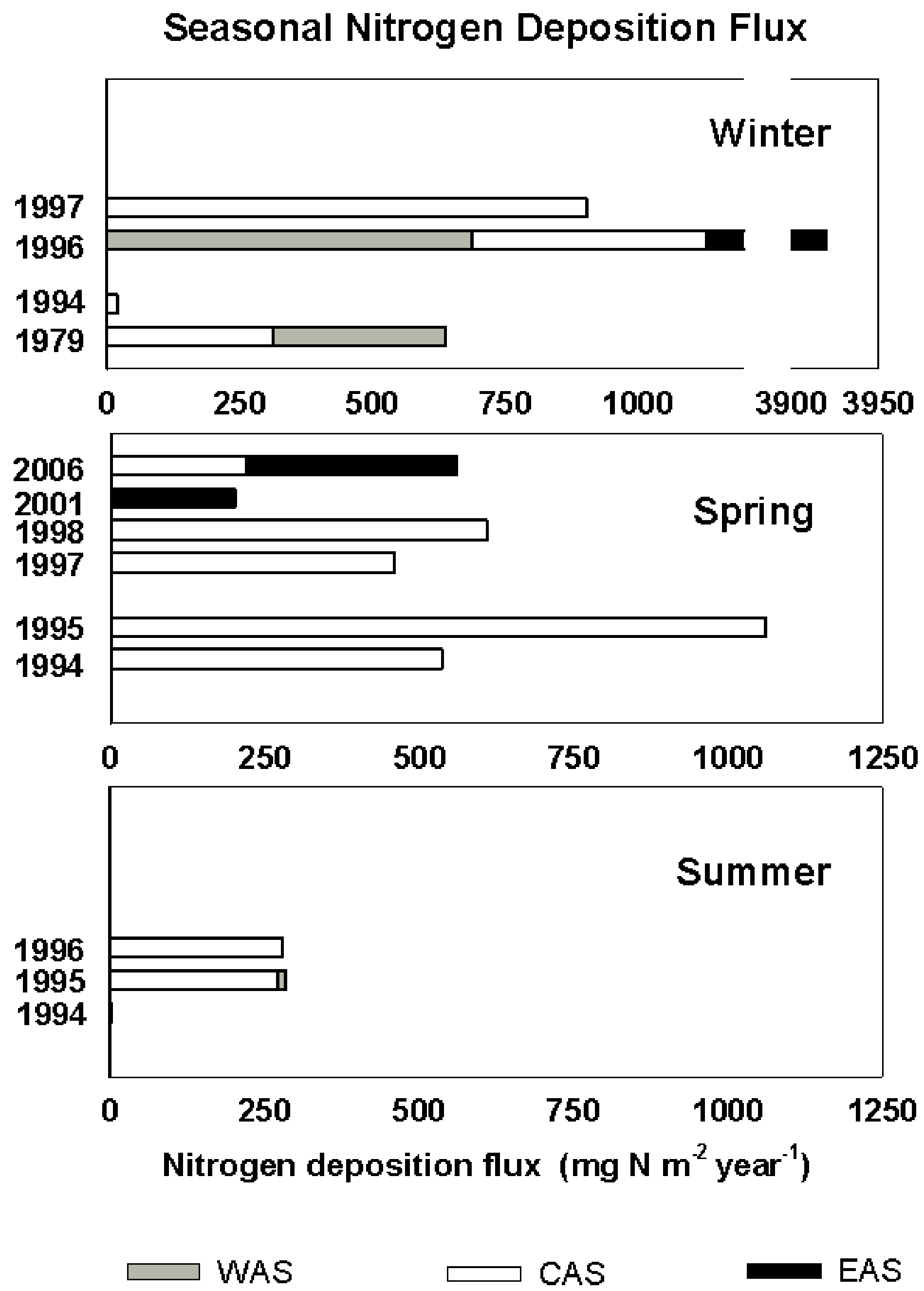

Figure 5.1: N_r deposition flux variation from the available data in winter, summer monsoons and spring intermonsoons in the Arabian Sea. Grey, yellow and blue colors represent data of the eastern Arabian Sea, the central Arabian Sea and the western Arabian Sea, respectively. Note split scale of x-axis in the top panel (winter).

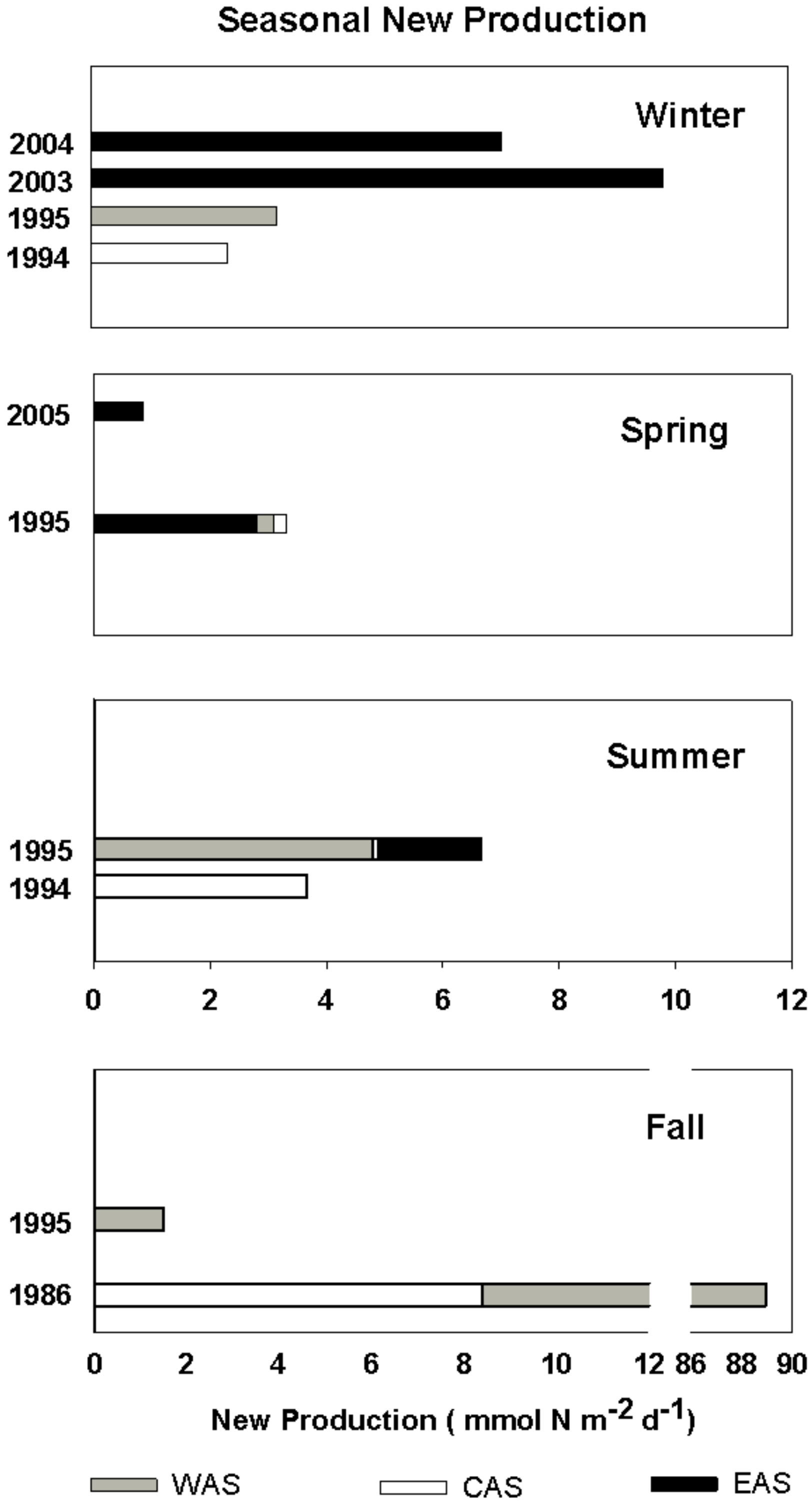

Figure 5.2: New productivity variations in winter, summer monsoons and spring, fall intermonsoons in the Arabian Sea. Grey, white and black colors represent data of the eastern Arabian Sea, the central Arabian Sea and the western Arabian Sea, respectively. Note the split scale of x-axis in the bottom panel (fall).

5.1.3 Spatiotemporal variations in the productivity and the atmospheric deposition flux

We observed higher primary productivity in the Arabian Sea than the Bay of Bengal; however, new productivity is comparable (Table 5.1). There is no such difference between the deposition fluxes. During the fall inter monsoon, productivity is quite high in the Arabian Sea. This is because, at two sampling stations (located very near the highly productive Oman coastal upwelling region) productivity was very high [*Owens et al.*, 1993] and our analysis is influenced by these two data. Aerosol data of the corresponding period are not available; nonetheless, the role of Arabian dust input, a well known source of nutrients to the western Arabian Sea, could be important. Deposition flux was higher during the winter monsoon than in any other season in the Arabian Sea. However, the percentage contribution of deposition flux to new productivity is higher during the spring inter monsoon.

In the second case B, new productivity is maximum (8.9 mmol N m^{-2} d^{-1}) and minimum (2.1 mmol N m^{-2} d^{-1}) in the eastern Arabian Sea during the winter monsoon and the spring inter monsoon, respectively (except anomalously higher new productivity in the western Arabian Sea during the fall inter monsoon, Table 5.2). New productivity is significantly higher in the eastern Arabian Sea during the winter monsoon and the summer monsoon than in the other three zones, attributable to winter mixing and upwelling, well known processes that occur in the respective seasons. All the three zones of the Arabian Sea depict comparable new productivity during the spring inter monsoon in 1995 (Figure 5.2), suggesting no significant spatial variations in new productivity, possibly because of a common process (could be N_2 fixation in the presence of diazotrophs) acting all over the Arabian Sea during this season. It is difficult to decipher any significant trend (increasing or decreasing) from the data set.

Flux estimations mostly pertain to the central Arabian Sea. Unlike new productivity, nitrogen deposition flux is higher in the central Arabian Sea (excluding anomalously higher flux in the eastern Arabian Sea during the winter monsoon, Figure 5.1). When the Arabian Sea is considered as a whole (section 3.1) we note that deposition flux is higher during the winter monsoon, and after dividing the Arabian Sea into three zones we find that deposition flux is higher mainly in the eastern Arabian Sea (Table 5.2). Winds blowing from the Indian subcontinent during the winter monsoon, may contribute to this flux. There is no significant variation in atmospheric deposition during different years in the spring inter monsoon and the summer monsoon (excluding the spring inter monsoon of 1995, Figure 5.1). Here also, no significant trend is observable from the available data set.

5.1.4 Contribution of atmospheric nitrogen deposition to new productivity in the northern Indian Ocean

In the case A, aerosol contribution is 1.4, 1.5 and 0.2% to new productivity in then Arabian Sea during the winter monsoon, the spring inter monsoon and the summer monsoon, respectively. These results show that aerosols contribute a maximum during the spring inter monsoon, which could be attributed to the stratification resulting in the low supply of nutrients from below, as indicated by low new productivity in this season. Atmospheric contribution is higher in the Arabian Sea, because upwelling is not significant during this period. Both the atmospheric deposition and its contribution to new productivity were higher during the winter monsoon, as winds blowing from the land to the ocean during the winter increase the atmospheric contribution. On the other hand, during the summer monsoon, both atmospheric deposition and its contribution to new productivity are low, as during summer most of the nutrients are either upwelled or regenerated (Table 5.1).

The contribution of atmospheric deposition to new productivity was maximum (1.5%) in the Arabian Sea and minimum (0.2%) in the Bay of Bengal during the same season i.e. the spring inter monsoon; however, the difference between the contributions during the winter monsoon and the spring inter monsoon in the Arabian Sea is insignificant.

Using NOAA-AVHRR data of duration 1996-2003, *Parameswaran et al.* [2008] observed the significant impact of continental aerosols in the Arabian Sea: during March-April from the Indian subcontinent and during June-September from Arabian deserts, while in the Bay of Bengal, influence of the subcontinent was more during November-May and minimal during June-September. These observations are consistent with the results presented here.

In the case B, when the Arabian Sea is divided into three zones, higher productivity is observed during the summer monsoon as expected, but the contribution from deposition flux was less. This suggests that the deposition was not an important source of nitrogen to the Arabian Sea, and nitrogen through upwelling from the deep could be the most important new source of nitrogen to the surface waters during this season. These observations belong mainly to the central Arabian Sea and the western Arabian Sea, where intense winds cause upwelling during this season (Table 5.2).

All the three components (atmospheric deposition, new productivity and contribution) are higher during the winter monsoon in the eastern Arabian Sea, clearly suggesting that atmospheric deposition is an important factor in this region and season (Table 5.2), as winds blow from the land to ocean in this season.

In the Bay of Bengal, simultaneous data for new productivity and atmospheric nitrogen are available only for the spring inter monsoon. New productivity during the spring inter monsoon in the Bay of Bengal is comparable to that during winter monsoon and summer monsoon in the Arabian Sea, while the aerosol contribution is extremely less (0.2%). Also, upwelling is not a contributor to new productivity in the Bay of Bengal [*Gauns et al.*, 2005]. The Bay of Bengal receives a large volume of river run-off (1.6$\times10^{12}$ m^3 y^{-1}) [*Subramanian*, 1993]. It is likely that nitrogen flux from river run-off could play a significant role in the coastal areas of the Bay of Bengal for the new productivity. Higher new productivity could be triggered by cold core eddy formation during the spring inter monsoon in open ocean area of the Bay of Bengal [*Prasanna Kumar et al.*, 2007; *Gandhi et al.*, 2011].

Due to the limited seasonal and spatial matching of aerosol and new productivity observations (Figures 5.1 and 5.2), it is difficult to infer the role of deposition flux in primary productivity in the Bay of Bengal; however, we conclude that there is a minor contribution of atmospheric deposition to new productivity in the Arabian Sea, the maximum being in spring.

5.1.5 Effect of rainfall variations (including El Nino) on the estimates of wet deposition flux and new productivity

In the wet deposition flux formula, rainfall seems to be the dominant component. Rainfall over the Indian subcontinent is derived from the northward movement of Inter Tropical Convergence Zone (ITCZ) during June-September and its withdrawal during October-November. Deficit in monsoon rainfall in this region is closely linked to El Nino (unusual warming of Eastern Tropical South Pacific in December), while this relation has weakened in the last decade [*Kumar et al.*, 1999]. Annual variation in the monsoon rainfall caused by all such factors (including El Nino-like events in the Indian Ocean known as Indian Ocean Dipole which also affects monsoon rainfall) is ∼10% [*Gadgil*, 2003]. When we use the rainfall estimate of *Ramesh Kumar and Prasad* [1997] and TRMM data, both significantly different, there is a ∼20% discrepancy in the calculation of the deposition flux (e.g., in 1996, the data of the eastern Arabian Sea, TRMM-based estimate is 3920 mg N m^{-2} y^{-1} while the other is 3114 mg N m^2 y^{-1}, Figure 5.1), which is well within the stated uncertainty of 20% in the flux data due to factors other than rain. So the error in rainfall data may not affect significantly atmospheric flux calculation at present, while more accurate rainfall data would obviously decrease the uncertainties in the analysis. El Nino effects may also be negligible since error in the estimated deposition flux is more than in the annual variation in rainfall. The observed data correspond to a few El Nino years such as 1994-1995, 1997-1998;

but none of the observations is attributable to El Nino. On the other hand, lower new productivity observed during 1994 and 1995 than the following year, and this could be attributable to El Nino (1994-1995). Productivity during spring seasons of El Nino years could be higher because *Trichodesmium* blooms are known to occur in relatively warmer environments, but this is difficult to decipher from our data set.

There is no clear observation about decreasing or increasing trends of deposition fluxes seasonally, annually or spatially. Large variations in N_r deposition have been observed over the four regions of the northern Indian Ocean, possibly due to episodic events, e.g., concurrent high rainfall (Figure 5.3).

5.1.6 Relationship between new productivity and the flux of reactive nitrogen through atmospheric deposition

Presuming a constant contribution of nitrogen from other sources, new productivity should increase linearly with atmospheric deposition flux. It is seen from Figure 5.3 that initial increase in the atmospheric input of N_r, the new productivity decreases, however, a further increase in N_r seems to enhance the new productivity. If we consider all the eight data points and fit a linear regression line, atmospheric flux deposition and the new productivity are positively ($r^2 = 0.60$, $P = 0.02$) correlated; but if one datum point (3920, 8.9) is removed, this correlation becomes insignificant. Therefore, the possibility of great impacts of atmospheric flux on new productivity can be ruled out, at least until the size of the data set increases substantially; in other words, this analysis shows that other factors such as upwelling influence the new productivity much more than the atmospheric deposition in the present day biogeochemistry. Nevertheless, these smaller nitrogen fluxes may be important for oligotrophic regions to increase the drawdown of atmospheric carbon dioxide.

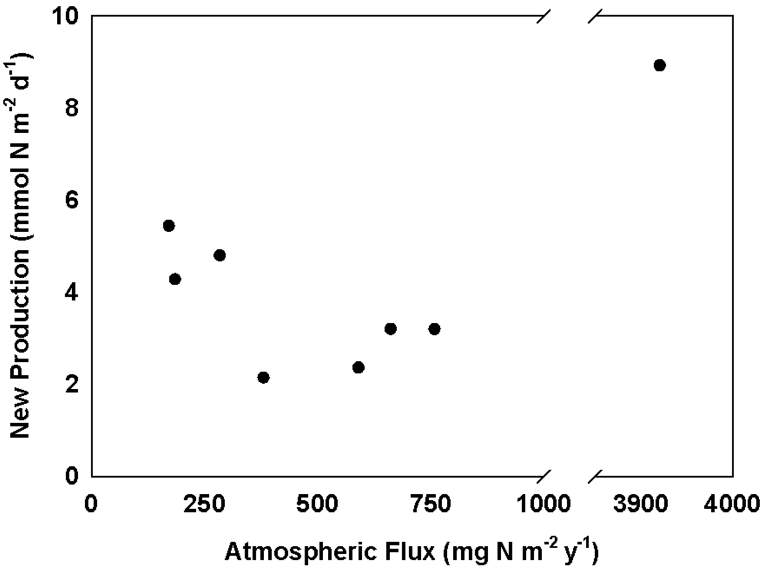

Figure 5.3: Relationship between atmospheric deposition and new productivity. Note the split scale of x-axis.

5.1.7 Changes in the Redfield Ratio and biodiversity

The Redfield ratio quantitatively links the marine nitrogen and phosphorus cycles in numerous biogeochemical applications. It is believed that all biological processes, other than N_2 fixation and denitrification, maintain nitrogen and phosphorus at a fixed ratio of 16:1, known as the Redfield ratio. Reactive nitrogen flux in the South Asian region has increased significantly in the last few decades, and consequently the atmospheric deposition of reactive anthropogenic nitrogen over the northern Indian Ocean is among the highest in the world [*Duce et al.*, 2008]. Such deposition fluxes are expected to alter the relative concentrations of marine macronutrients (N:P:Si) available for phytoplankton uptake, in turn resulting in a change in the phytoplankton community structure. As discussed by *Duce et al.* [2008], phosphorous concentration in the surface ocean is not significantly affected by anthropogenic activity and hence nitrogen deposition alone is likely to enhance N:P in surface water. Although the impact of atmospheric nitrogen deposition to marine new productivity is small, seasonal occurrences of potential dinitrogen fixers (*Trichodesmium*) in the Arabian Sea may be greatly affected. Unlike other plankton, the diazotrophs grow under very different environmental conditions (e.g., in the absence of nitrate and during warmer conditions) [*Karl et al.*, 2002].

The present study suggests that atmospheric fluxes have but a minor contribution to the new productivity in the northern Indian Ocean; however, the potential impacts of these fluxes in future would be determined by the change in anthropogenic activity. In other regions, increasing trends of N_r as estimated by *Galloway et al.* [2004], may have larger impacts (positive/negative).

5.1.8 Synthesis of the available estimates

We compare nitrogen deposition flux estimations obtained from earlier work and the present study in the northern Indian Ocean. *Duce et al.* [1991] estimated a nitrogen deposition flux of ∼2 Tg y^{-1} (F_{dNO_3}= 0.14, F_{dNH_4} = 0.17, F_{wNO_3} = 0.49, F_{wNH_4} = 1.17 Tg N y^{-1}) over the northern Indian Ocean using data obtained prior to 1984. This flux is dominated by wet ammonium flux. *Duce et al.* [1991] concluded that this large ammonium flux could be due to the source of ammonium from the ocean itself. *Bange et al.* [2000] estimated the total nitrogen deposition (both dry and wet) as $0.84+0.74 \approx 1.5$ Tg N y^{-1} in the Arabian Sea. Clearly the spatial and temporal variability in these estimates is quite significant.

Taking into account more data from the recent past, we have calculated ∼1.2 Tg N y^{-1} flux into the Arabian Sea. NO_2^- data is also included in this analysis. These fluxes are dominated by dry deposition of nitrate (F_{dNO_3}= 0.64, F_{dNO_2} = 0.01, F_{dNH_4} = 0.04, F_{wNO_3} = 0.19, F_{wNO_2} = 0.004, F_{wNH_4} = 0.29 Tg N y^{-1}). The nitrogen deposition flux over the Bay of Bengal is nearly half of that in the Arabian Sea i.e. 0.56 Tg N y^{-1} (F_{dNO_3}= 0.30, F_{dNH_4} = 0.02, F_{wNO_3} = 0.15, F_{wNH_4} = 0.09 Tg N y^{-1}). Hence the total N_r deposition over the northern Indian Ocean is ∼1.7 Tg N y^{-1}. The fluxes presented here agree well with earlier estimates within the uncertainties. Therefore, a significant temporal trend is not observable during the past three decades.

Duce at al. [2008] estimated a global average N_r deposition flux of ~700 mg N m^{-2} y^{-1}. Our estimate of the deposition flux over the Arabian Sea is ~833 mg N m^{-2} y^{-1} (no data from fall intermonsoon) and that over the Bay of Bengal, ~733 mg N m^{-2} y^{-1} (no data from winter and fall). These estimates are not significantly different considering the associated uncertainties (±20%). New productivity in the Arabian Sea is ~23 g N m^{-2} y^{-1} hence the contribution of N_r deposition flux to the new productivity is 3.6%. The contribution of N_r deposition flux to the new productivity in the Bay of Bengal is ~21 g N m^{-2} y^{-1} (no data from summer and fall), similar to that in the Arabian Sea.

5.1.9 Other nitrogen sources to the Arabian Sea

The Arabian Sea loses ~35 Tg N y^{-1} (which is ~40% of global N loss) through various N loss processes and thus has global importance [*Bange et al.*, 2000 and references therein]. Nitrogen gain into the Arabian Sea through N_2 fixation and rivers is ~4.5 Tg N y^{-1} [*Bange et al.*, 2000] and present estimates suggest that atmospheric deposition contributes ~1.2 Tg N y^{-1}. *Gandhi et al.* [2010a], on the basis of nitrate uptake rates during a *Trichodesmium* bloom in the northeastern Arabian Sea, have estimated that ~0.9 Tg N y^{-1} is fixed in the Arabian Sea. Nitrogen gain processes do not reach to a level where nitrogen loss is compensated. Since nitrogen gain is an order of magnitude less than the loss, the mystery about missing nitrogen sources still remains.

5.1.10 Other nitrogen sources to the Bay of Bengal

Riverine fluxes and vertical mixing by eddies are the other and main sources of nitrogen to the surface Bay of Bengal. Eddies cause an upward movement of the thermocline, and these can inject nutrients into the euphotic zone. Cyclonic eddies, which occur in the Bay during the October-December, can increase the biological productivity of the Bay by injecting nutrients into the otherwise oligotrophic waters

[*Prasanna Kumar et al.*, 2007; *Gandhi et al.*, 2010b]. But the effect is not seen in the upper surface, restricting the eddy effect to below 20 m during the fall inter monsoon and the spring inter monsoon of 2002-2003 [*Prasanna Kumar et al.*, 2007]. Productivity measurements during the same expedition, however, show higher new productivity in the Bay of Bengal [*Kumar et al.*, 2004a]. Nitrogen inputs through rivers are most likely utilized in the estuarine and coastal primary productivity (discussed in detail in the next section); riverine impact on open ocean biological productivity is negligible [*Duce et al.*, 2008]. Rivers of the Indian subcontinent contribute ∼0.004 Tg N y^{-1} to the northern Indian Ocean [*Subramanian*, 2008], negligible compared to the present estimate of the atmospheric deposition flux (1.73 Tg N y^{-1}) to the region. Observations during 2003 also did not show high Chl *a* or productivity associated with a cyclonic eddy [*Muraleedharan et al.*, 2007]. All these phenomena together suggest that the atmospheric inputs could be significantly higher during the above two seasons. However, our analysis, from the limited data on aerosols, does not reflect this. This also suggests that N_2 fixation could be significant in the Bay of Bengal, where no such measurements have been reported so far.

5.2 Contribution of riverine fluxes to new productivity

Rivers are known to be one of the major sources of dissolved inorganic nitrogen (DIN) to the coastal ocean and contribute to the primary productivity in the sunlit upper ocean. This study provides an analysis of DIN fluxes and its possible contribution to new productivity in the coastal northern Indian Ocean based on literature data.

Anthropogenic activities (such as deforestation and fertilizer use) have not only increased carbon dioxide (CO_2) in the Earth's atmosphere, but also nitrogen on the Earth's land surface [*IPCC*, 2007; *Gruber and Galloway*, 2008]. It is important to assess the sources and sinks of carbon and nitrogen as these two elements affect the Earth's climate significantly, and are coupled in some ways. The ocean is one of the major sinks of CO_2, and its efficiency of removing CO_2 by photosynthesis depends on the availability of nutrients (e.g., nitrogen, silicon, iron, phosphorus) in the sunlit upper ocean. The ocean takes up CO_2 along with DIN (in a particular ratio known as Redfield Ratio, C:N:P :: 106:16:1) during photosynthesis in the photic zone (up to the depth at which the light intensity decreases to 1% of that at the surface) and the conversion rate of inorganic carbon to organic carbon is known as primary productivity. Part of this primary productivity which is supported by new nutrients (mainly nitrate), introduced from outside into the photic zone, is termed as new productivity. On an annual time scale it is approximately equal to the rate of export of organic matter to the deep from the upper ocean [*Eppley and Peterson*, 1979].

Primary productivity in the surface ocean is often limited due to the unavailability of nutrients such as nitrate, phosphate and iron [*Eppley and Peterson*, 1979]. It is shown that the scarcity of nitrogen bearing nutrients (e.g., nitrate, nitrite, ammonia, urea and Dissolved Organic Nitrogen; DON) in coastal regions limits primary productivity while other nutrients are available [*Krupadam and Anjaneyulu*, 2000]. As a result of nitrogen limitation in the surface ocean, the riverine inorganic nitrogen flux is rapidly utilized in the coast itself. This enhances the importance of coastal ecosystems, as the coastal zone (depth $<$ 200 m) occupies only $\sim$7% of the total oceanic area and $<$ 0.5% of volume, but accounts for (i) $\sim$18-33% of oceanic biological productivity (ii) $\sim$80% of organic carbon burial (iii) $\sim$90% of sedimentary mineralization (iv) $>$50% of sedimentary denitrification (v) $\sim$50% of $CaCO_3$ deposition (vi) $\sim$90% of the world's fish catch (vii) $\sim$40% of the value of the world's ecosystem services and natural capital (viii) trapping the bulk of terrestrially-derived suspended matter, nutrients and other chemicals, including pollutants (ix) $\sim$40% of the world population living within 100 km of the coastline (16 out of 23 mega cities); that makes the coastal regions extremely vulnerable to anthropogenic perturbations [*Gattuso et al.*, 2007]. Nutrients derived through rivers are partially responsible for all the above effects. The sunlit upper ocean receives DIN through various sources e.g. upwelling, atmospheric deposition and riverine inputs; riverine DIN flux is known to be one of the main sources to the coastal ocean and, hence an important part of the global nitrogen cycle. It is well established that primary productivity on the ocean surface is limited by the availability of fixed inorganic nitrogen (nitrate, nitrite, and ammonium) in most oceans, including the northern Indian Ocean [*Broecker*, 1974; *Falkowski*, 1997]. The role of atmospheric deposition is relatively minor [*Duce et al.*, 2008; *Singh et al.*, 2011] and the contribution of riverine DIN flux to coastal new productivity in the northern Indian Ocean has not been assessed so far because of the paucity of data. With more data becoming available recently, it is possible now to assess the role of the riverine DIN flux in coastal new productivity.

The northern Indian Ocean provides a unique opportunity to assess the impact of DIN fluxes through both larger and smaller rivers on new productivity. This oceanic basin is divided into two: the Arabian Sea, and the Bay of Bengal (Figure 2.14). These regions are very different in many aspects; the eastern Arabian Sea receives relatively less water discharge (0.3×10^{12} m^3 y^{-1}) relative to the Bay of Bengal from the rivers of subcontinental origin, while the western Arabian Sea is adjacent to the Arabian desert. On the other hand, the Bay of Bengal receives a large amount of fresh water (1.6×10^{12} m^3 y^{-1}, with prodigious amounts of dissolved nutrients) through rivers from the subcontinent [*Subramanian*, 1993; *Prasad*, 1997]. The Bay of Bengal offers a good opportunity to quantify the impacts of river discharge on new productivity,as some of the world's larger rivers debouch into this basin [*Wyrtki*; 1971]. Here we estimate the DIN transport through major rivers debouching into the northern Indian Ocean and assess the contribution of this flux to marine new productivity.

Table 5.3 shows the analysis of DIN flux (measured in head waters and some in the river course) and its estimated contribution to the new productivity. DIN flux is calculated from the mean values of DIN concentration available in the literature. The numbers for % contribution have been calculated as (DIN flux / New productivity)×100, and under the hypothetical situation that all nutrients are transported efficiently to the ocean without any removal in the estuary. Listed seasons pertain to mainly to those of the DIN measurements, and new productivity data are obtained for times as close as possible (Tables 5.3, 5.4). Tabulated new productivity data are from the ^{15}N experiments done in the coastal areas of eastern and western India (Tables 5.3, 5.4). New productivity mainly varies from 2-4 mmol N m^{-2} d^{-1}, except in the coast near Mahanadi (where new productivity is ∼11 mmol N m^{-2} d^{-1}, equivalent export productivity ∼850 mg C m^{-2} d^{-1}). In the case of measurements done on the river course, a calculated contribution exceeding 100% (represents eutrophication condition) implies that DIN gets removed on the land or in the estuary. Possible reasons could be DIN uptake during primary productivity in the estuary and denitrification (an anaerobic microbial process that reduces nitrate to decompose organic matter). Such nitrate reduction reactions occur in the water column of high turbidity [*Bouwman et al.*, 2005; *Jickells*, 2005], and in the sediments.

As major Indian rivers debouch into the Bay of Bengal, a higher DIN flux is expected in the Bay than the Arabian Sea, which is consistent with our analysis (Figures 5.4 and 5.5). The maximum and minimum DIN fluxes are observed in the Ganga and so is its contribution to the new productivity. Variations in data (mainly DIN flux) are large (Table 5.3). *Subramanian* [2008] reported higher DIN concentration in the Ganga and the Cauvery rivers, which yields a higher flux and hence the unusually high contribution to the new productivity (Table 5.3, Figure 5.4).

5.2.1 Bay of Bengal

Our analysis based on data reported by *Subramanian* [2008] shows that the Bay of Bengal receives ∼9 Tg N y^{-1} through major Indian rivers to which Ganga alone

Table 5.3: DIN flux (mmol N m^{-2} d^{-1}) in the course river and its contribution (in %) to the new productivity (mmol N m^{-2} d^{-1}) in the northern Indian Ocean

Rivers debouching into the Bay of Bengal						
River	Season	DIN flux	$NP^{\times}$	$EP^{€}$	%Contribution	References
$Ganga^{\$}$	Annual Average	76.41	2.13	169	3587*	*Subramanian* [2008], *Kumar et al.* [2004a]
Ganga	April 1989	0.01	2.47	196	0.4	*Sarin et al.* [1992], *Krishnaswami and Singh* [2005], *Kumar et al.* [2004a]
Ganga	August 2003	2.44	2.13	169	115*	*Bickle et al.* [2005], *Kumar et al.* [2004a]
Brahmaputra	Annual average	3.74	2.13^{+}	169	175*	*Subramanian* [2008], *Kumar et al.* [2004a]
Brahmaputra	Three years average	1.47	2.13^{+}	169	69*	*Singh et al.* [2005], *Kumar et al.* [2004a]
Mahanadi	-	$NA^{\dagger}$	4.48	356	-	*Kumar et al.* [2004a]
Godavari	Annual average	3.55	3.87	308	92	*Subramanian* [2008], *Kumar et al.* [2004a]
Krishna	-do-	0.41	0.17	14	243*	*Subramanian* [2008], *Kumar et al.* [2004a]
Krishna	September 2002	0.15	0.17	14	88	*Das et al.* [2005], *Krishnaswami and Singh* [2005], *Kumar et al.* [2004a]
Cauvery	Annual average	2.24	0.63	50	356*	*Subramanian* [2008], *Kumar et al.* [2004a]
Rivers debouching into the Arabian Sea						
Indus	Annual average	3.87	2.48	197	156*	*Subramanian* [2008], *Kumar* [2004]
Indus	-do-	0.83	2.48	197	34	*Karim and Veizer* [2000], *Kumar* [2004]
Narmada	-do-	0.21	4.25	338	5	*Subramanian* [2008], *Kumar* [2004]
Nethravati	-do-	$NA^{\dagger}$	0.46	37	-	*Prakash et al.* [2008]
Mahi	-do-	0.001	-	-	-	*Subramanian* [2008]
$SWKR^{\theta}$	-do-	0.42	1.56	124	27	*Subramanian* [2008], *Prakash et al.* [2008]

$^{\times}$New productivity is measured as uptake rate of nitrate during the deck incubation, $^{€}$Export productivity (mg C m^{-2} d^{-1}) is calculated using Redfield ratio, $^{\$}$Also known as Ganges, *high values represent either the eutrophication of the coastal ocean or much of the DIN could be removed prior to discharge into the coastal ocean, $^{+}$New productivity near the Ganga and Brahmaputra is taken to be the same as they debouch at the same place, †Data not available, $^{\theta}$Small West-flowing Kerala Rivers (average of 15 rivers).

Table 5.4: DIN flux (mmol N m^{-2} d^{-1}) in the rivermouths/estuary and its contribution (in %) to the new productivity (mmol N m^{-2} d^{-1}) in the northern Indian Ocean

Rivers debouching into the Bay of Bengal						
River	Season	DIN flux	NP$^{\times}$	EP$^{€}$	%Contribution	References
Ganga$^{\$}$	Feb-May 1999-2001	0.09	2.47	196	4	*Mukhopadhyay et al.* [2006], *Kumar et al.* [2004a]
Ganga	Jun-Sep 1999-2001	0.46	2.13	169	22	*Mukhopadhyay et al.* [2006], *Kumar et al.* [2004a]
Ganga	August 2001	3.20	2.13	169	150*	*Lambs et al.* [2005], *Kumar et al.* [2004a]
Brahmaputra	-do-	1.78	2.23	177	84	*Lambs et al.* [2005], *Kumar et al.* [2004a]
Mahanadi	-do-	0.41	4.48	356	9	*Lambs et al.* [2005], *Kumar et al.* [2004]
Mahanadi	May-Jun 2004-2005	1.87	10.68	849	18	*Naik et al.* [2009], *Kumar et al.* [2004a]
Mahanadi	Oct-Nov 2004-2005	3.47	4.48	356	77	*Naik et al.* [2009], *Kumar et al.* [2004a]
Godavari	August 2001	0.40	3.87	308	10	*Lambs et al.* [2005], *Kumar et al.* [2004a]
Godavari	January 1996	306	4.35	346	7024*	*Krupadam and Anjaneyulu* [2000], *Kumar et al.* [2004a]
Godavari	July 1996	5420	3.87	308	140041*	*Krupadam and Anjaneyulu* [2000], *Kumar et al.* [2004a]
Krishna	August 2001	0.21	0.17	14	124*	*Lambs et al.* [2005], *Kumar et al.* [2004a]
Cauvery	-do-	0.004	0.63	50	0.7	*Lambs et al.* [2005, *Kumar et al.* [2004a]
Rivers debouching into the Arabian Sea						
Indus	Annual average	0.38	2.48	197	15	*Karim and Veizer* [2000], *Kumar* [2004]
Narmada	August 2001	0.38	4.25	338	9	*Lambs et al.* [2005], *Kumar* [2004]
Narmada	Mar-May 1979	0.01	4.25	338	1	*Zingde* [2005], *Kumar* [2004]
Narmada	February 1995	0.02	4.25	338	3	*Zingde* [2005], *Kumar* [2004]
Narmada	March 1997	0.03	4.25	338	5	*Zingde* [2005], *Kumar* [2004]
Nethravati	-do-	0.03	5.64	448	5	*Naik et al.* [2009], *Prakash et al.* [2008]

$^{\times}$New productivity is measured as uptake rate of nitrate during the deck incubation, $^{€}$Export productivity (mg C m^{-2} d^{-1}) is calculated using Redfield ratio,*high values represent either the eutrophication of the coastal ocean or much of the DIN could be removed prior to discharge into the coastal ocean.

contributes ∼5 Tg N y^{-1} (9 Tg N y^{-1} also includes the 3 Tg N y^{-1} transport through Padma, Meghna and other tributaries of the Ganga, which debouch into the Bay via Bangladesh). Most of the agricultural activities are supported by the Ganga waters in the northern India. Fertilizer use in the fields around the Ganga basin has been increasing [*Subramanian*, 2008]. This could have led to the large nitrate transport through the Ganga. All other rivers such as Godavari, Krishna have a minor DIN transport i.e. < 1 Tg N y^{-1}. Analysis based on the data presented by *Lambs et al.* [2005], suggests that the Bay receives 0.4 Tg N y^{-1} and 50% of this amount is transported through the Ganga.

We conclude from our analysis that a major fraction of DIN is carried by the Ganga, though the two studies [*Lambs et al.*, 2005; *Subramanian*, 2008] sampled different stations: those of *Subramanian* [2008] are on the river course while those of *Lambs et al.* [2005] are at the river mouth. It appears that 96% of this DIN does not reach the Bay and is consumed on the way.

DIN concentration measurements in the river course show that the contribution of riverine DIN flux to new productivity is always more than 100% except for a few, such as for April 1989, which only show a 0.37% contribution from the Ganga (Table 5.3). The Ganga also shows an abnormally high contribution i.e. 3,587% to new productivity in the adjacent area, from the data based on another report (Table 5.3). This must be interpreted in terms of eutrophication of coastal waters. Estuarine measurements show larger fluxes in the Mahanadi during October-November 2004 and 2005, but the contribution of this flux to marine new productivity is not the maximum from this river, but from the Ganga during August 2001 (Table 5.4). One of the largest Indian rivers, Brahmaputra, shows a higher contribution (84%) to new productivity. The Cauvery contributes a minimum (0.7%) to new productivity (Table 5.4), although it passes through vast areas of rice cultivation, with an excessive of nitrogenous fertilizers [*Subramanian*, 2008]. This is likely if mineralization of nutrients in the Cauvery estuary is rapid.

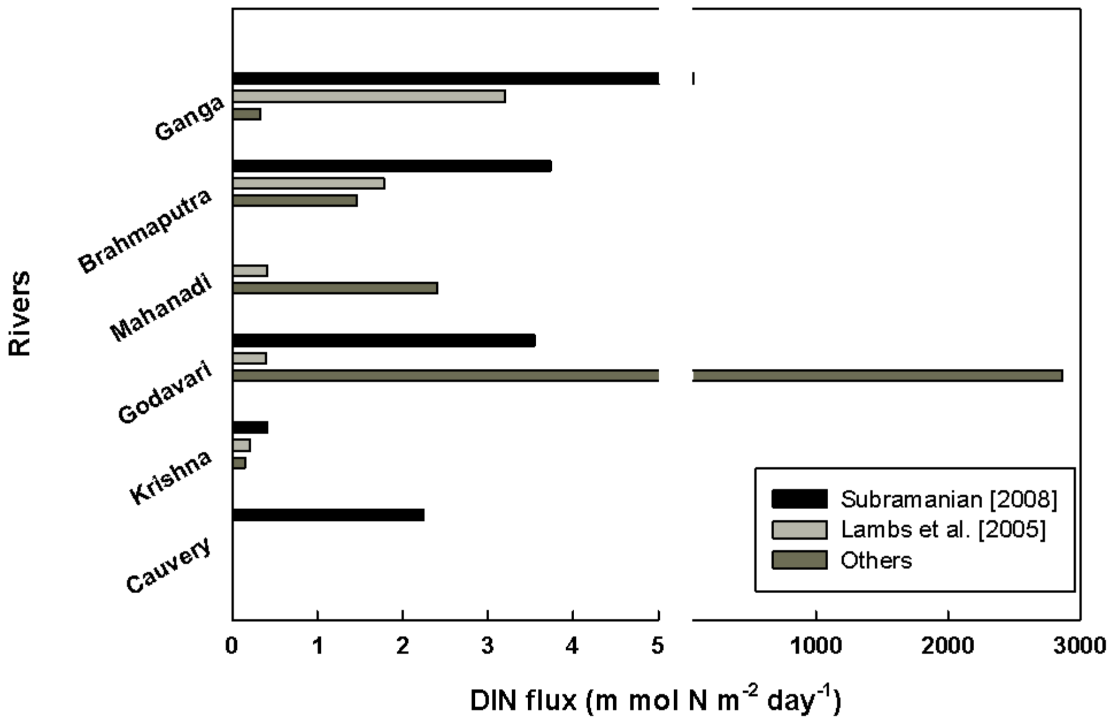

Figure 5.4: DIN fluxes to the Bay of Bengal from major Indian rivers (analysis based on the data obtained from different studies, others include *Krupadam and Anjaneyulu* [2000], *Das et al.* [2005], *Mukhopadhyay et al.* [2006], *Naik et al.* [2009], and *Singh et al.* [2005]). Note the break in the x-axis at 5 mmol N m^{-2} d^{-1}. Error bars indicate overall uncertainty (21%) in flux estimations.

5.2.2 Arabian Sea

Our estimation based on data reported by *Subramanian* [2008] shows that the Arabian Sea receives 0.3 Tg N y^{-1} (if the flux in west-flowing rivers in north are Kerala are not excluded, it is abnormally large i.e. 4.3 Tg N y^{-1}) and the Indus alone contributes 0.2 Tg N y^{-1} (DIN transport through other rivers is not statistically significant). Analysis based on the data presented by *Lambs et al.* [2005] and *Karim and Veizer* [2000] suggests an order of magnitude lesser values: i.e., the Arabian Sea receives 0.07 Tg N y^{-1} and the Indus contribution is 0.02 Tg N y^{-1}. Sampling locations by *Subramanian* [2008] are on the river course while the data of *Lambs et al.* [2005] and *Karim and Veizer* [2000] are from river mouths. This reveals that 81% of this DIN does not reach the Arabian Sea and is consumed on the way (mostly in the estuaries).

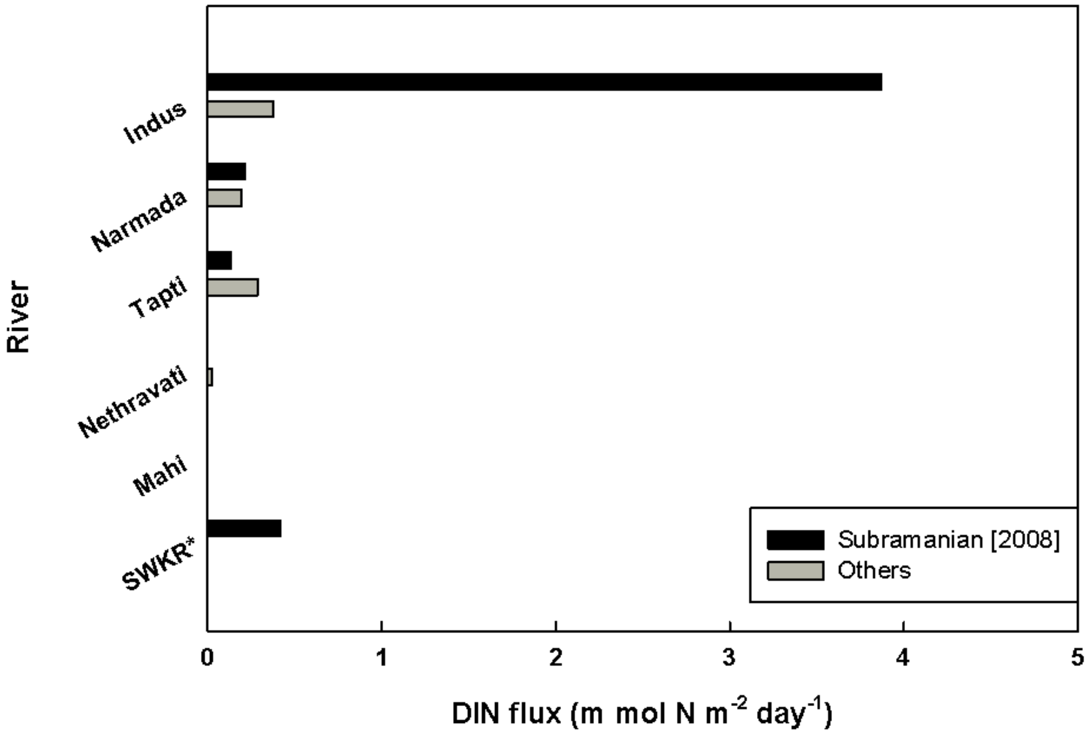

Figure 5.5: DIN fluxes to the Arabian Sea from major rivers that originate in the subcontinent (analysis based on the data obtained from different studies, ‘others’ include *Lambs et al.* [2005], *Karim and Veizer* [2000], and *Zingde* [2005]. *Small West-flowing Kerala Rivers (average value of 15 small rivers). Error bars indicate overall uncertainty (21%) in flux estimations.

Unlike the rivers debouching into the Bay, here rivers seldom show higher than 100% contribution to the new productivity except the Indus (Table 5.3). Estimates based on estuarine DIN concentrations show that although the Indus and the Narmada rivers transport equal amount of DIN, the marine new productivity is more in the coast near Narmada and hence its contribution to new productivity is less (Table 5.4).

Analysis of nutrient discharge through rivers to the Arabian Sea and the Bay of Bengal shows that most of the DIN is transported through rivers of Himalayan origin and most of it is consumed on the way because of the longer river courses. Globally 4-5% to the N input to agricultural systems is transported to the coastal seas [*Bouwman et al.*, 2005]. Our analysis also supports this and is in agreement with the conclusion of *Bouwman et al.* [2005] that most of the DIN is removed on the land before it reaches the ocean because part of the nitrogen is first reduced by crop removal, and the remaining is reduced by denitrification in the soil, followed by denitrification in groundwater systems. Field experiments may help quantify these losses.

5.2.3 Riverine flux versus coastal upwelling

Intense upwelling during summer (June-September) and vertical mixing in winter (December-February) make the Arabian Sea the more productive basin [*Kumar et al.*, 2010, *Gandhi et al.*, 2010a, *Singh et al.*, 2010]. On the other hand, river discharge stratifies the surface Bay of Bengal and inhibits upwelling [*Singh et al.*, 2010, and references therein]. As a result, the Arabian Sea is more productive relative to the Bay. However, new productivity is comparable in both the basins (Tables 5.3, 5.4). Sediment trap observations also suggest comparable organic matter transport to the deep in both basins [*Ramaswamy and Nair*, 1994]. Coastal upwelling, driven by local winds, is not strong enough to explain the higher new productivity in the Bay of Bengal [*Shetye et al.*, 1991, *Prasanna Kumar et al.*, 2004]. Eddies have been suggested to be one of the possible sources of nutrients in the Bay of Bengal [*Prasanna Kumar et al.*, 2004; *Gandhi et al.*, 2011]. We propose the riverine DIN flux to be a potential factor for the higher new productivity in the coastal Bay, though most of the riverine nutrients are removed in the estuaries. Nutrients produced through remineralisation of organic matter in the estuary may be transported into the ocean and thus could enhance new productivity.

Coastal upwelling introduces 65×10^{10} m^3 water from the deep to the surface in the Arabian Sea during the summer monsoon [*Rixen et al.*, 2000]. Assuming that this water (having a nitrate concentration of ∼5.56 μM) is spread over 1°×1° area, 2.44 mmol N m^{-2} d^{-1} is brought up during intense upwelling. Higher coastal new productivity (e.g. new productivity is 4.25 mmol N m^{-2} d^{-1} where the Narmada debouches) suggests a significant contribution from the rivers even during an intense upwelling period in the Arabian Sea.

5.2.4 Submarine ground water discharge

Submarine groundwater discharges nutrients into the ocean. Preliminary and limited results from a coastal site in southern India reported 86.4-142 μM nitrate in the submarine groundwater discharge [*Somayajulu*, 2008]. Groundwater flux is 2,300-23,000 m^3 s^{-1}, rarely comparable to the revirine flux [*Moore*, 1997]. Since nitrate is quite low in groundwater, this discharge does not contribute significantly to marine new productivity (<1%). In such cases, where groundwater discharge and upwelling are not significant, the riverine flux seems to be contributing significantly to higher marine new productivity (e.g. in the Bay of Bengal).

5.2.5 Changes in the Redfield Ratio and biodiversity

Sea surface water microorganisms take up C:N:P in a particular ratio which is known as Redfield Ratio. *Duce et al.* [2008] suggested that phosphorous concentration in the surface ocean is not significantly affected by anthropogenic activity and hence nitrogen fluxes alone are likely to enhance the N:P in the surface sea water. As most of the new productivity in the coastal ocean is supported by riverine DIN fluxes, this may result in increasing dissolved N:P. Any change in the Redfield ratio causes a change in the ecosystem composition, which may have positive/negative influence on the marine environments [*Paerl*, 1988]. It is shown recently that a major part of nitrogen is also lost in its organic form [*Perakis and Hedin*, 2002] i.e. DON. Unavailability of DON data precludes the assessment of its contribution to coastal new productivity. Quantification of DON fluxes along with

DIN may improve estimates of nitrogen loss through rivers and its contribution to new productivity, though DON contribution to productivity is yet to be evaluated in the Indian Ocean.

5.3 Conclusion

This study synthesizes important information needed to understand the atmospheric and riverine nitrogen fluxes (the nitrogen cycle) and their contribution to new productivity. No significant temporal trends either in the marine productivity or in the deposition fluxes are observable in the northern Indian Ocean. There is no significant spatial variation in the new productivity during the spring inter monsoon in the three zones of the Arabian Sea. However, a significant seasonal variation in the western Arabian Sea is observed during 1995. Aerosols deposit 1.73 Tg Nitrogen per year on the northern Indian Ocean, with a major fraction (68%) on the Arabian Sea. Atmospheric fluxes make a minor contribution to the marine new productivity (maximum up to 2.5% in the eastern Arabian Sea during the winter monsoon). However, this minor contribution is likely to become important in the near future and play a crucial role in the removal of excess atmospheric CO_2 through marine productivity. There is no definite correlation between the atmospheric flux and new productivity. Limited data suggest that depositional flux estimates are not affected by El Nino events, while new productivity is weakly linked.

We infer that a major fraction of the DIN transported through Indian rivers is removed on the land surface and in the estuaries; however, a significant contribution (∼13%, geometric mean) of this nitrogen to coastal new productivity is observed. Most of the riverine DIN flux (∼81% in the case of the Arabian Sea and 96% in the case of the Bay of Bengal) is not transported to the coastal ocean and is consumed on the course of the rivers or in the estuaries. Coastal Bay of Bengal and Arabian Sea receive ∼0.38 Tg N y^{-1} and ∼0.06 Tg N y^{-1}, respectively, through rivers. A large variation in the contribution of DIN through river fluxes to new productivity is found in both these basins. The contribution of riverine DIN to coastal new productivity is higher in the Bay of Bengal than in the Arabian Sea. Assessing riverine DON fluxes will provide better insight on nitrogen inputs.

Chapter 6

Summary and scope for future work

The present study is a step forward in understanding the physical and biogeochemical properties of the two northern Indian Ocean basins, i.e., the Arabian Sea - a region well recognized for the perennial occurrence of oxygen minimum zone but least-studied among such regions, and the Bay of Bengal - an ocean basin hitherto undersampled, Major finding of this study are as follows

6.1 Results from the N_2 fixation experiments

- The first direct measurements of N_2 fixation along with carbon uptake rates are reported and discussed which may not only be useful in global climate models but also help understand the marine biogeochemical cycles.

- Significant dinitrogen is fixed (~5% of the global N_2 fixation) during a *Trichodesmium* bloom in the Arabian Sea. The present estimate shows that the previous N_2 fixation rates can be considerably underestimated, however, the fixed nitrogen (6.2 Tg N y^{-1}) is still far less than the estimated nitrogen loss (~120 Tg N y^{-1}) through denitrification. N_2 fixation is the most important process among all the nitrogen gain processes and the Arabian Sea gains ~85% of its 'new' nitrogen through this process.

- In addition to the visual evidence of *Trichodesmium* bloom, lower values of δ^{15}N of PON associated with higher N_2 fixation rates confirm the presence of N_2 fixing algae. N_2 fixation rates are consistent with carbon uptake rates. The presence of microbes that are incapable of fixing N_2, leads to higher consumption ratios.
- Nitrogen fixation was observed in the Wadden Sea sediments, fixation rates were not as higher as hypothesized. Lower fixation rates could be possible if N_2 fixation exhibits seasonal variation.
- The present study is the first attempt to quantify the N_2 fixation rates in the Wadden Sea sediments using $^{15}N_2$ tracer technique. To understand this process better in the sediments, further studies during summer are suggested.
- the technique developed for measuring N_2 fixation in sediments can be used in future to measure the same in the sediments of the northern Indian Ocean.

6.2 Results from Simulation of nitrogen loss in the ocean

- An attempt is made to understand nitrogen loss process in the Arabian Sea theoretically and verify it using data available in literature.
- By using a modified Rayleigh equation, it is shown that ~50% of the nitrate lost during denitrification is compensated by organic matter raining from above. In another application to SOM decomposition, ~20% of the organic matter is compensated by an appropriate choice of $\delta^{18}O_r$ and ϵ.
- The revised Rayleigh equation is further extended to understand the observed variations in the δ^{18}O-S relation of sea surface water in the northern Indian Ocean. This is the first study to assess the spatiotemporal variations of this

relation in the northern Indian Ocean, using a new data set that can help to decrease the uncertainty in paleosalinity estimates for this region.

- A significant spatiotemporal variation in the δ^{18}O-S relation has been observed in the Bay of Bengal. A mass balance model suggests a higher slope when river discharge depleted in ^{18}O is added to the Bay of Bengal surface waters, as also reflected by the data. Significant fresh water resulting from the summer monsoon rains over the hinterland increases the slope relative to the pre/post monsoon in the Bay of Bengal.

- In the southeastern Arabian Sea most data suggest little variation in the slope (∼0.26) during the summer, as reproduced by the model where evaporation dominates over other processes. During late winter a higher slope of 0.45 is observed in the northeastern Arabian Sea than the southeastern Arabian Sea, caused possibly by the mixing of water transported from Indian coastal currents or river inputs to this region. In contrast, limited data obtained during the two cruises in the southeastern Arabian Sea form a cluster, possibly because of small differences between evaporation and precipitation.

- The derived mass balance equations can be useful to quantify the relative importance of runoff sources from different processes such as rain snow-melt and rain over land.

6.3 Results from atmospheric and riverine fluxes

- Atmospheric deposition and on riverine nitrogen fluxes are estimated from published nitrogen concentration data. Their contribution to new productivity is examined further.

- No significant temporal trends either in the marine productivity or in the deposition fluxes are observable in the northern Indian Ocean.

- There is no significant spatial variation in the new productivity during the spring inter monsoon in the three zones of the Arabian Sea. However, a significant seasonal variation in the western Arabian Sea is observed during 1995.

- Aerosols deposit 1.73 Tg Nitrogen per year into the northern Indian Ocean, with a major fraction (68%) on the Arabian Sea. Atmospheric fluxes make a minor contribution to the marine new productivity (maximum up to 2.5% in the eastern Arabian Sea during the winter monsoon). However, it is speculated that this minor contribution is likely to become important in the near future and play a crucial role in the removal of excess atmospheric CO_2 via marine productivity.

- Limited data suggest that depositional flux estimates are not affected by El Nino events, while new productivity is weakly linked.

- Major fraction of the DIN transported through Indian rivers is removed on the land surface and in the estuaries; however, a significant contribution (∼13%, geometric mean) of this nitrogen to coastal new productivity is observed. Most of the riverine DIN flux (∼81% in the case of the Arabian Sea and 96% in the case of the Bay of Bengal) is not transported to the coastal ocean and is consumed on the courses of the rivers or in the estuaries.

- Coastal Bay of Bengal and Arabian Sea receive ∼0.38 Tg N y^{-1} and ∼0.06 Tg N y^{-1}, respectively, through rivers. A large variation in the contribution of DIN through river fluxes to new productivity is found in both these basins. The contribution of riverine DIN to coastal new productivity is higher in the Bay of Bengal than in the Arabian Sea.

6.4 Scope for future work

Though a significant amount of work has been done in the present study, yet more work needs to be done on this topic for improving our understanding of the marine nitrogen and carbon cycles. The following is suggested as future plan, in continuation of the present study:

- The present study helps to understand the carbon and nitrogen cycling of the Indian Ocean in a better way. For a more precise annual nitrogen budget, a further study during *Trichodesmium* blooms in fall is suggested in the Arabian Sea.

- Imbalance in nitrogen budget still suggests a possibility of significant nitrogen fixation in the Bay of Bengal or in other such basins. There is a need to measure N_2 fixation in such basins.

- Lower N_2 fixation rates in the Wadden Sea could be possible if N_2 fixation exhibits seasonal variation. To understand this process better in the sediments a further study during summer is suggested.

- Presently we use satellite data for estimating phytoplankton biomass and primary productivity to some extent. Characterization of marine microbial communities using satellite data would add extra information on larger spatial scales.

- A more rigorous modeling including advection is required to understand δ^{18}O-S relation.

- Denitrification in the Arabian Sea is studied rigorously but the role of other mechanisms for nitrogen loss from the ocean i.e., anammox, is yet to be evaluated.

- Assessing riverine DON fluxes will provide better insight on nitrogen inputs to the ocean.

- Both simulations [*Wiggert et al.*, 2006] and observations [*Naqvi et al.*, 2010a] suggest that the marine productivity is limited by the availability of Fe in the western surface Arabian Sea. Hypothesis of Fe limitation needs to be checked in the other parts of the Indian Ocean.

- Hypothesis of high CO_2/low pH in the ocean (anticipated from the future climate changes) may affect global nitrogen cycling [*Huesemann et al.*, 2002] and nitrogen inputs due to N_2 fixation [*Hutchins et al.*, 2007]. Mesocosm experiments are required to test this hypothesis.

References

Accoe F. et al, 2002. Evolution of the δ^{13}C signature related to total carbon contents and carbon decomposition rate constants in a soil profile under grassland. *Rapid Communication in Mass Spectrometry* 16, 2184-2189.

Araguas-Araguas L., Froehlich K., Rozanski K., 1998. Stable isotope composition of precipitation over southeast Asia. *Journal of Geophysical Research* 103, 28721-28742.

Arrigo K. R., 2005. Marine microorganisms and global nutrient cycles. *Nature* 437, 349-355.

Albarede F., 1995. Introduction to geochemical modeling, Cambridge University Press, U.K., pp. 47-50.

Altabet M. A., McCarthy J. J., 1985. Temporal and spatial variations in the natural abundance of ^{15}N in PON from a warm-core ring. *Deep Sea Research I* 32, 755-772.

Austin W. E. N., Cage A. G., Scourse J. D., 2006. Mid-latitude shelf seas: a NW European perspective on the seasonal dynamics of temperature, salinity and oxygen isotopes. *The Holocene* 16, 937-947.

Baker A. R. et al, 2007. Dry and wet deposition of nutrients from the tropical Atlantic atmosphere: Links to primary productivity and nitrogen fixation. *Deep Sea Research I* 54, 1704-1720.

Baker A. R. et al, 2010. Estimation of atmospheric nutrient inputs to the Atlantic Ocean from 50N to 50S based on large-scale field sampling: Fixed nitrogen and dry deposition of phosphorus. *Global Biogeochemical Cycles* 24, GB3006, doi:10.1029/2009GB003634.

Bange H. W. et al, 2000. A revised nitrogen budget for Arabian Sea. *Global Biogeochemical Cycles* 14 (4), 1283-1297.

Bange H. W., Naqvi S. W. A., Codispoti L. A., 2005. The nitrogen cycle in the Arabian Sea. *Progress in Oceanography* 65, 145-158.

Barber R. T. et al, 2001. Primary productivity and its regulation in the Arabia Sea during 1995. *Deep Sea Research II* 48, 1127-1172.

Barford C. C. et al, 1999. Steady-state nitrogen isotope effects of N_2 and N_2O production in Paracoccus denitrificans. *Applied Environmental Microbiology* 65, 989-994.

Benway, H. M., Mix, A. C., 2004. Oxygen isotopes, upper ocean salinity, and precipitation sources in the eastern tropical Pacific. *Earth and Planetary Science Letters* 224, 493-507.

Bhattathiri P. M. A. et al, 1996. Phytoplankton production and chlorophyll distribution in eastern and central Arabian Sea in 1994-1995. *Current Science* 71, 857-862.

Bickle, M. J. et al, 2005. Relative contributions of silicate and carbonate rocks to riverine Sr fluxes in the headwaters of the Ganges. *Geochimica et Cosmochimica Acta* 69, 2221-2240.

Bigg, G. R., Rohling, E. J., 2000. An oxygen isotope data set for marine waters. *Journal of Geophysical Research* 105, C4, 8527-8535.

Bird C. et al, 2005. Spatial Distribution and Transcriptional Activity of an Uncultured Clade of Planktonic Diazotrophic γ-Proteobacteria in the Arabian Sea. *Applied And Environmental Microbiology* 71 (4), 2079-2085.

Blair N. et al, 1985. Carbon Isotopic Fractionation in Heterotrophic Microbial Metabolism. *Applied Environmental Biology* 50, 996-1001.

Bouwman A. F. et al, 2005. Exploring changes in river nitrogen export to the world's oceans. *Global Biogeochemical Cycles* 19, GB1002, doi:10.1029/2004 GB002314.

Bowen, G. J., Revenaugh, J., 2003. Interpolating the isotopic composition of modern meteoric precipitation. *Water Resources Research* 39:1299 Doi:10.1029/2003WR002086.

Brand W. A. et al, 1996. New methods for fully automated ratio determination from hydrogen at natural abundance level. *Isotopes in Environmental and Health Studies* 32, 263-273.

Brandes J. A. et al, 1998. Isotopic composition of nitrate in the central Arabian Sea and eastern tropical North Pacific: a tracer for mixing and nitrogen cycles. *Limnology and Oceanography* 43, 1680-1689.

Brandes J. A., Devol A. H., Deutsch C., 2007. New developments in the marine nitrogen cycle, *Chemical Reviews* 107, 577-589.

Broecker W. S., 1974. Chemical Oceanography (Harcourt Brace Jovanovich, New York), 214 pp.

Broecker W. S., Oversby V. M., 1971. Chemical equilibria in the earth. McGraw-Hill, New York, London.

Capone D. G., 1993. Determination of nitrogenase activity in aquatic samples using the acetylene reduction procedure. In Handbook of methods in aquatic microbial ecology edited by P. F. Kemp, B. F. Sherr, E. B. Sherr, and J. J. Cole, Lewis Publishers, Boca Raton, Fla. pp. 621-631.

Capone D. G. et al, 1997. *Trichodesmium*: a globally significant marine cynobacterium. *Science* 276, 1221-1229.

Capone D. G. et al, 1998. An extensive bloom of the N_2 fixing cyanobacterium *Trichodesmium* erythraeum in the central Arabian Sea. *Marine Ecological Progress Series* 172, 281-292.

Capone D. G., 2001. Marine nitrogen fixation: what's the fuss?, *Current Opinion in Microbiology* 4, 341-348.

Capone D. G. et al, 2005. Nitrogen fixation by *Trichodesmium* spp.: An important source of new nitrogen to the tropical and subtropical North Atlantic Ocean. *Global Biogeochemical Cycles* 19, GB2024, doi:10.1029/2004GB002331.

Carpenter E. J., Capone D. G., 2008. N_2 fixation in the Marine Environment, in Nitrogen in the Marine Environment, edited by D. G. Capone et al., 141-198, Elsevier.

Chao, L. L., 1974. Statistics, methods and analysis. McGraw-Hill Book Company, 237 p.

Chen Y. L., Chen H. Y., 2006. Seasonal dynamics of primary and new production in the northern South China Sea: The significance of river discharge and nutrient advection. *Deep Sea Research I* 53, 971-986.

Chen Y. L., Chen H. Y., Tuo S., Ohki K., 2008. Seasonal dynamics of new production from *Trichodesmium* N_2 fixation and nitrate uptake in the upstream Kuroshio and South China Sea basin. *Limnology Oceanography* 53(5), 1705-1721.

Church M. J. et al., 2009. Physical forcing of nitrogen fixation and diazotroph community structure in the North Pacific subtropical gyre. *Global Biogeochemical Cycles* 23, GB2020, doi:10.1029/2008GB003418.

Clark I. D., Fritz P., 1997. Environmental isotopes in hydrogeology. Levis Publisher, 328p.

Cleixner C. et al, 1993. Correlations between the ^{13}C Content of Primary and Secondary Plant Products in Different Cell Compartments and That in Decomposing Basidiomycetes. *Plant Physiology* 102, 1287-1290.

Cline J. D., Richards F. A., 1972. Oxygen deficient conditions and nitrate reduction in the eastern tropical North Pacific Ocean. *Limnology Oceanography* 17, 885-900.

Codispoti L. A., 2007. An oceanic fixed nitrogen sink exceeding 400 Tg N a^{-1} vs the concept of homeostasis in the fixed-nitrogen inventory. *Biogeosciences* 4, 233-253.

Craig H., 1957. Isotopic standards for carbon and Oxygen and correction factors for mass spectrometric analysis of carbon dioxide. *Geochemica et Cosmochimica Acta* 12. p. 133.

Craig, H., Gordon, L. I., 1965. Deuterium and oxygen-18 variations in the ocean and the marine atmosphere, in stable isotopes in Oceanographic Studies and Paleotemperatures. Edited by E. Tongiorgi, Lab. Di Geol. Nucl., Cons. Naz. Delle Ric., Pisa, Italy, pp. 9-130.

Criss R. E., 1999. Principles of stable isotope distribution. Oxford University Press, Oxford, UK, 254p.

Dalsgaard T. et al, 2003. N_2 production by the anammox reaction in the anoxic water column of Golfo Dulce, Costa Rica. *Nature* 422, 606-608.

Dansgaard W., 1964. Stable isotopes in precipitation. *Tellus* 16, 436-468.

Das A. et al, 2005. Chemical weathering in the Krishna basin and Western ghats of the Deccan Traps, India: Rates of basalt eathering and their controls. *Geochimica et Cosmochimica Acta* 69, 2067-2084.

Dekas A. E. et al, 2009. Deep-Sea Archaea Fix and Share Nitrogen in Methane-Consuming Microbial Consortia. *Science* 326, 422-426.

Delaygue G., et al, 2001. Oxygen isotope/salinity relation in the northern Indian Ocean. *Journal of Geophysical Research* 106, 4565-4574.

Delwiche C. C., Steyn P. L., 1970. Nitrogen isotope fractionation in soils and microbial reactions. *Environment Science and Technology* 4, 929-935.

Desa E. et al., 2005. Detection of *Trichodesmium* bloom patches along the eastern Arabian Sea by IRS-P4/OCM ocean color sensor and by in-situ measurements, *Indian Journal Marine Sciences* 34, 374-386.

Devassy V. P., Bhattathiri P. M. A., Qasim S. Z., 1978. *Trichodesmium* Phenomenon. *Indian Journal of Marine Sciences* 7, 168-186.

Devol A. H. et al., 2006. Denitrification rates and excess nitrogen gas concentrations in the Arabian Sea oxygen deficient zone. *Deep Sea Research I* 53, 1533-1547.

Devol A. H., 2008. Denitrification including anammox - in Nitrogen in the Marine Environment, 2^{nd} Edition, edited by Capone D., Bronk, D., Mulholland, M., Carpenter, E., Elsevier, Amsterdom, 263-301.

Deutsch C. et al., 2007. Spatial coupling of nitrogen inputs and losses in the ocean, *Nature* 445, 163-167.

Doney S. C., Schimel D. S., 2007. Carbon and climate system coupling on timescales from the Precambrian to the Anthropocene. *Annual Review of Environment and Resources* 32, 31-66.

Duce R. A. et al, 1991. The atmospheric input of trace species to the world ocean. *Global Biogeochemical Cycles* 5, 193-259.

Duce R. A. et al, 2008. Impacts of atmospheric anthropogenic nitrogen on the open ocean. *Science* 320, 893-897.

Dugdale R. C., Goering J. J., 1967. Uptake of new and regenerated forms of nitrogen in primary productivity. *Limnology and Oceanography* 12, 196-206.

Duplessy J. C., B A. W. H., Blanc P. L., 1981. Oxygen and carbon isotopic composition and biogeographic distribution of planktonic foraminifera in the Indian Ocean. *Palaeogeography, Palaeoclimatology, Palaeoecology* 33, 9-46.

Duplessy J. C., 1982. Glacial to interglacial contrasts in the northern Indian Ocean. *Nature* 295, 494-498.

Eppley R. W., Peterson B. J., 1979. Particulate organic matter flux and planktonic new production in the deep ocean. *Nature* 282, 677-680.

Epstein, S., Mayeda, T., 1953. Variation of O^{18} content of water from natural sources. *Geochimica et Cosmochimica Acta* 4, 213-224.

Falkowski P. G., 1997. Evolution of the nitrogen cycle and its influence on the biological sequestration of CO_2 in the ocean. *Nature* 387, 272-275.

Faure G., 1986. Principles of isotope geology. John Wiley & sons, Singapore.

Ferronsky V. I., Brezgunov V. S., 1989. Stable isotopes and ocean mixing, in Handbook of Environmental Isotope Geochemistry, Vol 3, The Marine Environment A, Edited by Fritz, P. & Fontes, J. Ch., Elsevier, Amsterdam, pp. 1-27.

Flemming B. W., Davis R. A. Jr., 1994. Holocene evolution, morphodynamics and sedimentology of the Spiekeroog barrier island system (Southern North Sea). *Senckenb Marit* 24,117-155.

Gadgil S., 2003. The Indian monsoon and its variability. *Annual Review of Earth and Planetary Sciences* 31, 429-467.

Galloway J. N. et al, 2004. Nitrogen Cycles: Past, Present and Future, *Biogeochemistry* 70, 153-226.

Gandhi N., 2010. Carbon fixation in the Hydrosphere: Quantification in the Indian region using ^{13}C and ^{15}N isotopes, Ph.D. thesis submitted to M.L.S. University, Udaipur, India, 206 p.

Gandhi N. et al, 2010a. Nitrogen uptake rates during spring in the NE Arabian Sea. *International Journal of Oceanography* 2010, doi:10.1155/2010/127493.

Gandhi N. et al, 2010b. Nitrogen uptake rates and new production in the northern Indian Ocean. *Indian Journal of Marine Sciences* 39 (2), 1-7.

Gandhi N., Singh A., Ramesh R., 2011. Nitrogen sources for new production in the NE Indian Ocean. *Advances in Geosciences* (accepted).

Gao et al, 2010. Aerobic denitrification in permeable Wadden Sea sediments. *The ISME Journal* 4, 417-426.

Gat J. R., Gonfiantini R., 1981. Stable Isotope Hydrology, Deuterium and Oxygen-18 in the Water Cycle. Technical Report Series No.210.,pp 103-142. IAEA, Vienna.

Gattuso, Jean-Pierre and Stephen V Smith (Lead Authors); J Emmett Duffy (Topic Editor). 2007. 'Coastal zone.' In: Encyclopedia of Earth. Eds. Cutler J. Cleveland (Washington, D.C.: Environmental Information Coalition, National Council for Science and the Environment).

Gauns M. et al, 2005.Comparative accounts of biological productivity characteristics and estimates of carbon fluxes in the Arabian Sea and the Bay of Bengal. *Deep Sea Research II* 52, 2003-2017.

Gibb S. W., Mantoura R. F. C., Liss, P. S., 1999. Ocean-atmosphere exchange and atmospheric speciation of ammonia and methylamines in the region of the NW Arabian Sea. *Global Biogeochemical Cycles* 13, 161-178.

Goes J. I. et al, 2005. Warming of the Eurasian Landmass in making the Arabian Sea more productive. *Science* 30, 545-547.

Gonfiantini, R., 1981. The δ notation and the mass-spectrometric measurement techniques, in Stable Isotope Hydrology: Deuterium and Oxygen-18 in the Water Cycle, Tech. Rep. Ser. 210, edited by J. R. Gat and R. Gonfiantini, 337 p., International Atomic Energy Agency, Vienna, Austria.

Gonzalez P. J. et al, 2006. Bacterial nitrate reductases: molecular and biological aspects of nitrate reduction. *Journal of Inorganic Biochemistry* 10, 1015-23.

Gruber N., Galloway J. N., 2008. An Earth-system perspective of the global nitrogen cycle. *Nature* 451, 293-296.

Han W., McCreary J. Jr., 2001. Modeling salinity distributions in the Indian Ocean, *Journal of Geophysical Research* 106, 859-877.

Harrison, W. G. et al, 1977. Marine diatoms in chemostats under silicate or ammonium limitation. III. Cellular chemical composition and morphology of three diatoms. *Marine Biology* 43, 19-31.

Hoefs J., 1980. Stable isotope Geochemistry. second edition, Springer-Verlag, Berlin.

Houghton R. A., 2007. Balancing the Global Carbon Budget. *Annual Review of Earth and Planetary Sciences* 35, 313-347.

Huesemann M. H., Skillman A. D., Crecelius E. A., 2002. The inhibition of nitrification by ocean disposal of carbon dioxide. *Marine Pollution Bulletin* 44, 142-148.

Hutchins D. A. et al, 2007. CO_2 control of *Trichodesmium* N_2-fixation, photosynthesis, growth rates, and elemental ratios: Implications for past, present, and future ocean biogeochemistry. *Limnology and Oceanography* 52, 1293-1304.

Huettel M. et al, 2003. Hydrodynamical impact on biogeochemical processes in aquatic sediments. *Hydrobiologia* 494. 231-236.

IAEA/WMO, 2006. Global Network of Isotopes in Precipitation. The GNIP Database. Accessible at: http://isohis.iaea.org

IPCC (Intergovernmental Panel on Climate Change) report, 2007. http://www.ipcc.ch/SPM2feb07.pdf

Jickells T., 2005. External inputs as a contributor to eutrophication problems. *Journal of Sea Research* 54, 58-69.

Jickells T., 2006. The role of air-sea exchange in the marine nitrogen cycle. *Biogeosciences* 3, 271-280.

Johansen A. M., Siefert R. L., Hoffmann M. R., 1999. Chemical characterization of ambient aerosol collected during the southwest monsoon and intermonsoon seasons over Arabian Sea: Anions and cations. *Journal Geophysical Research* 104, 26325-26347.

Jouzel J., Koster R. D., 1996. A reconsideration of the initial conditions used for stable water isotope models. *Journal of Geophysical Research* 101:22933-22938 doi:10.1029/96JD02362.

Jyothibabu R. et al, 2004. Differential response of winter cooling on biological production in the northeastern Arabian Sea and northwestern Bay of Bengal. *Current Science* 87, 783-791.

Jyothibabu R. et al, 2010. Re-evaluation of 'paradox of mezozooplankton' in the eastern Arabian Sea based on ship and satellite observations. *Journal of Marine Systems* 81, 235-251.

Karim A., Veizer J., 2000. Weathering processes in the Indus river Basin: implications from riverine carbon, sulphur, oxygen, strontium isotopes. *Chemical Geology* 170, 153-177.

Karim A., Veizer J., 2002. Water balance of the Indus River Basin and moisture source in the Karakoram and western Himalayas: Implications from hydrogen and oxygen isotopes in river water. *Journal of Geophysical Research* 107 (D18), 4362. doi:10.1029/2000JD000253.

Karl D. M. et al, 2002. Dinitrogen fixation in the world's oceans, *Biogeochemistry* 57, 47- 98.

Krishnamurti T. N. et al, 1998. Aerosol and pollutant transport and their impact on radiative forcing over the tropical Indian Ocean during the January-February 1996 pre-INDOEX cruise. *Tellus* 50B, 521-542.

Krishnamurthy A. et al, 2010. Impacts of atmospheric nutrient inputs on marine biogeochemistry. *Journal of Geophysical Research* 115, G01006, doi:10.1029/2009JG001115.

Krishnaswami S., Singh S. K., 2005. Chemical weathering in the river basins of Himalaya, India. *Current Science* 85, 841-849.

Krupadam R. J., Anjaneyulu Y.,2000. Cycling of nutrients in Gautami-Godavari Estuarine Ecosystem, Bay of Bengal-East Coast of India. *Research Journal of Chemistry and Environment* 4, 55-70.

Kumar A., Sarin M. M., Sudhir A. K., 2008. Mineral and anthropogenic aerosols in Arabian Seaatmospheric boundary layer: Sources and spatial variability. *Atmospheric Environment* 42, 5169-5181.

Kumar K. K., Rajagopalan B., Cane M. A., 1999. On the weakening relationship between the Indian monsoon and ENSO. *Science* 284, 2156-59.

Kumar S., 2004. Biogeochemistry of Nitrogen isotopes in Northern Indian Ocea. PhD Thesis. M. S. Univeristy of Baroda, Vadodara, INDIA.

Kumar S. et al, 2004a. High new production in the Bay of Bengal: Possible causes and implications. *Geophysical Research Letters* 31, L18304, doi:10.1029/2004GL021005.

Kumar S. et al, 2004b. Natural isotopic composition of nitrogen in suspended particulate matter in the Bay of Bengal. *Biogeosciences* 1, 63-70.

Kumar S., Ramesh R., 2005. Productivity measurements in the Bay of Bengal using ^{15}N tracer: Implications to the global carbon cycle. *Indian Journal of Marine Sciences* 34(2), 153-162.

Kumar S. et al, 2005. Signature of terrestrial influence on nitrogen isotopic composition of suspended particulate matter in the Bay of Bengal. *Current Science* 88 (5), 770-774.

Kumar S. et al, 2010. Nitrogen uptake in the northeastern Arabian Sea during winter cooling. *International Journal of Oceanography* vol. 2010, Article ID 819029, doi:10.1155/2010/819029.

Kuypers M. M. M. et al, 2003. Anaerobic ammonium oxidation by anammox bacteria in the Black Sea. *Nature* 422, 608-611.

Lam P. et al, 2009. Revising the nitrogen cycle in the Peruvian oxygen minimum zone. *Proceedings of National Academy of Sciences USA* 106, 4752-4757.

Lam P., Kuypers M. M. M., 2011. Microbial Nitrogen Cycling Processes in Oxygen Minimum Zones. *Annual Reviews of Marine Sciences* 3, 317-345.

Lambs L. et al, 2005. Oxygen and hydrogen isotopic composition of major Indian rivers: a first global assessment. *Hydrological Processes* 19, 3345-3355.

LeGrande A. N., Schmidt, G. A., 2006. Global gridded data set of the oxygen isotopic composition in seawater. *Geophysical Research Letters* 33, L12604, doi:10.1029/2006GL026011.

Letelier R. M., Karl D. M., 1996. Role of *Trichodesmium* spp. in the productivity of the subtropical North Pacific Ocean. *Marine Ecology Progress Series* 133, 263-273.

Longhurst A., 1998. Ecological geography of the sea. Academic Press, San Diego, 398 p.

Madhupratap M. S. et al, 1996. Mechanism of the biological response to winter cooling in the northeastern Arabian Sea. *Nature* 384, 549-552.

Mariotti A. et al, 1981. Experimental determination of nitrogen kinetic isotope fractionation: some principles; illustration for the denitrification and nitrification processes. *Plant Soil* 62, 413-430.

Matondkar S. G. P. et al, 2006. Setellite and ship studies of phytoplankton in the Northeastern Arabian Sea during 2000-2006 period. *Proceedings of SPIE* 6406, doi: 10.117/12.693693.

McCarthy J. J., Garside C., Nevins J., 1999. Nitrogen dynamics during the Arabian Sea northeast monsoon. *Deep Sea Research II* 46, 1623-1664.

Merlivat L., Jouzel J., 1979. Global Climatic Interpretation of the Deuterium-Oxygen 18 Relationship for Precipitation. *Journal of Geophysical Research* 84:5029-5033 doi: 10.1029/JC084iC08p05029.

Mills M. M. et al, 2004. Iron and phosphorus co-limit nitrogen fixation in the eastern tropical North Atlantic. *Nature* 429, 292-294.

Montoya J. P. et al, 1996. A Simple, High-Precision, High-Sensitivity Tracer Assay for N_2 Fixation. *Applied and Environmental Microbiology* 62, 986-993.

Montoya J. P. et al, 2004. High rates of N_2 fixation by unicellular diazotrophs in the oligotrophic Pacific Ocean. *Nature* 430, 1027-1031.

Mook W. G., 1982. The oxygen-18 content of rivers. Mitt. Geol.-Palaont. Inst. Univ. Hamburg, SCOPE/UNEP Sonderband 52: 565-570.

Mook W. G., 2006. Introduction to Isotope Hydrology: Stable and Radioactive isotopes of Hydrogen, Oxygen and Carbon. Taylor & Francis Group, London, Great Britain.

Moore W. S., 1997. High fluxes of radium and barium from the mouth of the Ganges-Brahmaputra River during low river discharge suggest a large groundwater source. *Earth and Planetary Science Letters* 150, 141-150.

Mukhopadhyay M. K. et al, 2006. Fluxes of nutrients from tropical river Hooghly at the land ocean boundary of Sundarbans, NE coast of Bay of Bengal, India. *Journal of Marine Systems* 62, 9-21.

Mulholland M. R. et al, 2006. Nitrogen fixation and release of fixed nitrogen by *Trichodesmium* spp. in the Gulf of Mexico. *Limnology Oceanography* 51, 1762-1776.

Mulholland M. R., Capone D. G., 2009. Dinitrogen Fixation in the Indian Ocean. *Geophyical Monograph Series* 185, 10.1029/2009GM000850.

Mulitza S. et al, 2010. Increase in African dust flux at the onset of commercial agriculture in the Sahel region, *Nature* 466, 226-228.

Muraleedharan K. R. et al, 2007. Influence of basin-scale and mesoscale physical processes on biological productivity in the Bay of Bengal during the summer monsoon. *Progress in Oceanography* 72(4), 364-383.

Naik S., Acharya B. C., Mohapatra A., 2009. Seasonal variations of phytoplankton in Mahanadi estuary, east coast of India. *Indian Journal of Marine Sciences* 38, 184-190.

Naqvi S. W. A., 1987. Some aspects of the oxygen deficient conditions and denitrification in the Arabian Sea. *Journal of Marine Research* 45, 1049-1072.

Naqvi S. W. A. et al, 2005. Biogeochemical ocean-atmosphere transfers in the Arabian Sea *Progress in Oceanography* 65, 116-144.

Naqvi S. W. A., 2008. The Indian Ocean, in Nitrogen in the Marine Environment, edited by: Capone, D. G., Bronk, D. A., Mulholland, M. R., Carpenter, E. J., Academic Press, pp. 631-681.

Naqvi S. W. A. et al, 2010a. The Arabian Sea as a high-nutrient, low-chlorophyll region during the late Southwest Monsoon. *Biogeosciences* 7, 2091-2100.

Naqvi S. W. A. et al, 2010b. Carbon and Nitrogen fluxes in the North Indian Ocean, in Carbon and Nitrogen Fluxes in Continental Margins edited by Liu et al, pp. 180-191.

Owens N. J. P., Galloway J. N., Duce R. A., 1992. Episodic atmospheric nitrogen deposition to oligotrophic oceans. *Nature* 357, 397-399.

Owens N. J. P. et al, 1993. Size-fractionated primary production and nitrogen assimilation in the northwestern Indian Ocean. *Deep Sea Research II* 40(3), 607-709.

Owens N. J. P., Watts L. J., 1998. ^{15}N and the assimilation of nitrogen by marine phytoplankton: the past, present and future? in Stable Isotopes: Integration of Biological, Ecological and Geochemical Processes.Environmental Plant Biology Series edited by H. Griffiths, BIOS Scientific Publishers Ltd, pp. 257-283.

Padmakumar et al, 2010. Preponderance of heterotrophic *Noctiluca scintillans* during a multi-species diatom bloom along the southwest coast of India. *International Journal of Oceans and Oceanography* 4, 55-63.

Paerl H. W., 1988. *Nuisance* phytoplankton blooms in coastal, estuarine and inland waters. *Limnology and Oceanography* 33, 823-847.

Parab S. G. et al, 2006. Monsoon driven changes in phytoplankton populations in the eastern Arabian Sea as revealed by microscopy and HPLC pigment analysis, *Continental Shelf Research* 26, 2538-2558.

Parameswaran K., Nair S. K., Rajeev K., 2008. Impact of aerosols from the Asian Continent on the adjoining oceanic environments. *Journal of Earth System Sciences* 117, 83-102.

Patra P. K. et al, 2007. Atmospheric deposition and surface stratification as controls of contrasting chlorophyll abundance in the North Indian Ocean. *Journal of Geophyical Research* 112, C05029, doi:10.1029/2006JC003885.

Paul A. et al, 1999. Simulation of Oxygen Isotopes in a Global Ocean Model. From FISCHER G, WEFER G (eds), Use of Proxies in Paleoceanography: Examples from the South Atlantic. Springer-Verlag Berlin Heidelberg, pp. 655-686.

Payne W. J., 1973. Reduction of nitrogenous oxide by micro-organisms. *Bacteriological Reviews* 37, 409-452.

Perakis S. S., Hedin L. O., 2002. Nitrogen loss from unpolluted South American forests mainly via dissolved organic compounds. *Nature* 415, 416-419.

Prakash S., 2008. Role of the ocean in the Global carbon cycle. Ph.D. thesis. The Maharaja Sayajirao University of Baroda Vadodara, India.

Prakash S., Ramesh R., 2007. Is the Arabian Sea getting more productive?. *Current Science* 92(5), 667-671.

Prakash S. et al, 2008. Quantification of New Production during a winter *Noctiluca scintillans* bloom in the Arabian Sea. *Geophysical Research Letters* 35, doi: 10.1029/2008GL033819.

Prasad T. G., 1997. Annual and seasonal mean buoyancy fluxes for the tropical Indian Ocean. *Current Science* 73, 667-674.

Prasanna Kumar S., Prasad T. G., 1996. Winter cooling in the northern Arabian Sea. *Current Science* 71 (11), 834-841.

Prasanna Kumar S., Prasad T. G., 1999. Formation and spreading of Arabian Sea high-salinity water mass. *Journal of Geophysical Research* 104. 1455-1464.

Prasanna Kumar S. et al, 2001. Physical forcing of biological productivity in the Northern Arabian Sea during the Northeast Monsoon. *Deep Sea Research II* 48, 1115-1126.

Prasanna Kumar S. et al, 2002. Why is the Bay of Bengal less productive during summer monsoon compared to the Arabian Sea?. *Geophysical Research Letters* 29, 22-35.

Prasanna Kumar S. et al, 2004. Are Eddies nature's trigger to enhance biological productivity in the Bay of Bengal?. *Geophysical Research Letters* 31, L07309, doi:10.1029/2003Gl019274.

Prasanna Kumar S., Narvekar J., 2005. Seasonal variability of the mixed layer in the Arabian Sea and its implication on nutrients and primary productivity. *Deep Sea Research II* 52, 1848-1861.

Prasanna Kumar S. et al, 2007. Eddy-mediated biological productivity in the Bay of Bengal during fall and spring intermonsoons. *Deep Sea Research I* 54, 1619-1640.

Prasanna Kumar S. et al, 2010. What drives the increased phytoplankton biomass in the Arabian Sea? *Current Science* 99, 101-106.

Qasim S. Z., 1982. Oceanography of northern Arabian Sea. *Deep Sea Research* 29, 1041-1068.

Ramaswamy V., Nair R.R., 1994. Fluxes of material in the Arabian Sea and Bay of Bengal-Sediment trap studies. *Proceedings of the Indian Academy of Sciences (Earth and Planetary Sciences)* 103, 189-210.

Ramesh R., Sarin M. M., 1992. Stable isotope study of the Ganga (Ganges) River system. *Journal of Hydrology* 139, 49-62.

Ramesh R., Singh A., 2010. Isotope fractionation in open systems: application to organic matter decomposition in ocean and land. *Current Science* 98(3), 406-411.

Ramesh Kumar M. R., Prasad T. G., 1997. Annual and interannual variation of precipitation over the tropical Indian Ocean. *Journal of Geophysical Research* 102, 18,519-18,527.

Rao R. R., Sivakumar R., 2003. Seasonal variability of sea surface salinity and salt budget of the mixed layer of the north Indian Ocean. *Journal of Geophysical Research* 108, doi:10.1029/2001JC000907.

Rashid H. et al, 2007. A ~25 ka Indian Ocean monsoon variability record from the Andaman Sea. *Quaternary Science Reviews* 26, 2586-2597.

Rao S. M., 2006. Practical Isotope Hydrology, New India Publishing Agency. p 59.

Rastogi N., 2005. Environmental Radionuclides and Chemical Constituents in Rain and Aerosols : Biogeochemical Sources and Temporal Variations. Ph.D. thesis submitted to M.L.S. University, Udaipur, India, 149 p.

Ray J. S., Ramesh R., 2000. Rayleigh fractionation of stable isotopes from a multicomponent source. *Geochimica et Cosmochimica Acta* 64(2), 299-306.

Rayleigh, 1902. On the distillation of binary mixtures. *Philosophical Magazine* 4, 521-537.

Rengarajan R., Sarin M. M., 2004. Atmospheric deposition fluxes of ^{7}Be, ^{210}Pb and chemical species to the Arabian Sea and Bay of Bengal. *Indian Journal of Marine Sciences* 33, 56-64.

Rhoads K. et al, 1997. Composition of the troposphere the Indian Ocean during the monsoonal transition. *Journal of Geophysical Research* 102, 18981-18995.

Richards F. A., 1965. Anoxic basins and fjords. Chemical Oceanography (eds) J. P. Riley and G. Skirrow, Academic press 1, 611-645.

Rixen T., Haake B., Ittekkot V., 2000. Sedimentation in the Arabian Sea: The role of coastal and open ocean upwelling. *Deep-Sea Research II* 47, 2155-2178.

Rohling E.J., Bigg, G. R., 1998. Paleosalinity and δ^{18}O: A critical assessment. *Journal of Geophysical Research* 103, 1307-1318.

Rostek F. et al, 1993. Reconstructing sea surface temperature and salinity using δ^{18}O and alkenone records. *Nature* 364, 319-321.

Rozanski K., Froelich K., Mook W. G., Stichler W., 2001. Environmental Isotopes in Hydrological Cycle, Principles and Applications. Volume 3: Surface Water, Mook WG (ed). UNESCO/IAEA:Paris.

Ryther J. H. et al, 1966. Primary organic production in relation to the chemistry and hydrography of the western Indian Ocean. *Limnology and Oceanography* 11, 371-380.

Sabine C. L. et al, 2004. The Oceanic Sink for Anthropogenic CO_2. *Science* 305, 367-371.

Sambrotto R. N., 2001. Nitrogen production in the northern Arabian Sea during the Spring Intermonsoon and Southwest Monsoon seasons. *Deep Sea Research II* 48, 1173-1198.

Sarin M. M. et al, 1992. Major ion chemistry of the Ganga source waters: weathering in the high altitude Himalaya. *Proceedings of Indian Academy of Sciences* (*Earth and Planetary Sciences*) 101, 89-98.

Sarin M. M., Rengarajan R., Krishnaswami S., 1999. Aerosol NO_3^- and ^{210}Pb distribution over the central-eastern Arabian Sea and their air-sea deposition fluxes. *Tellus* 51 B, 749-758.

Savidge G., Gilpin L., 1999. Seasonal influences on size-fractionated chlorophyll a concentrations and primary production in the north-west Indian Ocean. *Deep Sea Research II* 46, 701-723.

Savoie D. L., Prospero J. M., Nees R. T., 1987. Nitrate, non-sea-salt sulphate, and mineral aerosol over northwestern Indian Ocean. *Journal of Geophysical Research* 92, 933-942.

Schmidt G. A., LeGrande A. N., Hoffmann G., 2007. Water isotope expressions of intrinsic and forced variability in a coupled ocean-atmosphere model, *Journal of Geophysical Research* 112, D10103, doi:10.1029/2006JD007781.

Schafer P. H. et al, 1993. Cycling of inorganic nitrogen compounds between atmosphere and ocean in tropical areas off South east Asia. Monsoon Biogeochemistry, edited by V. Ittekkot and R.R. Nair, pp. 19-36, Geol.-Paaontologischen Inst. Der Univv. Hamburg, Hamburg, Germany

Schott F., McCreary J. P., 2001. The monsoon circulation of the Indian Ocean. *Progress in Oceanography*, 51, 1-123.

Seitzinger S. et al, 2006. Denitrification across landscapes and waterscapes: A synthesis. Ecol. Appl., 16,2064-2090, doi:10.1890/1051-0761.

Sharada M. K. et al, 2008. Role of biology in the air-sea carbon flux in the Bay of Bengal and Arabian Sea, *Journal of Earth System Science* 117, 429-447.

Sharp Z., 2007. Principles of stable isotope geochemistry. Pearson Prentice Hall, New jersey, USA, 2007, 344p.

Shetye S. R. et al, 1991. Wind-driven coastal upwelling along the western boundary of the Bay of Bengal during the southwest monsoon. *Continental Shelf Research* 11, 1397-1408.

Shetye S. R., 1999. Dynamics of circulation of the waters around India. Ocean Science: Trends and Future dirtections, B.L.K. Somayajulu ed., Indian National Science Academy, New Delhi, pp. 1-21.

Shiozaki T. et al, 2010. New estimation of N_2 fixation in the western and central Pacific Ocean and its marginal seas. *Global Biogeochemical Cycles* 24, GB1015, doi:10.1029/2009GB003620.

Singh A., Jani R. A., Ramesh R., 2010. Spatiotemporal variations of the $\delta^{18}O$-salinity relation in the northern Indian Ocean. *Deep Sea Research I*, doi:10.1016/j.dsr.2010.08.002 .

Singh A., Ramesh R., 2011. Contribution of riverine dissolved inorganic nitrogen flux to new production in the coastal northern Indian Ocean - an assessment. *International Journal of Oceanography*, (in the press).

Singh A., Gandhi N., Ramesh R., 2011. An assessment of the contribution of atmospheric deposition to new productivity in the northern Indian Ocean, submitted to *Journal of Geophysical Research*.

Singh S. K., Sarin M. M., Lanord C. F., 2005. Chemical erosion in the eastern Himalaya: Major ion composition of the Brahmaputra and δ^{13}C of dissolved inorganic carbon. *Geochimica et Cosmochimica Acta* 69, 3573-3588.

Slawyk G., Collos Y. , Auclair J. C., 1977. The use of the ^{13}C and ^{15}N isotopes for the simultaneous measurement of carbon and nitrogen turn over rates in marine phytoplankton. *Limnology and Oceanography* 22, 925-932.

Smith S. L., 2001. Understanding the Arabian Sea: Reflections on the 1994-1996 Arabian Sea Expedition. *Deep Sea Research II* 48, 1385-1402.

Solomon S. et al, 2007. Climate Change 2007: The Physical Science Basis: Contribution of Working Group I to the Fourth Assessment Report of the Intergovernmental Panel on Climate Change. New York: Cambridge Univ. Press.

Somayajulu B. L. K., 2008. Nuclear and isotopic techniques for the characterization of submarine groundwater discharge in coastal zones. IAEA, Vienna, IAEA-TECDOC-1595. ISBN 978-92-0-106408-0. ISSN 1011-4289.

Somayajulu B. L. K., Rengarajan R., Jani R. A., 2002. Geochemical cycling in the Hooghly estuary, India. *Marine Chemistry* 79, 171-183.

Spokes L. J. et al, 2000. Nitrogen deposition to the eastern Atlantic Ocean. The importance of southeasterly flow. *Tellus* 52B, 37-49.

Srivastava R., et al, 2007. Oxygen isotope and salinity variations in the Indian sector of the Southern Ocean. *Geophysical Research Letters* 34, L24603, doi:10.1029/2007GL031790.

Subramanian V., 1993. Sediment load of Indian Rivers. *Current Science* 64, 928-930.

Subramanian V., 2008. Nitrogen transport by rivers of south Asia. *Current Science* 94, 1413-1418.

Takeda S., 1998. Influence of iron availability on nutrient consumption ratio of diatoms in oceanic waters. *Nature* 393, 774-777.

Thadathil P. et al, 2007. Observed seasonal variability of barrier layer in the Bay of Bengal, *Journal of Geophysical Research* 112, C02009, doi:10.1029/2006JC003651.

Tindale N. W., Pease P. P., 1999. Aerosols over the Arabian Sea: Atmospheric transport pathways and concentrations of dust and sea salt. *Deep Sea Research II* 46, 1577-1595.

Tiwari M. et al, 2005. Early deglacial (~19-17 ka) strengthening of the northeast monsoon. *Geophysical Research Letters* 32, L19712, doi:10.1029/2005GL024070.

Tiwari M. et al, 2009. Spatial and temporal coherence of paleomonsoon records from marine and land proxies in the Indian region during the past 30 ka. Platinum Jubilee publication of the Indian Academy of sciences, Bangalore, India, pp. 1-19.

Topping J., 1962. Errors of observation and their treatment. Reinhold publishing corporation, New York, 106 p.

UNESCO, 1994. Protocols for the Joint Global Ocean Flux Study (JGOFS) core measurements, Manual and guides, 170, Scientific Committee on Oceanic Research 29. pp 120.

Vinayachandran P. N. et al, 1999. Intrusion of the southwest monsoon current into the Bay of Bengal. *Journal of Geophysical Research* 104, 1107711085.

Watts L. J., Owens N. J. P., 1999. Nitrogen assimilation and f-ratio in the northwestern Indian Ocean during an Intermonsoon period. *Deep Sea Research II* 46, 725-743.

Watts L. J. et al, 1999. Modelling new production in the northwest Indian Ocean region. *Marine Ecological Progress Series* 183, 1-12.

Weiss R. F., 1970. The solubility of nitrogen, oxygen, and argon in water and seawater. *Deep Sea Research* 17(4), 721-735.

Westberry T. K., Siegel D. A., 2006. Spatial and temporal distribution of *Trichodesmium* blooms in the world's oceans. *Global Biogeochemical cycles* 20, GB4016, doi: 10.1029/2005GB002673.

White A. E. et al, 2007. Summer surface waters in the Gulf of California: Prime habitat for biological N_2 fixation. G*lobal Biogeochemical Cycles* 21, GB2017, doi:10.1029/2006GB002779.

Wiggert J. D., Murtugudde R. G., Christian J. R., 2006. Annual ecosystem variability in the tropical Indian Ocean: Results of a coupled bio-physical ocean general circulation model. *Deep Sea Research II* 53, 644-676.

Wyrtki K., 1971. Oceanographic Atlas of the International Indian Ocean Expedition. *Amerind Publishing Co. Pvt. Ltd.*, New Delhi, India.

Wyrtki K., 1973. An equatorial jet in the Indian Ocean. *Science* 181, 1331-1338.

Yadava M. G., Ramesh R., 1999. Speleothems-useful proxies for past monsoon rainfall. *Journal of Scientific and Industrial Research* 58, 339-348.

Yadava M. G., Ramesh R., 2005. Monsoon reconstruction from radiocarbon dated tropical speleothems. *The Holocene* 15, 48-59.

Zingde M. D., 2005. Inputs into the Oceans from Land/Rivers and Pollution. Oceanology, Universities Press. Edited by Harsh K. Gupta, pp. 210.

Zumft W. G., 1997. Cell biology and molecular basis of denitrification. *Microbiology and Molecular Biology Reviews* 61, 533-616.

Publications

A: Papers in Refereed Journals:-

1. Ramesh, R., and **A. Singh** (2010), Isotope fractionation in open systems: application to organic matter decomposition in ocean and land. *Curr. Sci.*, 98(3), 406-411.
2. **Singh, A.**, R. A. Jani, and R. Ramesh (2010), Spatiotemporal variations of the δ^{18}O-salinity relation in the northern Indian Ocean, *Deep-Sea Res., Part I*, doi:10.1016/j.dsr.2010.08.002.
3. Thirumalai, K., **A. Singh**, and R. Ramesh (2010), A MATLAB^{TM} code to perform weighted linear regression with (correlated or uncorrelated) errors in bivariate data, *J. of the Geological Society of India* (in the press).
4. **Singh, A.**, and R. Ramesh (2010), Contribution of riverine dissolved inorganic nitrogen flux to new production in the coastal northern Indian Ocean - an assessment, *International J. of Oceanography* (in the press).
5. Gandhi, N., **A. Singh**, and R. Ramesh (2010), Nitrogen sources for new production in the NE Indian Ocean, *Advances in Geosci.* (in the press).
6. **Singh, A.**, N. Gandhi, and R. Ramesh (2010), An assessment of the contribution of atmospheric deposition to new productivity in the northern Indian Ocean, *J. Geophys. Res.* (under review).

7. Gandhi, N., **A. Singh**, S. Prakash, M. S. Sheshshayee, S. Shetye, and R. Ramesh (2010), First direct Nitrogen fixation measurements in the eastern Arabian Sea, *Global Biogeochem. Cycles* (under review).

B: **Papers in Proceedings of Conferences:-**

8. **Singh, A.**, Prakash, S., Ramesh, R., and M. Sudhakar (2007), Ocean Fertilization: Recent Results from the Southern Ocean, Proceedings of National Conference on 'Global Temperature Rise: An Indian Effort Towards Mitigation of Carbon di-oxide emissions: A Brain Storming Session' during September 21-22, 2007, Visakhapatnam, India.

9. **Singh, A.**, R. A. Jani and R. Ramesh (2009), Oxygen isotope-salinity relation in the Bay of Bengal, 11^{th} ISMAS Triennial International Conference on Mass Spectrometry (ISBN 978-81-904442-2-4), Ramoji Film City, Hyderabad during 24 to 28 November , 2009.

10. Ramesh, R., **A. Singh**, and N. Gandhi (2010), Applications of stable isotopes in oceanography, International Conference organized by National Association for Applications of Radioisotopes and Radiation in Industry (NAARRI), Mumbai on 'Isotope Technologies and Applications - New Horizons' during December 13-15, 2010.

C: **Abstracts presented in Conference/ Symposia:-**

11. Gandhi, N., **A. Singh**, and R. Ramesh (2007), An assessment of the nitrogen supply by aerosols to primary production in the northern Indian Ocean, International Symposium on Aerosol-Chemistry-Climate Interactions 2007, Physical Research Laboratory, Ahmedabad, India.

12. **Singh, A.**, and R. Ramesh (2008), Does δ^{18}O-salinity relationship vary in the northern Indian Ocean?, International conference on Terrestrial Planets:

Evolution through Time during 21 - 25 January 2008, Physical Research Laboratory, Ahmedabad, India.

13. **Singh, A.**, and R. Ramesh (2008), Nitrogen budget of the Arabian Sea, Biogeochemical Interactions between the Ocean and the Atmosphere (BIOCAT) summer school held during 15 - 19 September 2008, at IFM-GEOMAR, Kiel, Germany

14. **Singh, A.**, and R. Ramesh (2008), Balancing the nitrogen budget in the northern Indian Ocean, 50th anniversary symposium and 2008 general meeting of Scientific Committee of Oceanic Research (SCOR) held during 18 - 25 October 2008 at Woods Hole, Massachusetts, USA.

15. **Singh, A.**, and R. Ramesh (2009), Isotope fractionation equation for an open system, European Research Course on Atmospheres (ERCA), 2009 held during 12 January - 13 February 2009 at Grenoble, France.

16. Gandhi, N., **A. Singh**, S. Prakash, R. Ramesh, and M. S. Sheshshayee (2010), Role of eddy pumping in enhancing primary production in the Bay of Bengal, Workshop on Satellite Meteorology: 50 - year Journey held during 29th October, 2010 at the Science city, Ahmedabad, India.

17. Gandhi, N., **A. Singh**, S. Prakash, S. Kumar, and R. Ramesh (2010), Glimpses of Oceanographic Research at PRL, Workshop on Satellite Meteorology: 50 - year Journey held during 29th October, 2010 at the Science city, Ahmedabad, India.